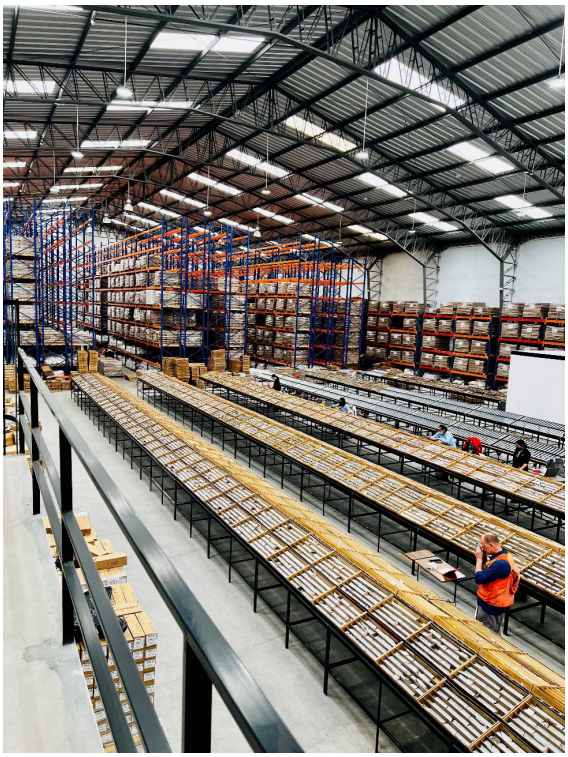

NI 43-101 Technical Report

for the Warintza Project, Ecuador (Amended)

Effective Date:
April 1, 2022

Prepared for:
Solaris Resources Inc.
Suite 555, 999 Canada Place
Vancouver, BC V6C 3E1

Qualified Person	Company
Mario E. Rossi	GeoSystems International, Inc.

Certificate of Qualified Person

I, Mario E. Rossi, do hereby certify that:

1. I am currently employed as President and Principal Geostatistician by GeoSystems International, Inc. 2385 NW Executive Center Dr., Suite 100, Boca Raton, Florida, 33431, USA.

2. This certificate applies to the report titled "NI 43-101 Technical Report, Warintza Project, Ecuador (Amended)," with an effective date of April 1, 2022 (the "Report").

3. I am a graduate of the Universidad Nacional de San Juan, Argentina, with a Mining Engineering Degree in 1985. I am also a graduate of Stanford University, California, USA, with a MSc in Geostatistics in 1988. I have been practicing my profession since 1985, and my relevant experience for the purpose of this Report includes work in resource estimation of a number of Cu-Mo-Au open-pit mines and development projects. I have worked on and been involved with National Instrument 43-101 studies on a number of projects, including several porphyry copper projects in Chile, Perú, and Argentina, among others.

4. I am a Registered Member of the Society of Mining Engineers (SME) of the USA, RM# 2770000.

5. I am also a Fellow with the Australasian Institute of Mining and Metallurgy (AusIMM), Fellow# 205464.

6. I visited the Warintza Project in Ecuador from October 27 to 29, 2021, including the Project site, Solaris offices in Patuca and Macas (Morona Santiago Province), the core logging and storage facilities in Quito, and ALS's sample preparation laboratory, also in Quito.

7. I am responsible for the overall content of this Report.

8. I have not had any prior involvement with the property.

9. I am independent of Solaris Resources Inc. as defined in Section 1.5 of National Instrument 43-101.

10. I have read the definition of "Qualified Person" set out in National Instrument 43-101 and certify that by reason of education, experience, independence, and affiliation with a professional association, I meet the requirements of a Qualified Person as defined in National Instrument 43-101.

11. I am not aware of any material fact or material change with respect to the subject matter of the Report that is not reflected in the Report and that, at the effective date of the Report, to the best of my knowledge, information, and belief, this Report contains all the scientific and technical information that is required to be disclosed to make the Report not misleading.

12. I have read the Report and National Instrument 43-101 - *Standards for Disclosure of Mineral Projects* and Form 43-101F1. This Report has been prepared in compliance with that instrument and form.

Dated this March 13, 2024 in Boca Raton, Florida, USA.

"Signed and Sealed"
Mario E. Rossi, RM-SME; Fellow, AusIMM; GeoSystems International, Inc.

Table of Contents

List of Tables

List of Figures

1.0 SUMMARY

1.1 Introduction

The purpose of this report is to disclose an updated mineral resource estimate ("MRE" or the "Resource") for the Warintza Project ("Warintza" or the "Project") located in southeastern Ecuador and owned by Solaris Resources Inc. ("Solaris" or the "Company").

Mario E. Rossi, FAusIMM, SME, IAMG, Principal Geostatistician of Geosystems International Inc. ("GSI"), prepared this technical report (the "Report"). Mr. Rossi is a Qualified Person ("QP") pursuant to National Instrument 43-101 ("NI 43-101") and is independent of Solaris Resources under Section 1.5 of NI 43-101. Mr. Rossi has over 35 years of experience in mining and geostatistics, mineral resource and reserves estimation, audits, and reviews in over 100 mining projects at various stages of development and operation. GSI is an independent, international mining consulting practice offering services specializing in porphyry deposits from exploration through feasibility, mine planning, and production.

This Report has an effective date of April 1, 2022. All information and assumptions discussed in this Report were determined as of the effective date. In Section 1, tables and production statistics are reported in metric units. All prices and costs used in this Report are based on US Dollars (USD).

Solaris is a Canadian-based metals mining company advancing a portfolio of copper assets in the Americas, focused on its Warintza Project in Ecuador which features a broad cluster of outcropping copper porphyry deposits anchored by a large-scale, high-grade open-pit resource inventory at Warintza Central. Ongoing efforts are focused on rapid resource growth and further discovery drilling. The Company offers additional discovery potential at its portfolio projects, Capricho and Paco Orco in Peru, Ricardo, and Tamarugo, via option agreements with Freeport-McMoRan in Chile and significant leverage to increasing copper prices through its 60% interest in the La Verde joint-venture with Teck Resources in Mexico.

Solaris' headquarters is located at Suite 555, 999 Canada Place, Vancouver, BC, V6C 3E1, Canada, and the Company is listed on the Toronto Stock Exchange under the symbol "SLS" as well as on the OTCQB Venture Market under the symbol "SLSSF". Further information is available at www.solarisresources.com.

The Report supersedes the Technical Report titled "Resource Estimate of the Warintza Central Cu-Mo Porphyry Deposit" with an effective date of December 13, 2019.

1.2 Property Description and Ownership

The Warintza Project is located in southeastern Ecuador, in the Province of Morona Santiago. It occupies the district of San Miguel de Conchay and San Antonio in the Limón Indanza Canton and San Carlos de Limón in the San Juan Bosco Canton. In the Project area, there are communities that identify themselves as belonging to the Shuar original peoples (96%) and to mixed ethnicity (4%).

The Project is situated 85 kilometers ("km") east of the major city of Cuenca in a rural part of the Cordillera del Cóndor, an inland mountain range forming the border between Ecuador and Peru. The Property is centered at 3º10' S latitude and 78º17' W longitude (PSAD-56 UTM Zone 17S: 800186E; 9648676N). The Project can be accessed by an unimproved road from the nearest national Highway 45, approximately 20

km from the Warintza Project. An unsealed, approximately 550 meters ("m") long, airstrip at the village of Warintza provides additional access to the Project by airplane or helicopter.

The Project is 100% owned by Solaris and includes nine metallic mineral concessions covering 268 square kilometers ("km²") ("Warintza Property" or the "Property"). Four concessions with an area of 10 km² are permitted for exploration activities, including drilling and path construction. There are four additional concessions contiguous with the original concession and one concession to the northwest.

The climate of the Project is classified as tropical, with an average annual temperature of 23.0°C and average annual rainfall of 1,827 millimetres ("mm"). Rainfall is significant year-round but peaks in May, whereas the temperature is consistent year-round. From a mineral exploration point of view, the Property can be explored year-round.

The terrain surrounding the Project is mountainous to rolling hills and valleys, with elevations from 1,000 m to 2,700 m above mean sea level.

1.3 Geology and Mineralization

The Property is underlain by Jurassic supracrustal volcanic and sedimentary rocks of the Mishuallli Member of the Chapiza Formation, as well as Jurassic granitoids of the Zamora Batholith. These rocks are intruded by a series of plutonic and porphyritic intrusions of intermediate composition, from quartz-monzonite, through to granodiorite, to diorite, emplaced as outliers of the Zamora batholith in proximity to its eastern contact with Misahualli volcanic and volcano-sedimentary rocks.

Porphyry copper bearing dikes and stocks at Warintza Central were principally emplaced in precursor plutonic stocks, whereas Warintza South and Warintza East intruded Misahuallí volcanic and volcano-sedimentary rocks. Late Jurassic syn-mineralization porphyry that hosts the Warintza Central deposit is of similar age to other nearby porphyry and epithermal deposits in the Zamora copper-gold belt (e.g., Fruta del Norte, Mirador).

Warintza Central is a calc-alkalic copper-molybdenum porphyry deposit with copper mineralization (but not molybdenum) partly redistributed by supergene processes to form leached and underlying supergene-enriched zones that both overlie primary mineralization. Three other discoveries have been made on the Property, including Warintza West, Warintza East, and Warintza South, but only partially drill-tested, with additional copper-molybdenum anomalies at Yawi and El Trinche and elsewhere on the Property.

1.4 Mineral Resource Estimate

The MRE was prepared by the QP and includes estimates of copper ("Cu"), molybdenum ("Mo"), and gold ("Au") resources and was based on over 64,500 m of diamond drilling data. Additionally, the QP also estimated in-situ density values from 1,599 samples available.

Cu grades were estimated based on 10 separate domains, while Mo was based on seven domains and Au on four domains. These domains are, in turn, based on the underlying geologic model prepared by Solaris, validated by the QP, and include a lithology model, an alteration model, and a mineralization model. Available structural information was used in the interpretation of the Warintza geologic model.

Detailed statistical and geostatistical analyses were used to develop the grade estimation strategy, including the definition of an appropriate composite length; the restriction of outlier grades (capping); contact (grade profile) analysis for all domains and for the three metals; the use of correlogram models to understand and apply the continuity of grades within each domain; and the overall grade estimation strategy applied in the resource estimates.

The grades estimated into the block model were properly validated using statistical and visual tools, concluding that the grade estimates are reasonable.

Resource classification was implemented on the nominal notion that at least two drill holes are required within 100 m to declare block Indicated mineral resources, with all other estimated blocks classified as Inferred mineral resources. There are no Measured mineral resources classified at Warintza. The final coding into the resource model blocks of the classification was completed by interpreting by hand, on plan level, the Indicated mineral resource areas. No Indicated mineral resources were classified in the Warintza East and El Trinche areas or at elevations below 545 m.

The mineral resources have been developed according to the 2014 CIM Definition Standards and were prepared according to CIM Best Practice Guidelines (CIM, 2019), reported in accordance with Canadian Securities Administrators' National Instrument 43-101. Mineral resources are not mineral reserves and do not have demonstrated economic viability. There is no certainty that all or any part of the mineral resources will be converted into mineral reserves.

To assess the "Reasonable Prospects for Eventual Economic Extraction," the QP constrained the overall estimated grades by running a pit optimization on the block model. The results of the pit optimization were used solely to test the "Reasonable Prospects for Eventual Economic Extraction" by an open-pit and do not represent an attempt to estimate mineral reserves.

Although it is not certain that additional drilling will add to the current resource base, the incorporation of 87% of the current mineral inventory into the open-pit-constrained resource highlights the fact that the current resource base and constraining pit is limited by the current drilling and the early stage of the Project. The Inferred open-pit mineral resources in the Warintza Central deposit within the constraining optimized pit shell are reported at a 0.3% CuEq cut-off grade, summarized in Table 1.

Table 1: Warintza Mineral Resource at 0.3% CuEq Cut-Off Grade, Effective April 1, 2022

Cut-off	Resource Category	Tonnage Above Cutoff	Grade Above Cutoff				Contained Metal Above Cutoff			
CuEq (%)		(Mt)	CuEq (%)	Cu (%)	Mo (%)	Au (g/t)	CuEq (Mt)	Cu (Mt)	Mo (Mt)	Au (Moz)
0.3	Indicated	579	0.59	0.47	0.03	0.05	3.45	2.7	0.15	0.93
	Inferred	887	0.47	0.39	0.01	0.04	4.17	3.48	0.13	1.08

Notes to Table 1:

1. *The mineral resource estimates are reported in accordance with the CIM Definition Standards for Mineral Resources & Mineral Reserves, adopted by CIM Council May 10, 2014.*

2. *Reasonable prospects for eventual economic extraction assume open-pit mining with conventional flotation processing and were tested using NPV Scheduler™ pit optimization software with the following assumptions: metal prices of US$3.50/lb Cu, US$15.00/lb Mo, and US$1,500/oz Au; operating costs of US$1.50/t + US$0.02/t per bench for mining, US$4.50/t milling, US$0.90/t G&A; recoveries of 90% Cu, 85% Mo, and 70% Au.*
3. *Resource includes grade capping and internal dilution. Grade was interpolated by ordinary kriging, populating a block model with block dimensions of 25m x 25m x 15m.*
4. *Mineral resources that are not mineral reserves do not have demonstrated economic viability.*
5. *Copper equivalent assumes recoveries of 90% Cu, 85% Mo, and 70% Au, based on preliminary metallurgical test work and metal prices of US$3.50/lb Cu, US$15.00/lb Mo, and US$1,500/oz Au. CuEq formula: CuEq (%) = Cu (%) + 4.0476 × Mo (%) + 0.487 × Au (g/t).*
6. *The Qualified Person is Mario E. Rossi, FAusIMM, RM-SME, Principal Geostatistician of Geosystems International Inc.*
7. *All figures are rounded to reflect the relative accuracy of the estimate.*
8. *The effective date of the mineral resource estimate is April 1, 2022.*

Table 2: Warintza Mineral Resource Estimate Summary and Cut-Off Grade Sensitivity

Cut-off	Category	Tonnage	Grade				Contained Metal			
CuEq (%)		(Mt)	CuEq (%)	Cu (%)	Mo (%)	Au (g/t)	CuEq (Mt)	Cu (Mt)	Mo (Mt)	Au (Moz)
0.2%	Indicated	736	0.52	0.40	0.02	0.05	3.84	2.95	0.18	1.11
	Inferred	1,558	0.37	0.31	0.01	0.03	5.80	4.80	0.19	1.63
0.3% (Base Case)	**Indicated**	**579**	**0.59**	**0.47**	**0.03**	**0.05**	**3.45**	**2.70**	**0.15**	**0.93**
	Inferred	**887**	**0.47**	**0.39**	**0.01**	**0.04**	**4.17**	**3.48**	**0.13**	**1.08**
0.4%	Indicated	442	0.67	0.54	0.03	0.05	2.97	2.38	0.12	0.77
	Inferred	539	0.55	0.47	0.01	0.04	2.96	2.53	0.08	0.71

Notes to Table 2:

1. *The mineral resource estimates are reported in accordance with the CIM Definition Standards for Mineral Resources & Mineral Reserves, adopted by CIM Council May 10, 2014.*
2. *Reasonable prospects for eventual economic extraction assume open-pit mining with conventional flotation processing and were tested using NPV Scheduler™ pit optimization software with the following assumptions: metal prices of US$3.50/lb Cu, US$15.00/lb Mo, and US$1,500/oz Au; operating costs of US$1.50/t + US$0.02/t per bench for mining, US$4.50/t milling, US$0.90/t G&A; recoveries of 90% Cu, 85% Mo, and 70% Au.*
3. *Resource includes grade capping and internal dilution. Grade was interpolated by ordinary kriging, populating a block model with block dimensions of 25m x 25m x 15m.*
4. *Mineral resources that are not mineral reserves do not have demonstrated economic viability.*
5. *Copper equivalent assumes recoveries of 90% Cu, 85% Mo, and 70% Au, based on preliminary metallurgical test work and metal prices of US$3.50/lb Cu, US$15.00/lb Mo, and US$1,500/oz Au. CuEq formula: CuEq (%) = Cu (%) + 4.0476 × Mo (%) + 0.487 × Au (g/t).*
6. *The Qualified Person is Mario E. Rossi, FAusIMM, RM-SME, Principal Geostatistician of Geosystems International Inc.*
7. *All figures are rounded to reflect the relative accuracy of the estimate.*
8. *The effective date of the mineral resource estimate is April 1, 2022.*

1.5 Conclusions and Recommendations

Warintza is a highly prospective Cu-Mo-Au porphyry deposit within the Cordillera del Cóndor. Exploration efforts in the belt have identified numerous porphyry, Au skarn, and epithermal Au deposits, all related to Late Jurassic magmatism. Warintza is a typical porphyry system that has the potential to become a world-class Cu-Mo-Au resource, while the potential for other deposit types exists but have not been explored.

After less than two years and less than 65,000 m of core drilling, which have tested mainly the Warintza Central area, this MRE shows a very significant tonnage amenable to open-pit mining. It also shows that the mineralization is open in several directions and that there are several additional deposits which have significant target footprints, adjacent and nearby to Warintza Central, that require further exploration.

Infill drilling is required within both Warintza Central and Warintza East, but more importantly, drilling to date has not defined the limits of mineralization, with a reasonable expectation that additional drilling will result in an increase in the known dimensions of the mineralization.

Straightforward grass-roots exploration techniques work well in the Cordillera del Cóndor. Numerous porphyry deposits have been discovered in the area by initial panned concentrate stream sediment sampling, followed by prospecting, rock sampling, ridge soil sampling, grid soil sampling, and finally, scout drill-testing of geochemical anomalies. At Warintza, there are additional targets that have yet to be investigated by drilling.

Warintza Central and Warintza East are the subjects of this MRE. Both are open at depth and laterally. These are good prospects for additional drilling to expand the Resource in both areas.

Early exploration at Warintza prior to Solaris' involvement was hampered by community and social issues, and although this still presents a risk, efforts by the Company have allowed for the development of a supportive relationship and advancement of the Project. The return of the surface rights covering the Shuar communities, along with ongoing community consultation and community development efforts, have culminated in the Company entering into an Impact and Benefits Agreement with the host communities.

Metallurgical testing is ongoing, and a full characterization of Warintza's mineralization is still pending. It is merited that, in the near-term, a Preliminary Economic Assessment ("PEA") be developed, which will require a more complete understanding of the mineralization's response to beneficiation methods. From the testing completed to date, plus comparisons to similar porphyry deposits, it is likely that mineralization is amenable to conventional metallurgical processes.

Additional diamond core drilling for the Warintza Central deposit is recommended. There are two simultaneous objectives: resource expansion and increase in resource confidence (categorization). Among these two objectives, if additional geologic information warrants it, targeting new areas of higher-grade mineralization (supergene enrichment or high-grade primary mineralization) should be prioritized.

Infill, resource expansion, exploration and geometallurgical drilling (at PQ diameter) and studies to support a PEA based on an updated MRE should be completed. The combined objectives are likely to require an additional 44,000 m of drilling, with the resource expansion drilling component at Warintza

Central and Warintza East and follow-up drilling at the Warintza West discovery amounting to approximately 24,000 m of this total. Together, these programs would cost approximately $25 million, inclusive of camp costs, infrastructure development, and community costs. Further infill drilling, geometallurgical and geotechnical drilling, together with other technical, environmental and market studies in support of a Pre-Feasibility Study could cost an additional $40 million.

2.0 INTRODUCTION

2.1 Terms of Reference

Solaris, a TSX-listed company with headquarters in Vancouver, British Columbia, Canada, commissioned the Author to prepare this Report on the Warintza Project in Ecuador to update the previous mineral resource estimate at the Project. Solaris is an Augusta Group company, a management group focused on the mining sector and highly specialized in exploration and development-stage projects. Solaris' common shares are listed on the Toronto Stock Exchange and trade under the symbol "SLS" as well as on the OTCQB Venture Market under the symbol "SLSSF".

Essentially, all the technical information and much of the Ecuadorian legal and regulatory information in this Report was obtained by the Author from employees or representatives of Solaris and its subsidiary, Lowell Mineral Exploration Ecuador S.A. ("Lowell"). This includes documents received and personal communications in the form of face-to-face conversations, telephone conversations, and email.

Mr. Rossi visited the Warintza Project in Ecuador from October 27 to 29, 2021. Mr. Rossi visited the Project site, Solaris' offices in Macas and Quito, and the sample preparation laboratory in Quito.

2.2 Units, Currency, and Abbreviations

Unless otherwise stated, all currencies are expressed in USD with metric units applied throughout this Report. 'Section' and 'Item' have been used interchangeably in this Report. Abbreviations and units are shown in Table 3.

Table 3: Abbreviations and Measurement Units

%	Percent
% w/w	% Of Solid Mass in Liquid Mass
°	Degrees
°C	Degrees Celsius
µm	Micron
3D	Three-Dimensional
AAS	Atomic Absorption Spectrometry
AB	Air Blast
AG	Auger
Ag	Silver
ARD	Acid Rock Drainage
As	Arsenic
Au	Gold
BD	Bulk Density
BLEG	Bulk Leach Extractable Gold
BOCO	Base of Complete Oxidation
Capex	Capital Expenditure
BWI	Bond's work index
CIM	Canadian Institute of Mining, Metallurgy, and Petroleum
cm	Centimeter(s)
CMP	Composite
CN	Cyanide
COEF	Coefficient
COG	Cut-off Grade
CRM	Certified Reference Material
CSV	Comma Separated Value
Cu	Copper
CuEq	Copper equivalent
CV	Coefficient of Variation
DBA	Database Administrator
DC	Diamond Core
DD	Diamond Drill
DFS	Definitive Feasibility Report
DH	Drill Hole
DDH	Diamond Drill Hole
EIA	Environmental Impact Assessment
EIS	Environmental Impact Study
EM	Electromagnetic

EMP	Environmental Management Plan
EMS	Environmental Management Systems
EOH	End of Hole
EOM	End of Month
EPA	Environmental Protection Agency (USA)
EPCM	Engineering, Procurement and Construction Management
EPMA	Electron Probe Microanalysis
ESE	East-Southeast
ESIA	Environmental And Social Impact Assessment
EXP	Exploration
FA	Fire Assay
FS	Feasibility Study
g	Gram(s)
G&A	General And Administration
g/cm^3	Grams Per Cubic Centimetre
g/t	Grams Per Tonne
Ga	Giga-Annum
GIS	Geographic Information System
GPS	Global Positioning System
h	Hour(s)
ha	Hectare(s)
HSE	Health, Safety, And Environment
ICMC	International Cyanide Management Code
ICP AES	Inductively Coupled Plasma Emission Spectrometry
ICP MS	Inductively Coupled Plasma Mass Spectrometry
ID^2	Inverse Distance Squared
ID^3	Inverse Distance Cubed
IFC	International Finance Corporation
IFRS	International Financial Reporting Standards
ILR	Intensive Leach Reactor
IP	Induced Polarization
ISO	International Standards Organization
IT	Information Technology
JV	Joint Venture
K	Thousand
kg	Kilogram(s)
kL	Kilolitre
Km	Kilometer(s)
km^2	Square Kilometers
koz	Kilo Ounce/Thousand Ounce (Troy)

kt	Thousand Tonnes
kW	Kilowatt
L	Litre
lbs	Pounds
m	Meter(s)
m^2	Square Meter(s)
m^3	Cubic Meter(s)
M	Million
M+I	Measured and Indicated
Ma	Million Years Ago
MAMSL	Meters Above Mean Sea Level
masl	Meters Above Sea Level
mm	Millimetre(s)
Mo	Molybdenum
MOU	Memorandum Of Understanding
MRE	Mineral Resource Estimate
Mt	Million Tonnes
Mtpa	Million Tonnes Per Annum
N	North
NE	Northeast
NI 43-101	Canadian Securities Administrators National Instrument 43-101
NNE	North-northeast
NPV	Net Present Value
NSR	Net Smelter Revenue
OK	Ordinary Kriging
OPEX	Operating Expenditure
oz	Ounce (Troy)
oz/ton	Troy Ounce Per Short Ton
PAG	Potentially Acid Generating
Pb	Lead
pH	Acidity Scale
PFS	Prefeasibility Study
ppb	Part Per Billion
ppm	Part Per Million
PSAD-56	Provisional South American datum
P80	80% Passing Through Grind Test
Q1, Q2, Q3, Q4	Quarter One, Quarter Two, Quarter Three, Quarter Four
QA/QC	Quality Assurance/Quality Control
QA	Quality Assurance
QC	Quality Control

QEMSCAN	Quantitative Evaluation of Materials by Scanning Electron Microscopy
QP(s)	Qualified Person(s)
QQ	Quantile-Quantile
QSP	Quartz Sericite Pyrite
Qtz	Quartz
QV	Quartz Veins
RBU	Remuneración Básica Unificada (Annual Ecuadorian Wage Calculation)
RC	Reverse Circulation
RCD	Reverse Circulation with Diamond Tail
RF	Revenue Factor
RHS	Right Hand Side
RQD	Rock Quality Designations
Sb	Antimony
SBM	Sub-Celled Block Model
SCC	Sericite-clay-chlorite
SD	Standard Deviation(s)
SE	Southeast
SEC	U.S. Securities and Exchange Commission
SG	Specific Gravity
SGS	SGS Laboratories
SiO_2	Silicon Dioxide (Silica)
SMU	Selective Mining Unit
SOX	Strongly Oxidized
SQL	Structured Query Language
t	Tonne(s)
t/m^3	Tonnes Per Cubic Metre
TOFR	Top of Fresh Rock
Tpa	Tonnes Per Annum
TSF	Tailings Storage Facility
TSX	Toronto Stock Exchange
UCS	Unconfined Compressive Strength
US$	United States Dollars
USB	Universal Serial Bus
UTM	Universal Transverse Mercator
VTEM	Versatile Time-Domain Electromagnetic Surveying
W	West
WOX	Weakly Oxidized
XRD	X-Ray Diffraction
XRF	X-Ray Fluorescence
Zn	Zinc

3.0 RELIANCE ON OTHER EXPERTS

For the purpose of this Report, the QP has relied on Solaris for information regarding legal and environmental information, as noted below.

3.1 Mineral Tenure, Surface Rights, Agreements, and Environmental Information

The QP has not reviewed the mineral tenure nor verified the legal status, ownership of the Property or underlying property agreements, and environmental information. The QP has fully relied upon and disclaims responsibility for information derived from Solaris experts derived from multiple documents as set out herein. This information is used in Sections 4 and 20 of the Report.

The information regarding mineral tenure was based upon a legal opinion dated April 25, 2022, and other advice prepared by Solaris' local Ecuadorian counsel, Robalino Abogados.

4.0 PROPERTY DESCRIPTION AND LOCATION

4.1 Project Location and Area

The Warintza Property is located in southeastern Ecuador in the province of Morona Santiago and the Limon Indaza Canton and San Carlos de Limón in the San Juan Bosco Canton. It is located 235 km southeast of Ecuador's capital, Quito (as the crow flies), and 85 km ESE from the city of Cuenca (Figure 1). The Property is centered at 3º10' S latitude and 78º17' W longitude (PSAD-56 UTM Zone 17S: 800186E; 9648676N) within the Cordillera del Cóndor, a mountain range in the eastern Andes that locally forms the border between Ecuador and Peru.

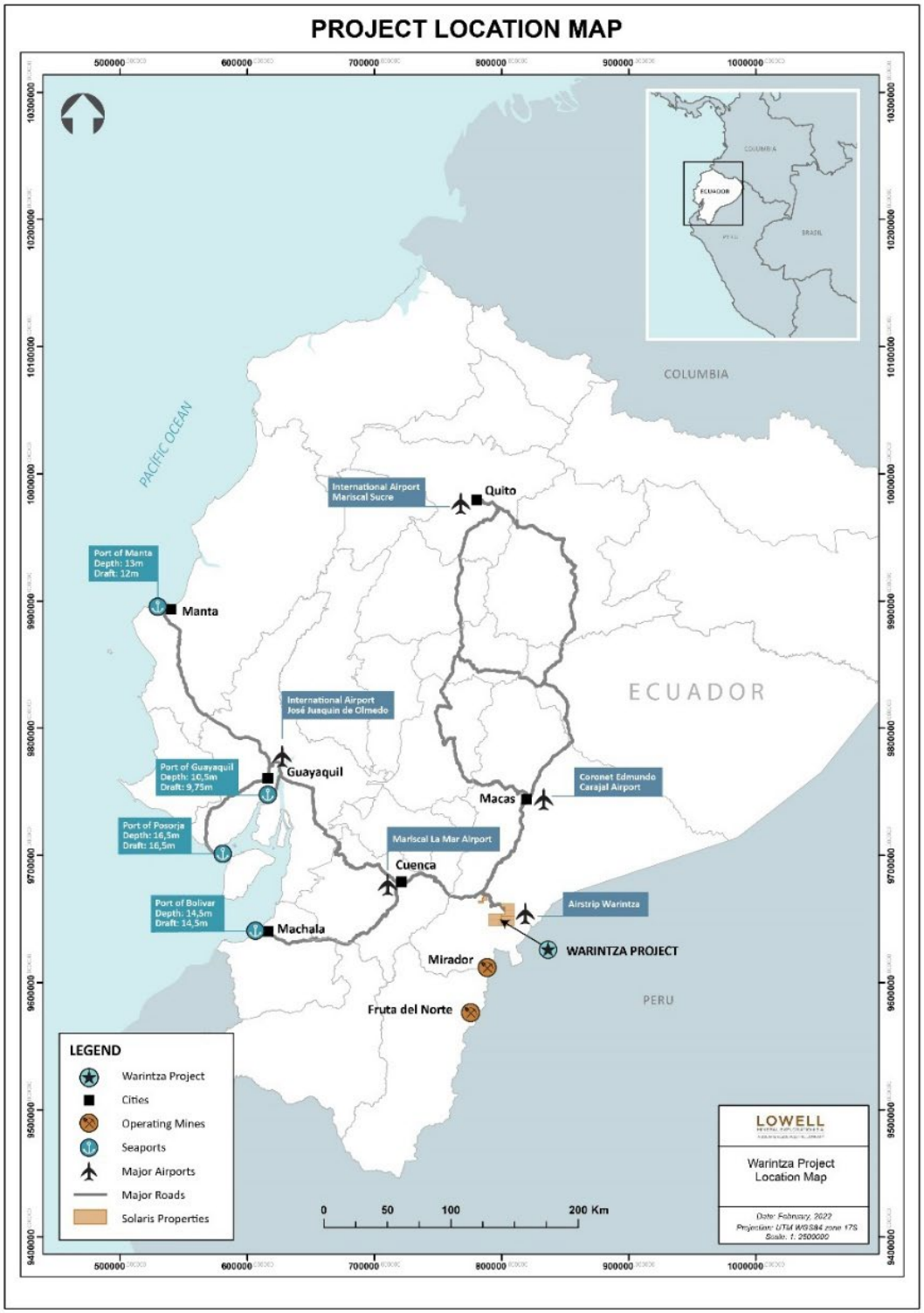

Figure 1: Location Map of the Warintza Project

4.2 Licenses and Mineral Tenure

The Property is covered by nine metallic mineral concessions that collectively cover approximately 268 km² (26,777 hectares) and represented in Table 4. The mineral concessions are 100%-owned by Solaris.

Solaris has entered into a "Cooperation, Benefits and Access Agreement for the Development of the Warintza Project" (also referred to as Impact and Benefits Agreement), dated March 2022 with the local communities within the area of influence of the Warintza Project that, among other things, grants Solaris access and use of surface rights at the Warintza Project.

Table 4: Warintza Concessions

Name	Concession Number	Area (Ha)	Type	Registration Date	Good to Date
CAYA 21	101083	2,500	Concession	25/5/2010	7/2/2041
CAYA 22	101092	2,500	Concession	25/5/2010	7/2/2041
CURIGEM 9	100081	4,050	Concession	25/5/2010	27/10/2041
CURIGEM 9-1	10000938	950	Concession	8/4/2022	10/8/2032
CLEMENTE	90000337	1,601	Concession	31/3/2017	31/3/2042
MAIKI 01	90000310	4,072	Concession	8/3/2017	8/3/2042
MAIKI 02	90000311	4,304	Concession	8/3/2017	8/3/2042
MAIKI 03	90000313	2,500	Concession	31/3/2017	31/3/2042
MAIKI 04	90000314	4,300	Concession	8/3/2017	8/3/2042
	Grand Total	**26,777**			

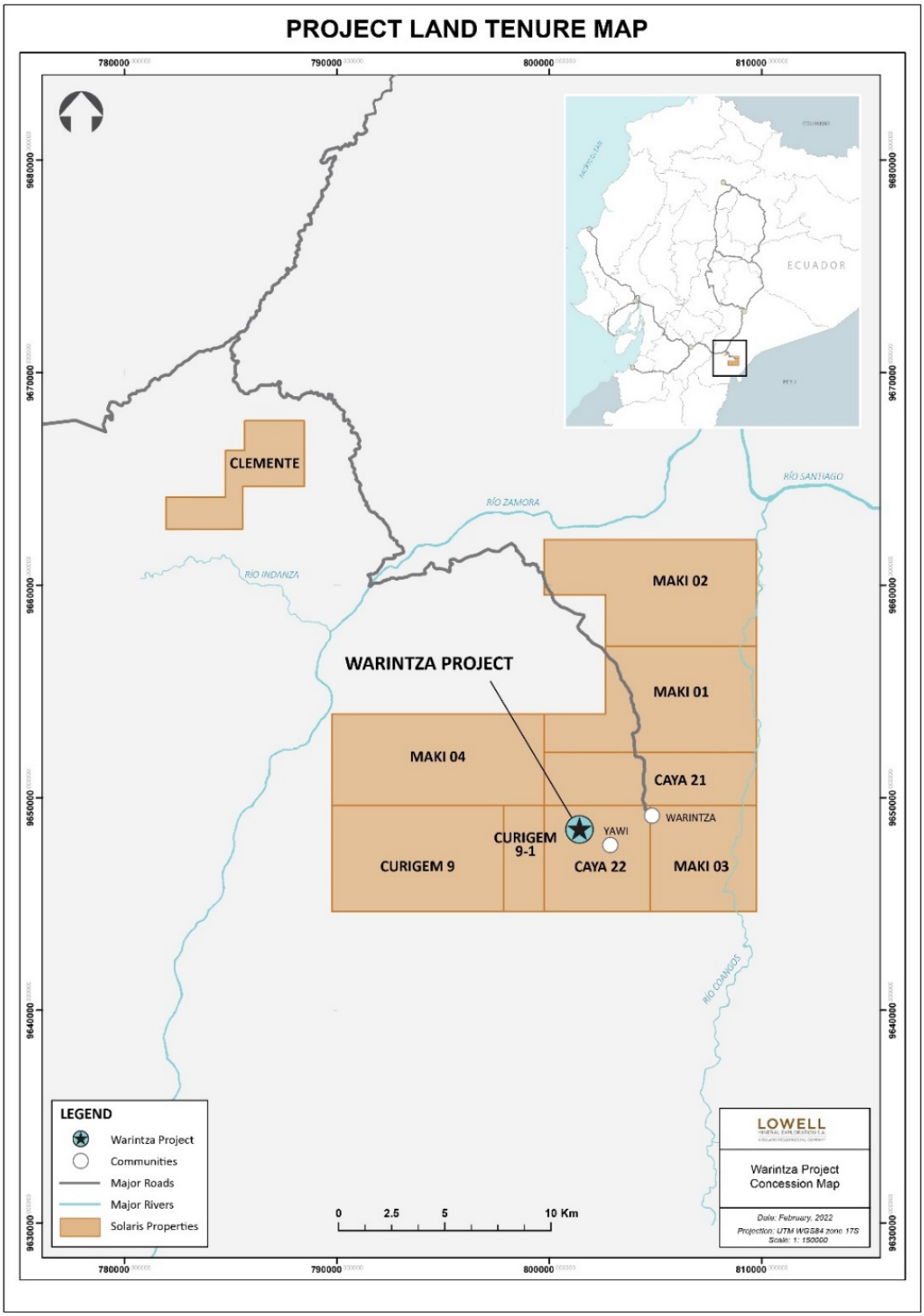

Figure 2: Location of Warintza Concessions

4.3 Royalties

A 2% net smelter royalty (NSR) is payable to South32 Royalty Investments Pty Ltd. (formerly BHP Billiton) on the Curigem 9, Curigem 9.1, Caya 21, and Caya 22 concessions. In addition, the Government of Ecuador mandates an NSR of between 3% to 8% for its benefit, which is negotiated and established in the exploitation agreement. To the Authors' knowledge, there are no other royalties, back-in rights, or other agreements or encumbrances of a similar nature on the Property.

4.4 Mineral Rights in Ecuador

Concessions have a term of 25 years and can be renewed for additional periods of 25 years if applications for renewal are submitted before the expiration of the concessions. In order to maintain concessions in good standing, a fee must be paid by March 31 each calendar year for the Conservation Patent. The fees are based on a calculated annual minimum wage, Remuneración Básica Unificada ("RBU"). For each hectare, the Conservation Patent fees start at 2.5% of the RBU per annum for the "initial exploration stage" and increase as the project advances (Table 5). The concessions are currently in the initial exploration stage.

Exploration expenditures are required annually based on the area of the concessions, and required expenditures increase each year. Excess spending can be carried over for a portion of the following year's required expenditure.

The annual Conservation Patent payments for the Property have been made as of the issuance of this Report and are valid until March 31, 2023.

Table 5: Exploration and Exploitation Phases

Project Stage	Length of Time	RBU per hectare
Initial Exploration	Up to four years from the time the concessionaire obtained all the previous administrative acts, according to Art. 26 of the Mining Law.	2.5%
Advanced Exploration	Up to four years, the application must be made prior to the end of the Initial Exploration Period. The application must include a waiver of part of the surface initially granted.	5%
Economic Evaluation	Up to two years, starting once the Initial Exploration Period or the Advanced Exploration Period has ended. May be extended, on application, for up to an additional two years.	5%
Exploitation	Commences on the request of the concessionaire, which must be made prior to the end of the Economic Evaluation Period. Various requirements and conditions apply.	10%

4.5 Environmental Obligations

Environmental liabilities are discussed in Section 20.

4.6 Permits

Permits are discussed in Section 20.

5.0 ACCESIBILITY, CLIMATE, LOCAL RESOURCES, INFRASTRUCTURE, AND PHYSIOGRAPHY

5.1 Topography, Elevation, and Vegetation

The Warintza Property is located in an area of rugged terrain mixed with rolling hills and valleys, covered by heavy forest in areas and scrub or cleared land in others, with a humid tropical climate. Elevations within the concessions range from a low of approximately 1000 m above sea level in the main drainage to a high of approximately 2,700 m on the ridge tops. Typical hillside slopes are between 25º and 40º, with some local slopes that are nearly vertical.

The nearest major population centre is Macas. Small villages, including Warintza (~600 people) and Yawi (~200 people), occur proximal to the Property, with these communities party to an Impact and Benefits Agreement with the Company.

The Warintza area is classified as Af (tropical climate) in the Köppen-Geiger climate system. Over the course of a typical year, low temperatures range from 8°C to 10°C, while high temperatures range from 17°C to 20°C. Approximate rainfall over the course of a typical year averages 1,827 mm and is illustrated in Figure 3 below. From a mineral exploration point of view, the Warintza Property can be explored year-round.

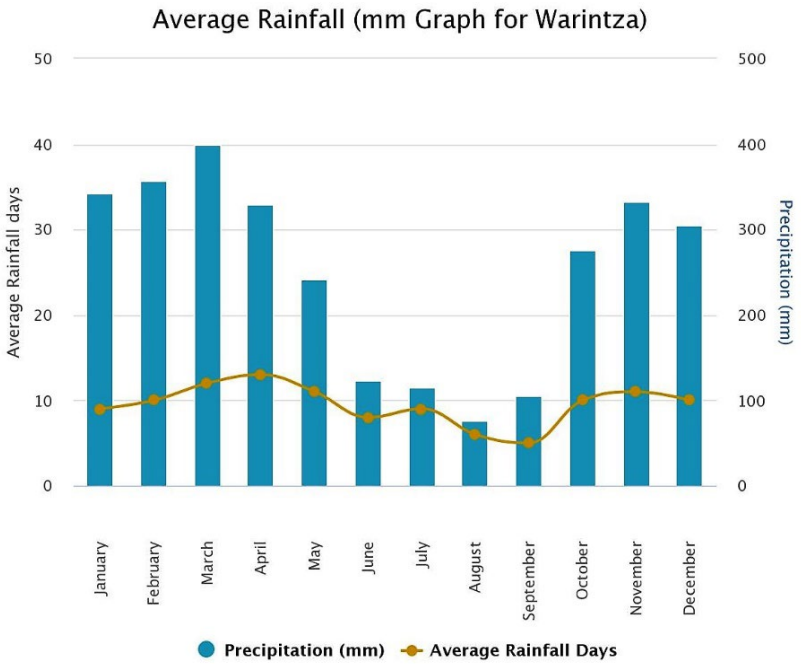

Figure 3: Monthly Average Rainfall, Warintza Project
Source: www.worldweatheronline.com

5.2 Access

The nearest national Highway 45 is within approximately 20 km of the Warintza Project (Figure 4), with direct unimproved road access established. An unsealed, approximately 550 m long, airstrip at the village of Warintza provides additional good access to the Project (Figure 5) by airplane or helicopter.

The Project site includes four remote camps that provide access to drill platforms for exploration drilling. The walk from the village to the main campsite on the Project takes approximately one hour on a route that is four km long with an elevation gain of approximately 250 m.

5.3 Proximity to Population Centre and Transport

The nearest supply center connected to the national transportation infrastructure is the town of Macas, which provides good road connections and a commercial airport capable of handling commercial jet aircraft. Small aircrafts chartered in Macas can reach the airstrip at Warintza in approximately 30 minutes. The highly changeable weather and cloud cover can delay flights.

From the western end of the airstrip, the Warintza Central deposit is accessible on foot via a series of trails that are the principal means of transportation of crew and equipment. The exploration program is also supported by helicopters to transport equipment, supplies, and core to transfer facilities.

5.4 Infrastructure and Personnel

The Project is not connected to existing electrical power infrastructure; however, the national electric grid is located approximately 20 km to the northwest of the Project nearby national highway 45. Solaris signed an MOU in March 2022 with the State electric company, Electric Corporation of Ecuador ("CELEC EP"), to supply low-cost, locally-sourced hydroelectric power to the Project. The author is aware of CELEC EP updating the Ecuadorian environmental plan for a 2.4 GW Santiago hydroelectric project development, which is a forthcoming, fully-permitted project on the northern property boundary of Warintza. It is highly likely that the Santiago hydroelectric power project will be a possible source of power for mine operations.

No studies have yet addressed the suitability of sites for infrastructure (e.g., tailings, processing plant sites) or the availability of resources (e.g., water, power, personnel) at Warintza.

Given the abundant rainfall and many streams on the Property, it is reasonable to assume that ample water supplies exist. The Author is not aware of any studies relating to specific sources for possible mine process waters.

Solaris employs many local residents in its exploration programs and has implemented training and education programs. However, there is no history of mining in the immediate vicinity, and hence no mining workforce is directly available. In a development scenario, a responsible operator would likely utilize as much local labor as possible and implement training programs to develop the skills required for mining, possibly incorporating personnel from the two major mines in operation in the neighboring province of Zamora-Chinchipe.

Other projects in Ecuador with similar terrain, climate, and access (e.g., Mirador and Fruta del Norte located 48 km and 70 km, respectively, SSW of Warintza) have recently shown that similar conditions do not preclude mining. Detailed studies, however, are required to determine the sufficiency of surface rights and the availability of power, water, personnel, and mining infrastructure sites at Warintza. These are beyond the scope of this Report.

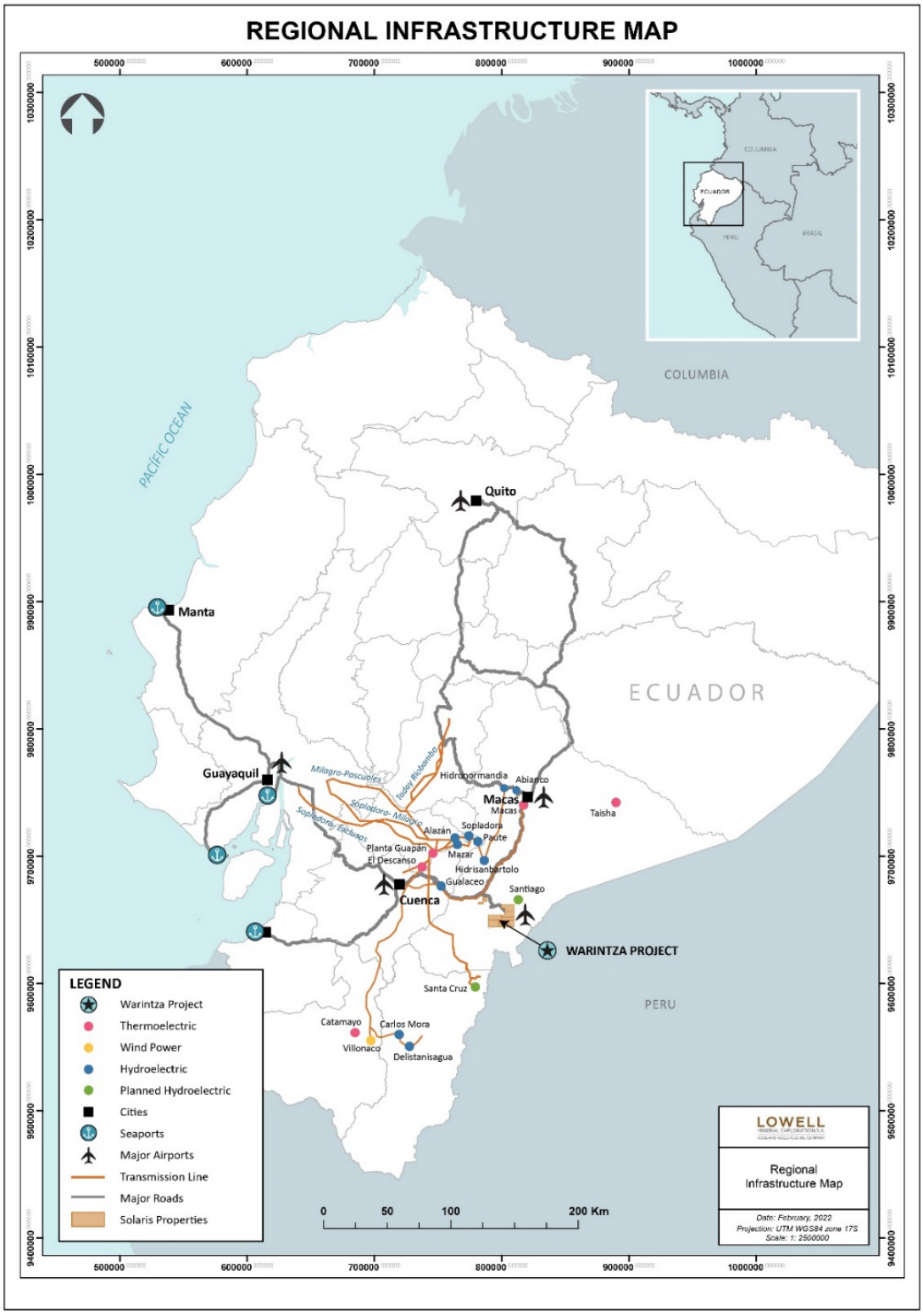

Figure 4: Regional Infrastructure Map

Figure 5: Unsealed Airstrip Access at Warintza Village
Viewed Towards the Southwest. Warintza Central Deposit Underlies the Ridge in the Centre

6.0 HISTORY

The following description of the Warintza Project history is largely derived from Sivertz et al. (2006) and Ronning and Ristorcelli (2018).

6.1 Property Ownership Changes

Prior to 1994, no mineral exploration had been reported in the Warintza area. In that year, Gencor Limited ("Gencor") began grassroots exploration of the Pangui project in southeastern Ecuador, which was directed at identifying Au mineralization in the Oriente foreland basin (Gendall et al., 2000). Following corporate restructuring of Gencor in 1997, Billiton PLC ("Billiton") continued the Pangui project. Between 1994 and 1999, Billiton completed regional-scale geochemical and airborne magnetic-electromagnetic

(EM) geophysical surveys over a large area and more detailed mapping and geochemical surveys of targets within it, ultimately leading to the initial drilling of several of the 10 regional-scale porphyry and skarn targets that were identified.

In April 2000, Billiton and Corriente Resources Inc. ("Corriente") entered into an agreement covering 230 km² of mineral concessions in the southeastern part of Ecuador, which included Warintza. Under the agreement, Corriente could earn a 70% interest in each of the Billiton projects by completing a feasibility study and meeting certain financial and work commitments (Corriente Resource Inc. Annual Information Form, 2000). At the completion of each feasibility study, Billiton could elect to (a) back-in for a 70% interest by providing production financing, (b) retain a 30% working interest, or (c) dilute to a 15% Net Profit Interest ("NPI"). Corriente also entered into an exploration management arrangement whereby Lowell Mineral Exploration Ecuador S.A. could earn up to 10% of Corriente's interest in certain properties in exchange for managing the exploration of the properties.

In 2002, Corriente purchased 100% of three of its optioned Ecuadorian properties (Mirador, San Carlos, and Panantza) from Billiton in return for a 2% NSR, of which 1% could be purchased for $2 million. In November 2003, Corriente announced that it had purchased 100% of the remaining Ecuadorian concessions it held under option from Billiton, including Warintza, for a 2% NSR with no buy-down and no back-in rights (Corriente Resources Inc. Annual Report, 2003).

By this time, Lowell had vested its 10% interest in Corriente's Ecuadorian properties, including Warintza, Mirador, San Carlos-Panantza. In 2004, Lowell swapped its 10% interest in Corriente's Ecuadorian properties for 100% interest in the Warintza Property (Corriente Resources Inc. Annual Report, 2004).

The four concessions (Caya 21, Caya 22, Curigem 9, and Curigem 9.1) were voluntarily placed under force majeure in 2006 by Lowell. Except for surface sampling in 2005-06, Lowell carried out no significant exploration on the Warintza Property after its acquisition in 2004. Instead, Lowell's efforts were directed toward obtaining a social license for exploration and mining from the local Shuar communities.

In July 2013, Lowell Copper Inc. completed a reverse takeover of Waterloo Resources Ltd. to form Lowell Copper Ltd. ("Lowell Copper").

In October 2016, Lowell Copper merged with Gold Mountain Mining Corporation and Anthem United Inc. to create a new company, JDL Gold Corp. ("JDL").

In March 2017, JDL merged with Luna Gold Corp. to form Trek Mining Inc. ("Trek"). In December 2017, Trek merged with NewCastle Gold Ltd. and Anfield Gold Corp. to form Equinox Gold Corp. In August 2018, Equinox spun out its copper assets, including the Warintza Property, into Solaris.

6.2 Exploration by Previous Owners

As described above, Warintza was a target that was generated from grassroots exploration in the Cordillera del Cóndor initiated by Gencor in 1994. Records of this early work at Warintza are unavailable, but according to Gendall et al. (2000), the first-pass exploration technique was panned concentrate stream sediment sampling. Anomalous drainages were followed up with prospecting and mapping in creeks and soil sampling of ridges in easily accessible areas. Collectively, these data sets led to the identification of four porphyry targets: Warintza Central, Warintza East, Warintza West, and Warintza South.

Once Billiton awarded the continuation of the exploration of the Warintza Project to Corriente, they proceeded to scout drill test the Warintza Central target, and, based on early success, ultimately drilled 33 core holes (6,530 m) in two campaigns: February-April 2000 (16 holes; 2,391 m) and July-August 2001 (17 holes; 4,140 m). Drilling confirmed Warintza Central as a supergene-enriched Cu-Mo porphyry deposit. At the same time, mapping and litho-geochemical sampling were carried out over Warintza West (Vaca and León, 2001).

6.2.1 Surface Geochemistry

Analytical data for the surface samples collected by previous operators (quantities summarized in Table 6) have been compiled into a database.

Table 6: Summary of Surface Samples from the Warintza Property
Source: Equity (2019)

Sample Type	Count
Soil	981
Rock channel	256
Rock chip	240
Rock panel	15

Results for Cu and Mo soil and rock samples are summarized in the figures below. Cu in soil and rock does not perfectly outline the Warintza Central deposit, but it does effectively highlight the general area of the porphyry centre (Figure 6). Mo in soil and rock geochemistry is somewhat more restricted, but the patterns are similar (Figure 7).

The soil sampling pattern in both figures demonstrates the progression from ridge soil sampling to the establishment of a more detailed grid over the deposit. Rock samples are largely restricted to stream drainages where outcrop exposures are more abundant. Overall, surface sampling is a highly effective tool to identify exposed porphyry deposits, such as Warintza. Note that not all soil/rock anomalies have been drill-tested, and sampling is largely limited to easily accessible areas.

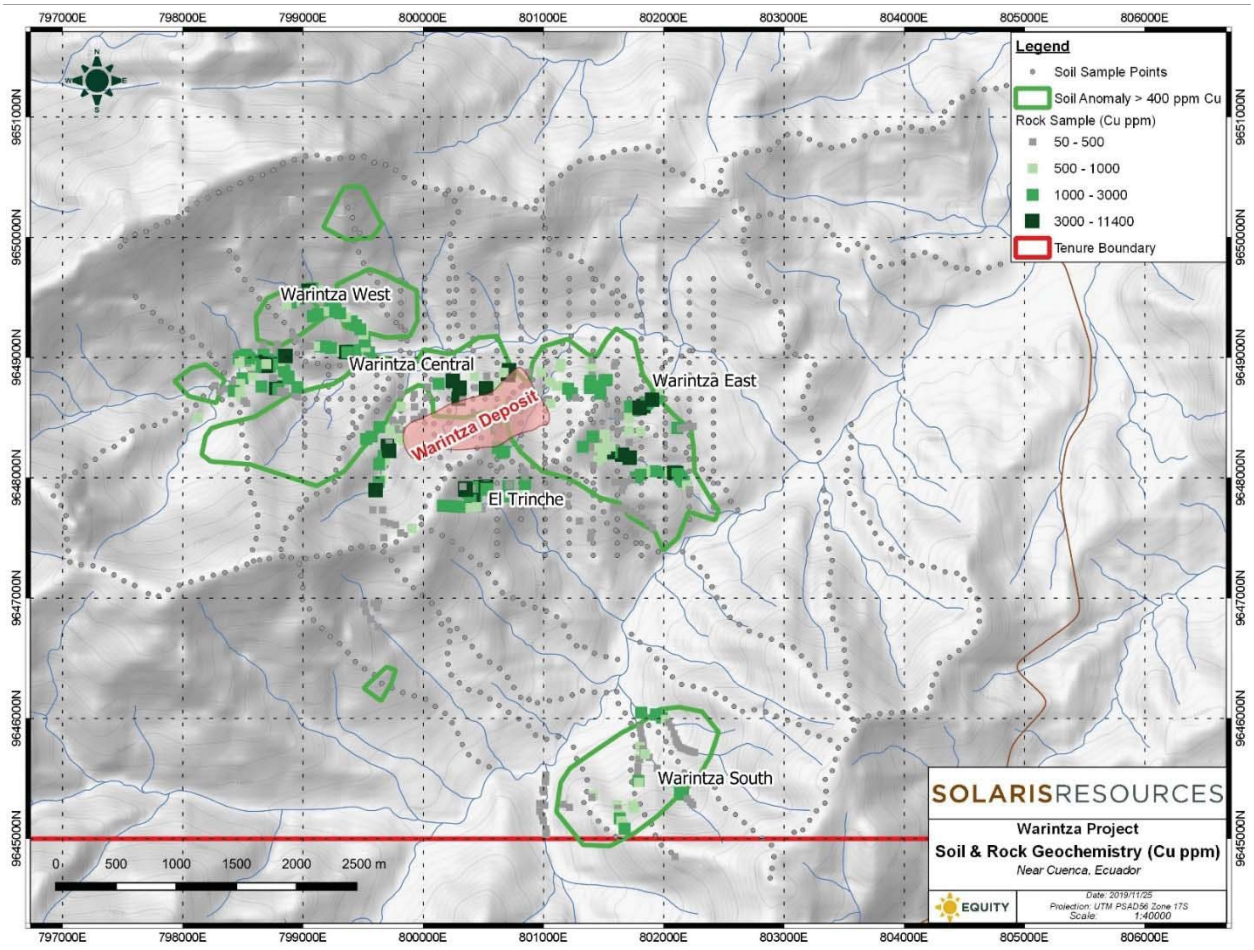

Figure 6: Property Soil and Rock Geochemistry Summarizing Cu Results
Source: Equity 2019

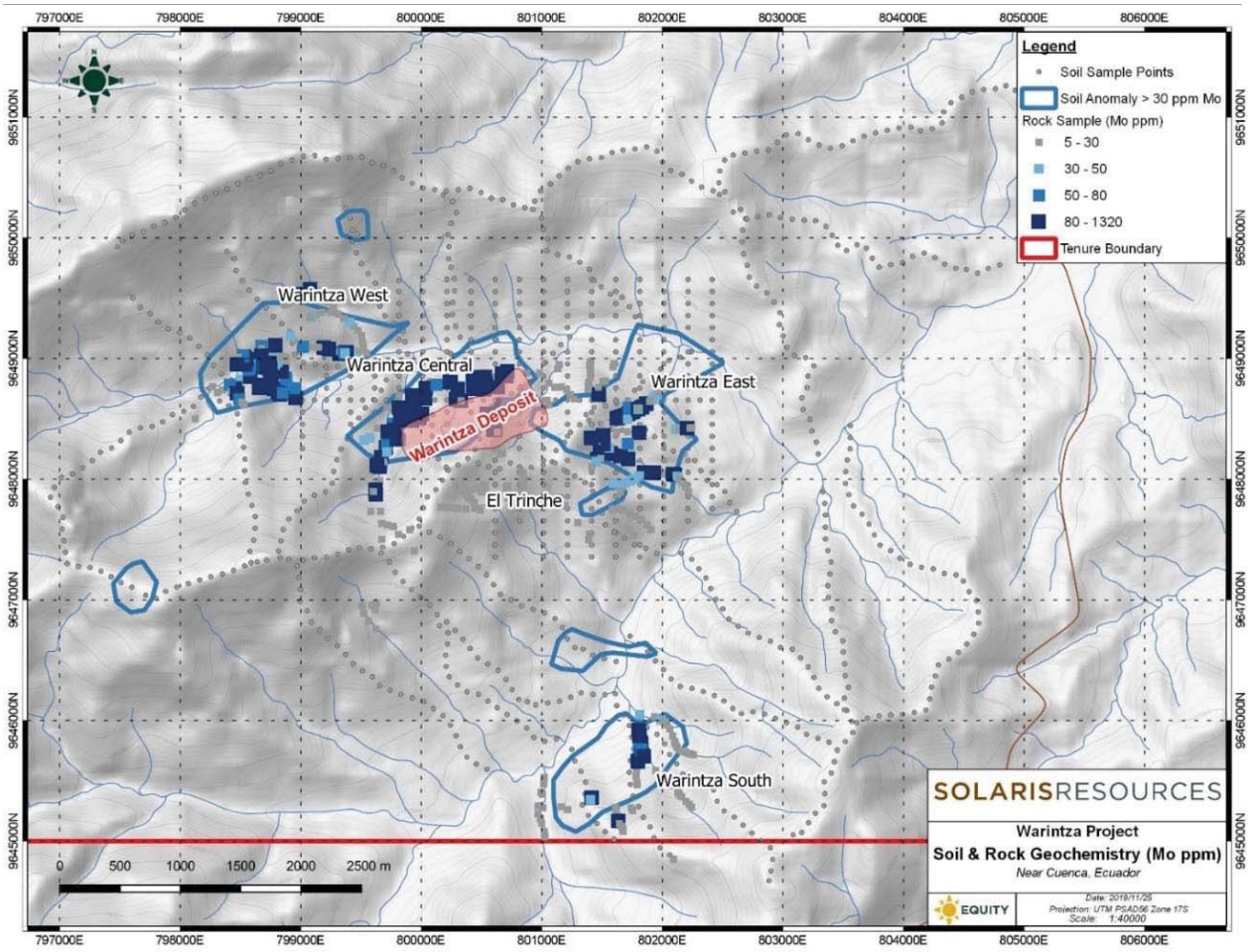

Figure 7: Property Soil and Rock Geochemistry Summarizing Mo Results
Source: Equity (2019)

6.2.2 Geophysics

Internal program summary reports indicate that an airborne magnetics-EM survey was flown in 1999. The data from this survey is not available.

6.3 Mineral Resource Estimates

Following the 2000-2001 Warintza drilling, three mineral resource estimates were prepared in 2001 and 2005 for the Warintza Central deposit (Vaca and León, 2001 and Suárez, 2005).

None of these early estimates were prepared in accordance with NI 43-101 and all of them were superseded by later estimates prepared in accordance with NI 43-101. As such, they are not considered significant and are not discussed further.

6.3.1 Mineral Resource Estimate (Ronning and Ristorcelli, 2006)

In 2006, Mine Development Associates prepared a mineral resource estimate on the Warintza Central deposit for Lowell Copper Holdings Inc. (formerly known as Lowell Copper Inc.) (Ronning and Ristorcelli, 2006). It is based on data from all 33 holes and 2,142 analyses of Cu, Mo, and Au. Au was not included in the resource estimate as the Au grades were deemed too low to be of value.

The resource estimate used a geologically constrained model, dividing the Cu mineralization into three zones: leached, supergene-enriched, and hypogene or primary. All the Mo mineralization was modelled as primary, and it spans all three of the Cu zones. Only the supergene-enriched and primary zones were included in the mineral resource estimation.

The Warintza Central mineral resource estimate used kriging for estimation. Trials using two other estimation techniques—one employing a nearest-neighbor algorithm and the other an inverse distance squared algorithm—were also completed. A comparison of the results led to the conclusion that at the current drill spacing, the kriged model would give the most appropriate estimate.

Cu assays were capped at 1.5% Cu (primary) and 2.7% Cu (supergene-enriched). Only the primary zone was materially impacted by capping (reducing the mean grade by 4%), with no material difference to the mean grade of the supergene-enriched zone.

Variograms were calculated using 10 m composites for each Cu zone and for Mo, then used to estimate grades for individual blocks.

The 2006 mineral resource estimate used a CuEq cut-off grade; CuEq was calculated using an in-situ value ratio of six Cu to one Mo. At a cut-off grade of 0.3% CuEq, the Warintza Central deposit was estimated to contain an Inferred mineral resource of 195,000,000 tonnes grading 0.61% CuEq, or 0.42% Cu, and 0.031% Mo. Table 7, Table 8, and Table 9 present Ronning and Ristorcelli's (2006) Inferred mineral resource estimate for the Warintza Central deposit.

Table 7: Warintza Central Deposit Inferred Mineral Resource Estimate – Primary Zone

Cutoff CuEq%	Tonnes	CuEq%	Cu%	Copper (tonnes)	Copper (lbs)	Mo%	Molybdenum (tonnes)	Molybdenum (lbs)
0.30	**141,000,000**	**0.56**	**0.37**	**528,000**	**1,164,000,000**	**0.031**	**44,000**	**97,000,000**
0.35	133,000,000	0.58	0.39	513,000	1,131,000,000	0.032	42,000	92,600,000
0.40	114,000,000	0.61	0.42	477,000	1,051,600,000	0.032	36,000	79,400,000
0.45	91,000,000	0.66	0.47	425,000	937,000,000	0.032	29,000	63,900,000
0.50	76,000,000	0.69	0.50	379,000	835,600,000	0.033	25,000	55,100,000
0.55	63,000,000	0.73	0.53	334,000	736,300,000	0.033	21,000	46,300,000
0.60	51,000,000	0.76	0.56	285,000	628,300,000	0.034	17,000	37,500,000
0.70	30,000,000	0.85	0.63	189,000	416,700,000	0.036	11,000	24,300,000
0.80	16,000,000	0.93	0.70	113,000	249,100,000	0.038	6,000	13,200,000
0.90	9,000,000	1.01	0.76	68,000	149,900,000	0.041	4,000	8,800,000
0.95	6,000,000	1.04	0.79	47,000	103,600,000	0.042	3,000	6,600,000

Source: Ronning and Ristorcelli (2006)

Table 8: Warintza Central Deposit Inferred Mineral Resource Estimate – Enriched Zone

Cutoff CuEq%	Tonnes	CuEq%	Cu%	Copper (tonnes)	Copper (lbs)	Mo%	Molybdenum (tonnes)	Molybdenum (lbs)
0.30	**54,000,000**	**0.72**	**0.54**	**292,000**	**643,700,000**	**0.029**	**16,000**	**35,300,000**
0.35	52,000,000	0.73	0.55	288,000	634,900,000	0.030	16,000	35,300,000
0.40	50,000,000	0.75	0.57	283,000	623,900,000	0.031	15,000	33,100,000
0.45	47,000,000	0.77	0.58	271,000	597,500,000	0.032	15,000	33,100,000
0.50	44,000,000	0.79	0.59	261,000	575,400,000	0.032	14,000	30,900,000
0.55	41,000,000	0.81	0.61	251,000	553,400,000	0.033	14,000	30,900,000
0.60	37,000,000	0.83	0.63	233,000	513,700,000	0.034	13,000	28,700,000
0.70	27,000,000	0.90	0.69	185,000	407,900,000	0.036	10,000	22,000,000
0.80	19,000,000	0.97	0.74	141,000	310,900,000	0.038	7,000	15,400,000
0.90	11,000,000	1.06	0.81	90,000	198,400,000	0.040	4,000	8,800,000
0.95	9,000,000	1.09	0.85	77,000	169,800,000	0.040	4,000	8,800,000

Source: Ronning and Ristorcelli (2006)

Table 9: Warintza Central Deposit Inferred Mineral Resource Estimate – Total

Cutoff CuEq%	Tonnes	CuEq%	Cu%	Copper (tonnes)	Copper (lbs)	Mo%	Molybdenum (tonnes)	Molybdenum (lbs)
0.30	**195,000,000**	**0.61**	**0.42**	**820,000**	**1,807,800,000**	**0.031**	**60,000**	**132,300,000**
0.35	185,000,000	0.62	0.43	801,000	1,765,900,000	0.031	58,000	127,900,000
0.40	164,000,000	0.65	0.46	759,000	1,673,300,000	0.031	51,000	112,400,000
0.45	138,000,000	0.69	0.50	696,000	1,534,400,000	0.032	44,000	97,000,000
0.50	120,000,000	0.73	0.53	641,000	1,413,200,000	0.032	39,000	86,000,000
0.55	104,000,000	0.76	0.56	584,000	1,287,500,000	0.033	34,000	75,000,000
0.60	88,000,000	0.79	0.59	519,000	1,144,200,000	0.034	30,000	66,100,000
0.70	57,000,000	0.87	0.66	374,000	824,500,000	0.036	21,000	46,300,000
0.80	35,000,000	0.96	0.73	254,000	560,000,000	0.038	13,000	28,700,000
0.90	20,000,000	1.03	0.79	158,000	348,300,000	0.041	8,000	17,600,000
0.95	15,000,000	1.07	0.83	124,000	273,400,000	0.041	6,000	13,200,000

Source: Ronning and Ristorcelli (2006)

Mine Development Associates' 2006 mineral resource estimate was prepared in accordance with NI 43-101 and uses resource categories stipulated by NI 43-101. The Company is not treating the 2006 historical estimate as a current mineral resource because it is superseded by the MRE presented herein (Section 14).

6.3.2 Mineral Resource Estimate (Ronning and Ristorcelli, 2018)

In 2018, Mine Development Associates updated their previous mineral resource estimate on the Warintza Central deposit for Equinox and Solaris (Ronning and Ristorcelli, 2018). It was based on the same database and geological model as used in the 2006 estimate and used the same estimation parameters. The 2018 mineral resource estimate was identical to the 2006 estimate, except for rounding differences and the inclusion of estimates above different cut-off grades (Table 10, Table 11, and Table 12).

Table 10: Warintza Central Deposit Inferred Mineral Resource Estimate – Primary Zone

Cutoff CuEq%	Tonnes	CuEq%	Cu%	Copper (tonnes)	Copper (lbsX1000)	Mo%	Molybdenum (tonnes)	Molybdenum (lbsX1000)
0.25	149,170,000	0.55	0.36	542,000	1,194,905,000	0.031	46,000	101,413,000
0.30	**140,532,000**	**0.56**	**0.37**	**526,000**	**1,159,631,000**	**0.031**	**44,000**	**97,003,000**
0.35	133,454,000	0.58	0.39	515,000	1,135,381,000	0.032	42,000	92,594,000
0.40	114,476,000	0.61	0.42	479,000	1,056,014,000	0.032	36,000	79,366,000
0.45	90,576,000	0.66	0.47	423,000	932,555,000	0.032	29,000	63,934,000
0.50	75,616,000	0.69	0.50	377,000	831,143,000	0.033	25,000	55,116,000
0.55	62,936,000	0.73	0.53	333,000	734,139,000	0.033	21,000	46,297,000
0.60	50,756,000	0.76	0.56	284,000	626,113,000	0.034	17,000	38,223,747
0.70	30,058,000	0.85	0.63	189,000	416,674,000	0.036	11,000	24,251,000

Source: Ronning and Ristorcelli (2018)

Table 11: Warintza Central Deposit Inferred Mineral Resource Estimate – Enriched Zone

Cutoff CuEq%	Tonnes	CuEq%	Cu%	Copper (tonnes)	Copper (lbs)	Mo%	Molybdenum (tonnes)	Molybdenum (lbs)
0.25	57,465,000	0.69	0.52	301,000	663,591,000	0.028	16,000	35,274,000
0.30	**54,462,000**	**0.72**	**0.54**	**294,000**	**648,159,000**	**0.029**	**16,000**	**35,274,000**
0.35	51,901,000	0.73	0.55	287,000	632,727,000	0.030	16,000	35,274,000
0.40	49,626,000	0.75	0.57	281,000	619,499,000	0.031	15,000	33,069,000
0.45	47,410,000	0.77	0.58	274,000	604,067,000	0.032	15,000	33,069,000
0.50	44,236,000	0.79	0.59	263,000	579,816,000	0.032	14,000	30,865,000
0.55	40,705,000	0.81	0.61	249,000	548,951,000	0.033	13,000	28,660,000
0.60	36,823,000	0.83	0.63	232,000	511,472,000	0.034	12,000	27,545,000
0.70	26,809,000	0.90	0.69	184,000	405,651,000	0.036	10,000	22,046,000

Source: Ronning and Ristorcelli (2018)

Table 12: Warintza Central Deposit Inferred Mineral Resource Estimate – Total

Cutoff CuEq%	Tonnes	CuEq%	Cu%	Copper (tonnes)	Copper (lbs)	Mo%	Molybdenum (tonnes)	Molybdenum (lbs)
0.25	206,635,000	0.59	0.41	843,000	1,858,497,000	0.030	62,000	136,687,000
0.30	**194,994,000**	**0.61**	**0.42**	**820,000**	**1,807,791,000**	**0.031**	**60,000**	**132,277,000**
0.35	185,356,000	0.62	0.43	802,000	1,768,107,000	0.031	58,000	127,868,000
0.40	164,102,000	0.65	0.46	760,000	1,675,513,000	0.031	51,000	112,436,000
0.45	137,986,000	0.69	0.50	696,000	1,534,417,000	0.032	44,000	97,003,000
0.50	119,852,000	0.73	0.53	640,000	1,410,958,000	0.032	39,000	85,980,000
0.55	103,641,000	0.76	0.56	582,000	1,283,090,000	0.033	34,000	74,957,000
0.60	87,580,000	0.79	0.59	516,000	1,137,585,000	0.034	30,000	65,784,000
0.70	56,867,000	0.87	0.66	373,000	822,324,000	0.036	21,000	46,297,000

Source: Ronning and Ristorcelli (2018)

Mine Development Associates' 2018 mineral resource estimate was prepared in accordance with NI 43-101 and classifies resources in accordance with CIM Definition Standards for Mineral Resources and Mineral Reserves (May 2014). The Company is not treating the 2018 historical estimate as a current mineral resource because it is superseded by the MRE presented herein (Section 14).

6.4 Historical Production

No ore production has been reported for the Warintza Property. There is no record of formal historical mining activity for the other target areas.

7.0 GEOLOGICAL SETTING AND MINERALIZATION

7.1 Regional Geology

This section summarizes the regional geologic setting and the salient geologic characteristics of the porphyry Cu-Mo-Au mineralization of the Warintza cluster located in the Cordillera del Cóndor range in the Andes of southeastern Ecuador. The herein defined Warintza cluster comprises of a series of discrete and partially coalescent porphyry Cu-Mo±Au deposits and prospects at Warintza Central, Warintza East, Warintza West, and Warintza South, of which the Warintza Central deposit currently is at the most advanced exploration stage. This section is based on a series of first-hand reviews of Warintza core by the Author during the second half of 2021. This section first describes the geologic setting of the Zamora belt to be followed by sections on the geology, alteration, and mineralization of the various target areas that compose the Warintza cluster, as per on-going exploration.

7.1.1 Subandean and Cordillera del Cóndor Geology

The Cordillera del Cóndor and Warintza cluster are located in the Subandean zone, a geologic domain underlining the eastern foothills of the Andes (Figure 8). On the west, the Cordillera del Cóndor is flanked by the Paleozoic and Mesozoic metamorphic belts and accreted terranes of the Cordillera Real (Aspden and Litherland, 1992; Litherland et al., 1994).

The Subandean zone was the site of rifting during the Permo-Triassic, where red-beds and alkaline volcanic rocks accumulated (e.g., Mitu Group in Peru) and were followed by deposition of carbonate sequences in the Late Triassic to Early Jurassic, as exemplified by the Pucará Group in central and northern Peru and the stratigraphically equivalent Santiago Formation in southeastern Ecuador (Tschopp, 1953). In the Jurassic, an andesite-dominated, calc-alkaline magmatic arc developed from Colombia, through Ecuador and into northern Peru, and gave rise to the Misahuallí Formation in Ecuador (Litherland et al., 1994) and equivalent formations in northern Peru, along with a series of batholithic-sized intrusions.

The volcanic-dominated sequences of the arc are considered partially equivalent to the Chapiza Formation, a continental red-bed package deposited farther east (Jaillard, 1997). Rocks of the Jurassic arc and the Chapiza Formation are unconformably overlain by a sequence of shallowly dipping, fluvial quartz sandstone of the Early Cretaceous Hollín Formation, which, in turn, is unconformably overlain by shale and limestone of the Napo Formation (Tschopp, 1953).

The Hollín and Napo Formations extend eastward beneath Cenozoic sedimentary strata of the Santiago basin, where they form part of the large hydrocarbon-bearing Oriente basin (Jaillard, 1997).

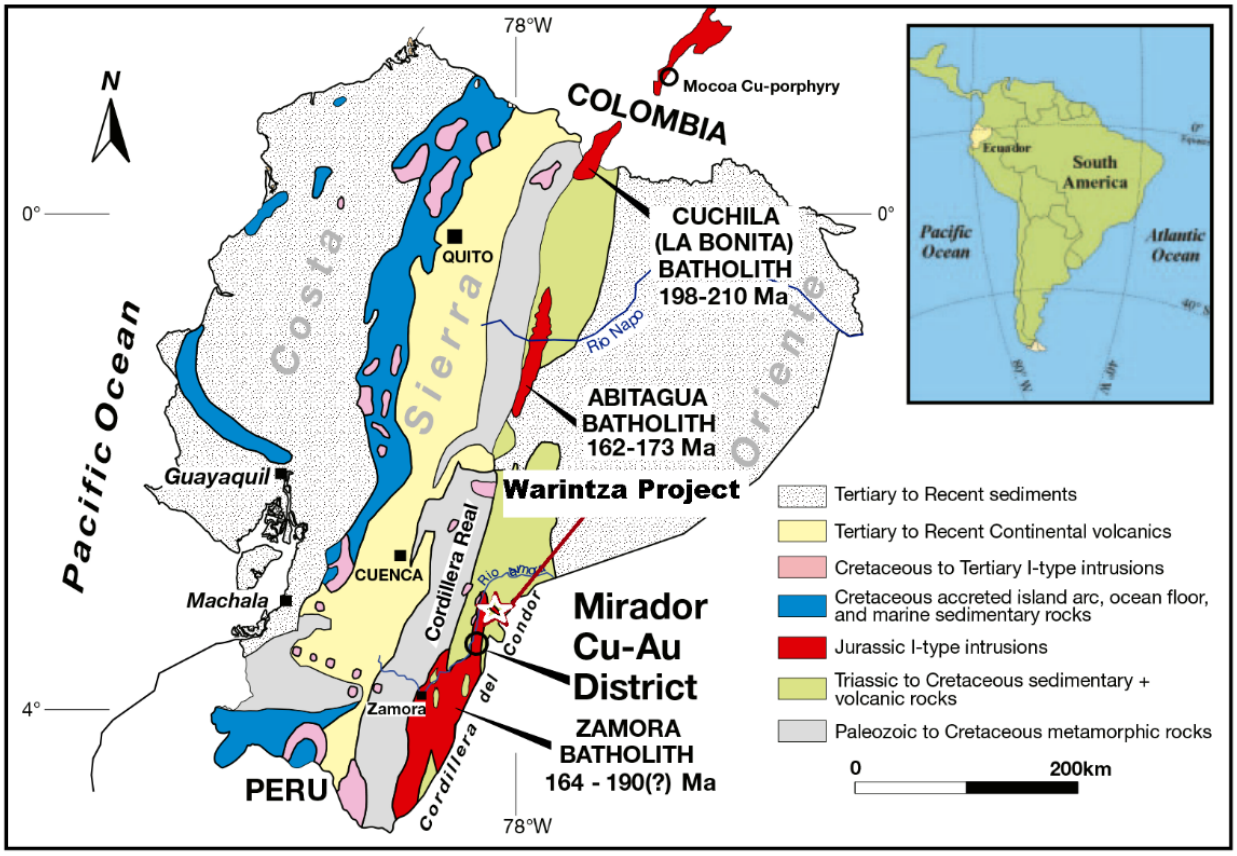

Figure 8: Location of the Warintza Cluster Within Zamora Batholith
Source: Modified from Drobe et al. (2013)

The main expressions of the Jurassic arc magmatism along the Cordillera del Cóndor are the subduction-related, I-type, predominantly dioritic to granodioritic plutons of the >200 km-long, north-northeast-trending Zamora batholith (Litherland et al., 1994; Drobe et al., 2013; Leary et al., 2016). Early isotopic dating by the K-Ar and Rb-Sr method yielded ages of ~190 to 170 Ma for main-stage batholith emplacement (Litherland et al., 1994), but more modern dates by the Ar-Ar (hornblende) and U-Pb (zircon) methods have returned younger, Middle-Late Jurassic ages (~164-160 Ma; Chiaradia et al., 2009; Drobe et al., 2013).

Extensive roof pendants of shallowly dipping and metamorphosed, locally skarnified, volcano-sedimentary rocks within the Zamora batholith were included in the Late Triassic Piuntza unit of the Santiago Formation, while similar sequences adjacent to the batholith were assigned to the Misahuallí unit of the Chapiza Formation (Litherland et al., 1992, 1994). This stratigraphic convention is followed in this report. Volcanic rocks of the Misahuallí sequence yield Ar–Ar ages between ~172 and 162 Ma (Middle Jurassic; Romeuf et al., 1995, Spikings et al., 2001). However, more recently, rocks assigned to Misahuallí andesitic volcanism at Fruta del Norte were dated at ~157 to 154 Ma (Leary et al., 2016).

In conjunction, the Zamora batholith and Misahuallí volcanic rocks are considered to represent the terminal events of a long-lived, subduction-related continental magmatic arc established on the western margin of the Amazon craton, with the Zamora batholith representing the plutonic roots and the Misahuallí rocks being the extrusive expressions, of the arc.

7.1.2 Regional Metallogeny

The principal ore deposits and prospects in the Subandean zone of southeastern Ecuador are hosted by the Zamora batholith and its associated volcano-sedimentary rocks and form part of a Jurassic metallogenic belt that extends from southern Colombia to northern Peru (Sillitoe and Perelló, 2005). With the exception of Fruta de Norte (Leary et al., 2016), most deposits and prospects are of porphyry Cu or skarn Au-Cu type (Gendall et al., 2000; Fontboté et al., 2004; Chiaradia et al., 2009; Drobe et al., 2013).

The Warintza cluster is part of the north-trending, 120 km-long, Late Jurassic Zamora Cu-Au belt (Drobe et al., 2013, Figure 9). The porphyry Cu and skarn mineralization in the region was originally named the Pangui belt by Gendall et al., (2000) and included deposits along the Río Zamora from San Carlos- Panantza deposits on the north to Mirador on the south, with Warintza as an eastern outlier. More recently, the belt has been expanded to comprise the Au skarn mineralization at Nambija and the epithermal Au deposit at Fruta del Norte (Drobe et al., 2013; Leary et al., 2016).

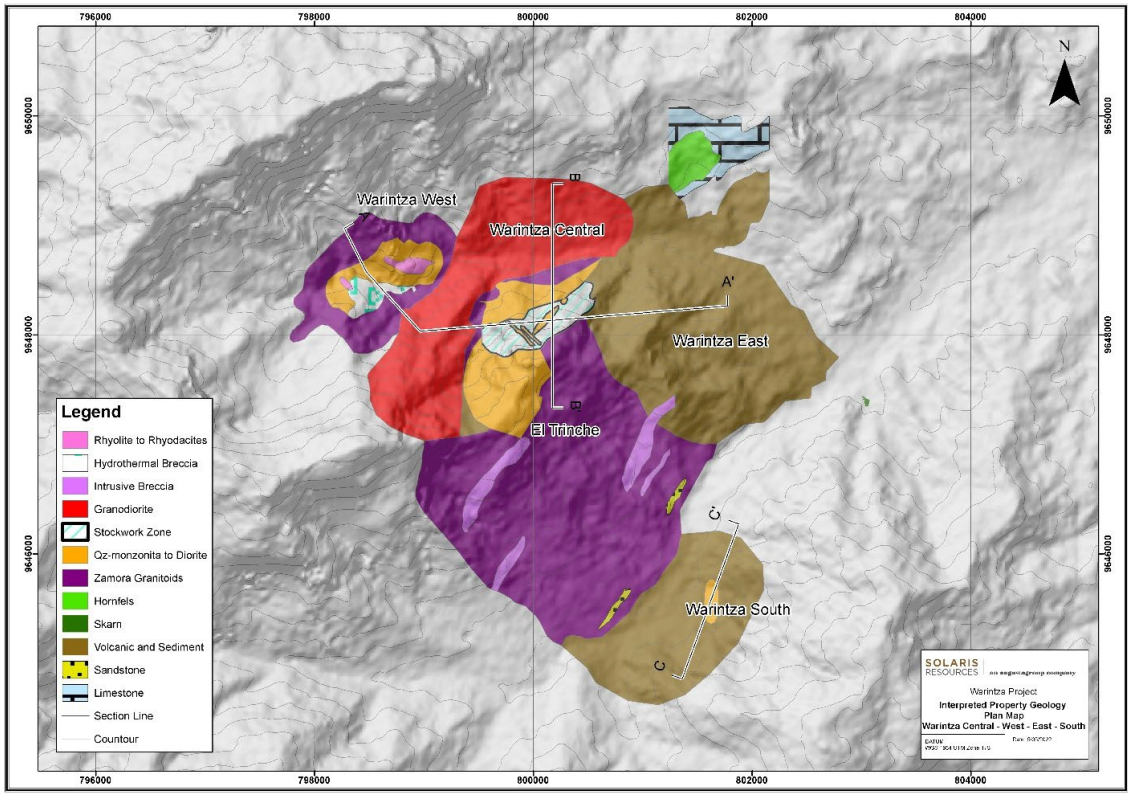

Figure 9: Simplified Geologic Map of Warintza Cluster
Source: Solaris Resources Inc. (2022)

The northern deposits within the belt are Cu-Mo, whereas the southern deposits are Cu-Au, the latter exemplified by Mirador. Most deposits are genetically associated with the late-stage, plagioclase- and hornblende-bearing, andesitic to dacitic porphyry phases of the Zamora batholith, in part coeval with the calc-alkaline andesitic volcanism of the Misahuallí unit. Late Jurassic U-Pb (zircon) and Re-Os (molybdenite) ages from 157 to 153 Ma for the porphyry Cu-bearing subvolcanic intrusions and mineralization (Chiaradia et al., 2009; Drobe et al., 2013) confirm the comagmatic relationship between these late-stage phases of the batholith and porphyry Cu formation.

7.2 Geologic Features of the Warintza Cluster

The Warintza cluster (Figure 10) comprises of a series of discrete and partially coalescent porphyry Cu-Mo±Au deposits and prospects at Warintza Central, Warintza East, Warintza West, and Warintza South, of which the Warintza Central deposit currently is at the most advanced exploration stage. A number of Cu-Mo soil geochemical anomalies likely represent additional porphyry-style mineralization, thereby covering an area of approximately 30 km². A broadly east-west-trending, approximate seven km-long, likely structurally controlled corridor of porphyry Cu centers is defined by the alignment of Warintza West, Warintza Central, and Warintza East, whereas Warintza South is located approximately three km to the south. All deposits and prospects display geologic features of the Cu-Mo clan, although Au is erratically present in some. For simplicity, in the following sections of this report, the term “porphyry Cu” implies a general Cu-Mo-(Au) association of principal metals.

Geologically, the Warintza cluster is associated with a series of plutonic and porphyritic intrusions of intermediate composition, from quartz-monzonite, through granodiorite to diorite, emplaced as outliers of the Zamora batholith in proximity to its eastern contact with Misahualli volcanic and volcano-sedimentary rocks. Porphyry Cu-related contain variable proportions of plagioclase, biotite, and hornblende as principal phenocryst components.

With the exception of Warintza East, quartz is a minor phenocryst phase in most productive intrusions, although some is present in certain late mineral phases at Warintza West. Porphyry Cu-bearing dikes and stocks at Warintza Central were principally emplaced in precursor plutonic stocks, whereas Warintza South and Warintza East intruded Misahuallí volcanic and volcano-sedimentary rocks.

Warintza West is hosted by a magmatic-hydrothermal stockwork zone formed at the expense of a quartz-monzodioritic intrusion emplaced into a composite, dioritic to granodioritic pluton. Although no isotopic ages are available for Warintza, the geologic relationships suggest that the porphyry Cu mineralization of the cluster is part of the Zamora (Pangui) belt, a correlation also established in the literature (Gendall et al., 2000; Drobe et al., 2013; Leary et al., 2016).

The geologic structure of the Warintza cluster is poorly defined to date. The marked east-west alignment of porphyry Cu centers from Warintza West, through Warintza Central, to Warintza East implies an important, structural control on porphyry Cu emplacement.

The internal east-west-trending lithologic, alteration, and mineralization grains at Warintza Central and Warintza East also evidence significant structural control during porphyry Cu evolution. Regional, likely fault-related, topographic lineaments controlling the distribution of major rivers and tributaries are apparent on satellite images available for the region, including the Piuntz river that runs along the

northern border of Warintza Central. However, detailed structural mapping, in progress, is hampered by the large vegetation cover and the deeply weathered state of the rocks at the surface.

In any case, since their emplacement in the Late Jurassic, rocks of the Warintza cluster and associated porphyry Cu mineralization are inferred to have been involved in the far-field deformation associated with the accretion of oceanic terranes to the Ecuadorian forearc from the Late Cretaceous to the Paleocene (Vallejo et al., 2006), producing the rapid uplift, unroofing, and exhumation of the Cordillera Real at ~75-60 Ma (Spikings et al., 2001), with corresponding structural implications.

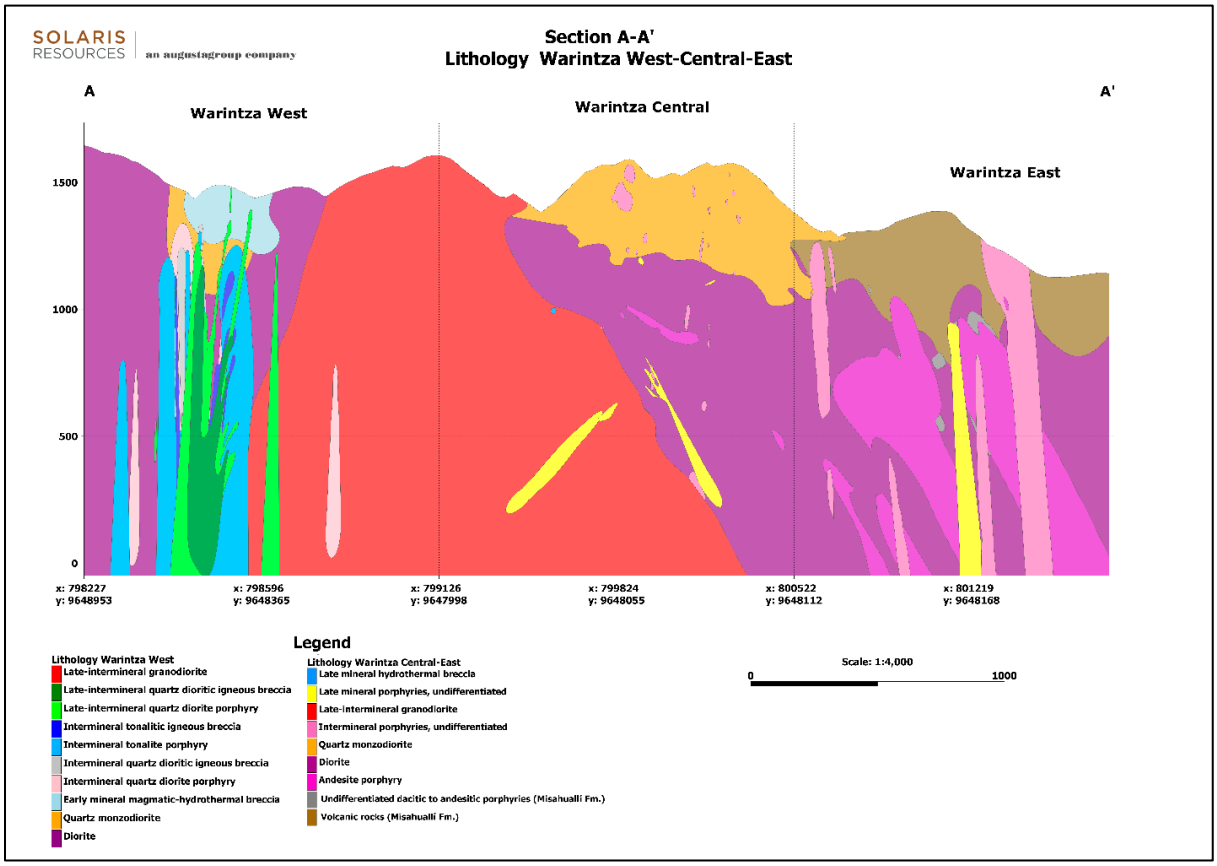

Figure 10: Simplified Geologic Cross Section of Warintza Cluster
Source: Solaris Resources Inc. (2022)

7.3 Warintza Central

Main lithologic units

The east-trending Warintza Central porphyry Cu deposit is hosted by composite stocks that form two principal pre-mineralization units, namely upper quartz-monzodiorite and lower diorite bodies (Figure 11).

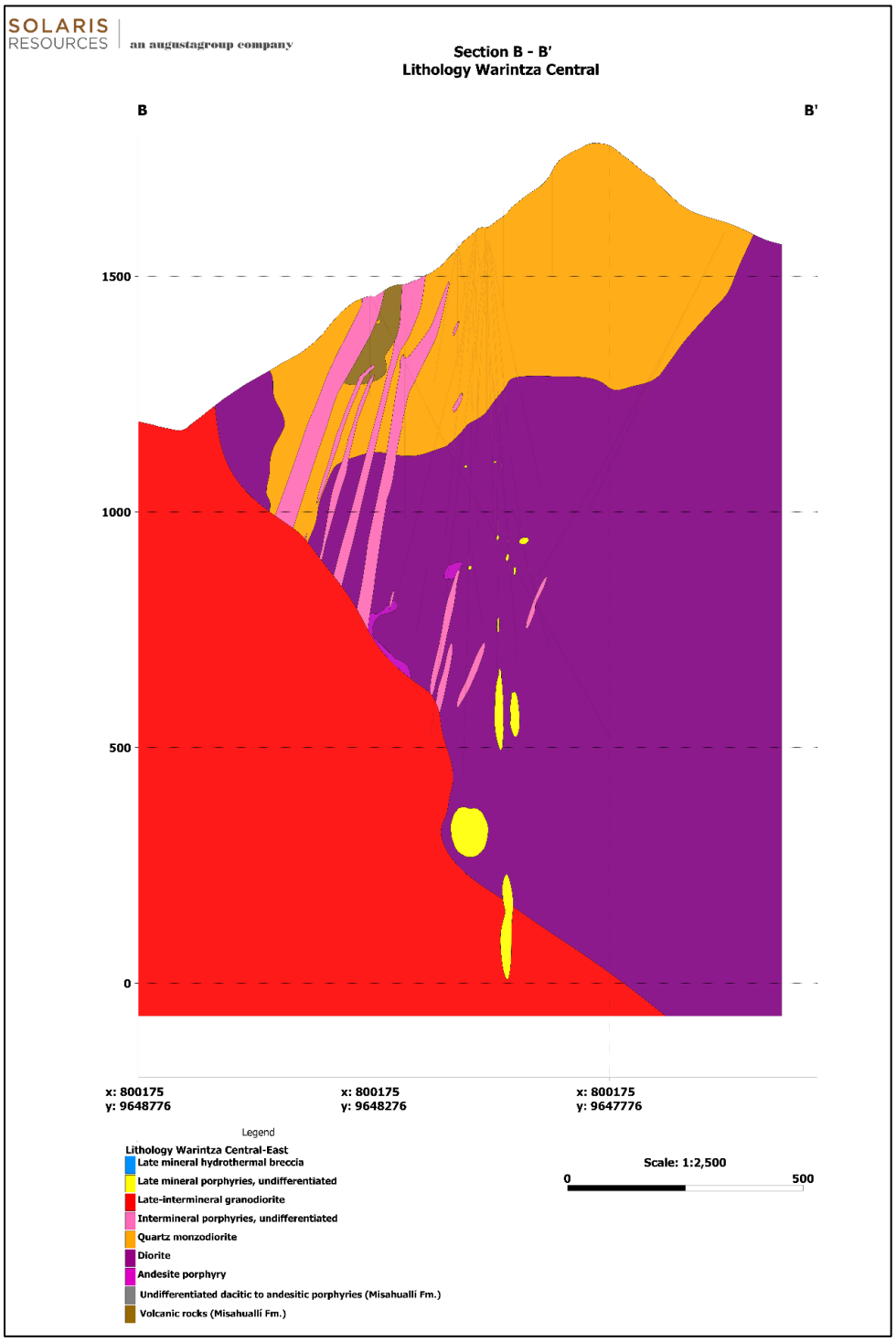

Figure 11: Simplified Geologic Cross Section Through Warintza Central
Source: Solaris Resources Inc. (2022)

Both were emplaced into volcanic and volcano-sedimentary assemblages of the Misahuallí sequence. The upper quartz-monzodiorite body is typically fine-grained, equigranular in texture, although hydrothermal alteration has amply modified original rock-forming constituents. In the case of the lower dioritic body, drilling has shown its original hornblende- and biotite-bearing composition at depth. Contacts between the two units have not been observed due to the intense hypogene alteration and supergene effects, the latter including a rubble zone at the transition from sulfate-leached (gypsum) to sulfate-stable (anhydrite) environments. Geological relationships suggest that both the lower diorite body and the upper quartz-monzodiorite bodies likely represent composite precursor intrusions with respect to the porphyry Cu mineralization. An intrusion of this size was almost certainly constructed by multiple magma pulses injected in relatively quick succession, such that early phases may have been still plastic when the successively younger phases were emplaced, with the consequent masking of internal contacts.

To the east, the Warintza Central stocks are in contact with rocks assigned to the Misahuallí sequence, a predominantly andesitic unit with locally thin interbeds of calcareous and siliceous sedimentary strata, as well as volcaniclastic and coarse-grained fragmental materials. Coarse-grained andesite porphyry dominates with depth and likely represents classic subvolcanic Misahuallí rocks. A few poorly constrained marker beds could be taken to imply a relatively shallowly dipping attitude of the whole sequence, in agreement with descriptions of Misahuallí rocks elsewhere in the area and regionally (Litherland et al., 1994).

Numerous dike-like porphyry-bodies are present at Warintza Central and eastern extensions. These are typically characterized by coarse-grained textures with predominance of plagioclase and hornblende phenocrysts, plus additional proportions of quartz eyes, all set in a fine-grained to aphanitic groundmass of similar compositions. Andesitic and dacitic compositions predominate. The porphyry dikes are of varied dimensions, including thin, meter-wide intercepts in drill holes that locally coalesce to form larger bodies. Two principal phases are present: 1) early, intermineral phases are andesitic to daciandesitic in composition, are variably altered, and are cut by pyrite- and/or chalcopyrite-bearing porphyry-style veinlets of EDM, A, B, C, and D types (see below); 2) late mineral phases are typically dacitic and characterized by well-defined quartz eyes, aphanitic groundmass, and by a fresher appearance in which weak illitic mica predominates. Veinlets are typically absent in these later phases, although pyritic D and later polymetallic varieties occur locally.

Drilling has confirmed that much of the Warintza Central deposit is floored by a large, coarse-grained, porphyritic to sub-equigranular, magnetite-stable, plagioclase-, biotite-, and hornblende-bearing stock of granodioritic composition. This body typically cuts and truncates mineralization and veinlets hosted by all rocks described above. However, veinlets with epidote, pyrite, biotite, and trace chalcopyrite are locally present, hence its late-mineralization timing.

Hydrothermal breccias are rare at Warintza Central, and only a few late-mineralization phreatomagmatic pebble dikes associated with late-stage porphyry dikes have been identified. Nevertheless, poorly developed composite bodies of aplite, irregular, and abnormally thick quartz veinlets and wavy quartz segregations, coarse-grained pegmatoidal pods of anhydrite—plus gray-green micaceous aggregates and patches of anhydrite with or without chalcopyrite and pyrite—are all common. Because these zones are typically entirely contained in diorite, they are tentatively interpreted to be the product of local magmatic-hydrothermal fluid ponding and concentration during stock evolution.

Alteration and Mineralization

With the exception of the late-mineralization dikes and the basal granodiorite, all other rocks at Warintza Central underwent various assemblages of sequential potassic and green-gray mica (mixed chlorite and fine-grained muscovite) alteration during Cu-Mo-Au introduction, before being overprinted by predominantly pyritic fine-grained white mica (sericite) and irregularly distributed base-metal veinlets. Supergene sulfide leaching and enrichment affected the shallow parts of the deposit.

The following tentative sequence of alteration-mineralization and accompanying veinlet events (e.g., Sillitoe, 2010) are apparent:

1) Early, pre-mineralization biotitization of all ferromagnesian components in diorite porphyry at depth (and likely of upper quartz-monzodiorite body at higher elevations), accompanied by incipient formation of early biotite ("EB") and biotite-bearing halo type-veinlets of early dark micaceous ("EDM") affiliation. This Cu poor event introduced trace chalcopyrite in addition to pyrite.

2) Intermediate, pervasive, bulk halo-type alteration characterized by the coalescence of EDM veinlets in two principal assemblages controlled by original rock composition: i) gray-green mica assemblages predominantly in the diorite stock and ii) gray mica, andalusite, and K-feldspar assemblages in the upper, quartz-monzodiorite body. This event was rich in Cu and introduced the bulk of the disseminated chalcopyrite. Pyrite is also present, and both chalcopyrite and pyrite (and corresponding cpy:py ratios) are zonally distributed, displaying vertical and lateral zonation and defining specific sulfide domains, in which pyrite always formed first and was followed by deposition of chalcopyrite.

3) Intermineral introduction of classic A and B quartz-veinlets carrying lower amounts of Cu in the form of chalcopyrite, although Mo as molybdenite was the principal metal component of B veinlets. Pyrite is always conspicuously present and were both, chalcopyrite and pyrite occur together; chalcopyrite formed always second to pyrite. Both A and B veinlets cut earlier-formed EDM veinlets and associated halos.

4) Late-intermineral, predominantly veinlet-controlled green-gray mica assemblages with chalcopyrite and pyrite. These veinlets are important contributors to the Cu metal endowment of Warintza Central, being characterized by sulfide-bearing centerlines with additional quartz, medium- to fine-grained gray mica and chlorite, and variably developed halos of similar components. Chalcopyrite is characteristically present along the centerline of the veinlets, defining millimetric hairline fractures and sub centimeter-wide veinlets. In places, these veinlets can be continuous or semi-continuous for up to several meters of core-length. These veinlets are similar to the C-type veinlets of Gustafson and Quiroga (1995). C-type veinlets are normally seen overprinting EDM halos and crosscutting A and B veinlets. At the edges and deeper parts of Warintza Central, magnetite-bearing, pyrite veinlets with one or more of epidote, chlorite, and albite cut through A and B quartz veinlets, suggesting their C-equivalent timing of emplacement.

5) Late, pyrite-dominated D veins and veinlets with associated fine-grained white mica (sericite) alteration halos. This event was Cu destructive and transformed some or all the pre-existing

chalcopyrite into pyrite, as defined by the observed paragenetic relationships between these two minerals.

6) Terminal-stage, characterized by erratic hairline fractures and thin veinlets of quartz and carbonate with polymetallic base-metal mineralization and associated fine-grained white mica (sericite) alteration halos.

Notably, the majority of the quartz-bearing A and B veinlets occur in the shallower parts of the system and assist in definition of an east-trending and steep zone of moderate-intensity quartz stockworks, predominantly in the quartz-monzodiorite body. Anhydrite is present in most veinlet types, and hydrothermal magnetite accompanies the C-veinlets in deeper parts at Warintza Central and extensions to the east. In such cases, magnetite is paragenetically late with respect to chalcopyrite and pyrite. Deep seated biotite-stable EDM veinlets in diorite also contain various proportions of magnetite.

Hypogene Sulfide Zoning

A well-defined geometry is present at Warintza Central, in which upper and shallower parts of the deposit are invariably dominated by pyrite over chalcopyrite. This is apparent in all intermineral alteration-mineralization events, including early EDM halos as well as A-, B-, and C- veinlets. Middle and central (interior) parts of Warintza Central are richer in chalcopyrite and typically contain cpy>py to cpy=py ratios in all Cu-producing events. Rocks, particularly diorite, are totally replaced by texturally destructive halo-type alteration with abundant disseminated chalcopyrite. C veinlets, which assist to increase bulk Cu contents, are also dominated by chalcopyrite. A and B veinlets also contain chalcopyrite, albeit in minor proportions.

In all cases, chalcopyrite followed pyrite in paragenetic sequence. Deeper parts of the system are characterized by lower sulfide contents in all Cu productive alteration-mineralization phases. Chalcopyrite and pyrite continue to be present, but the proportion of the total volume of sulfides is radically lower, and the Cu tenor decreases gradually with depth. A and B veinlets are erratic and scarce and, where present, are essentially free of sulfides or carry very limited amounts.

Laterally, the same features are observed, with Cu grades decreasing gradually due to the dominance of pyrite over chalcopyrite and the lower total sulfide contents in all assemblages. To the south, drilling at the El Trinche has shown this target area to be part of the pyritic halo of Warintza Central, with EDM, A, B, C, and D veinlets all carrying predominantly pyrite, albeit locally accompanied by minor proportions of chalcopyrite.

Supergene Effects

The upper parts of Warintza Central developed a first cycle, immature supergene chalcocite blanket beneath an irregular leached capping zone. The latter can be as thin as a couple of meters but, where better developed, is followed at depth by a formal and thicker chalcocite blanket. Importantly, the metal values of the leached capping are identical to the Cu and Mo values of the soil geochemistry, indicating that much of the soil anomaly over Warintza Central is in-situ and a reflection of the mineralization at depth.

Rocks affected by meteoric waters are typically porous, with open fractures and veinlets of all types characterized by abundant cavities due to the sequential hydration of the original anhydrite, its transformation to gypsum, and eventual washing out.

Extensions to the East

The eastern extensions, as explored by numerous holes, share the same geologic and mineralization elements of Warintza Central with the bulk of the Cu as chalcopyrite contained in associations dominated by east-trending swarms of C-type veinlets. Garnet-bearing prograde skarn and the epidote-chlorite-magnetite-pyrite-chalcopyrite retrograde skarn assemblages formed at the expense of certain volcano-sedimentary horizons in the Misahuallí sequence and confirm their relatively proximal position within the thermal aureole of Warintza Central.

7.4 Warintza East

On the basis of its geology and alteration-mineralization features, Warintza East is interpreted as a separate center along the Warintza trend (Figure 10). Here, the causative porphyry phases are of predominantly felsic composition and characterized by discrete, coarse-grained, quartz–eye-rich, rhyodacitic bodies intruding fine-grained to slightly porphyritic andesitic rocks of the Misahuallí sequence and assemblages the Andesitic Center (Andesite Porphyry Center of the resource model), to be described below. The rhyodacitic bodies display moderate to intense Mo-bearing quartz-stockworks of predominantly B-type veinlets. Cu values are notably lower in the rhyodacite than in the adjacent andesitic country rocks, the latter containing more abundant chalcopyrite, thereby suggesting that Warintza East is characterized by a zoned mineralization pattern, with a Mo-rich center and a Cu-Mo halo.

Andesite Porphyry Center

Part of the area between Warintza Central and Warintza East comprises a composite, predominantly andesite-bearing intrusion, in which coarse-grained porphyritic andesite is typically intruded by fine-grained, aphanitic dikes of similar composition. Both are entirely transformed to fine-grained assemblages of hydrothermal biotite. Sections of igneous/contact breccia are common where intrusions of the complex approach Mishuallí country rocks, and centimeter- to meter-sized lithic clasts and blocks hosted by the andesitic igneous matrix of the intrusive phase are characteristic. This center has been previously named Mafic Complex in internal reports and formalized as Andesite Porphyry in the resource model for Warintza Central.

The Andesite Porphyry Center is early intermineral in timing because it contains clasts of prograde garnet skarn, A-type veinlets, and anhydrite relicts, as well as blocks of felsic porphyry with delicate UST-textured and wormy quartz veinlets. It is locally cut by sulfide-bearing, A-type quartz veinlets, centimeter-wide aplite vein-dikes, and anhydrite-cemented hydrothermal breccia bodies. Through-going C veinlets with pyrite, chalcopyrite, and magnetite are common. To the west, diorite and intermineral dikes of Warintza Central cut rocks of the Andesite Porphyry Center and its contained veinlets, while the felsic dikes of Warintza East intrude it to the east.

8.0 DEPOSIT TYPES

The Warintza Central deposit is a Cu-Mo porphyry associated with calc-alkalic igneous rocks. Porphyry deposits are typically large tonnage, low-grade, hypogene resources, featuring (1) localization of Cu- and Mo-bearing sulphide in veinlet networks and as disseminated grains in altered wall rocks, (2) alteration and ore mineralization occurring at one to four km depth and related to magma emplaced at size to eight plus km depth, typically above subduction zones, (3) multi-phase intrusive rock complexes emplaced immediately before, during, and/or immediately after mineralization, and (4) zones of phyllic-argillic and marginal propylitic alteration that overlap or surround potassic alteration (Berger et al., 2008).

Oxidation and acid leaching of primary mineralization may produce zones of (supergene) enrichment near the base of a weathered zone (Hartley and Rice, 2005; Sillitoe, 2005) that, in some deposits, are important to their economic viability. Porphyry deposits associated with calc-alkalic rocks are typically larger than those associated with alkalic rocks, both in terms of alteration footprint and metal endowment.

The deposit model for porphyry Cu-Mo deposits is relatively well-developed and accepted (e.g., Lowell and Guilbert, 1970; and more recent reviews by Sillitoe, 2000; Richards, 2003; Richards, 2005; Sillitoe and Thompson, 2006) and lends itself to several exploration methods. Geological mapping and diamond drilling can define alteration patterns, vein network densities, multi-phase intrusive centers, and geochemical zonation that can help establish the viability of porphyry mineralization and/or establish vectors toward (higher grade) mineralization. The relatively large footprint of these deposits is amenable to surface geochemical methods, such as soil, silt, and/or rock geochemistry surveys. Disseminated sulphide mineralization and, in some systems, magnetite-destructive alteration can respond to ground-based induced polarization (“IP”) and ground- or air-based magnetic surveys. The spectral scanning method—both airborne and on drill core—is a more recently developed method that produces more objective maps of alteration and vein patterns.

9.0 EXPLORATION

9.1 Introduction

Some of the early regional exploration work by Billiton that led to the discovery of the Warintza mineralization has been alluded to earlier in this Report. For example, Billiton commissioned a regional helicopter magnetic and electromagnetic survey that was flown over the region in January to February 1999. They found that the areas now known to contain porphyry deposits are partially encircled by resistivity highs and are centered on reduced-to-pole magnetic lows.

No exploration was conducted on the Project between 2006 and 2019.

9.2 Geochemical Sampling

The Project has a historical analytical database including information from stream sediment, soil, and rock sampling. Surface samples were collected by the previous operators and are summarized in Table 13.

Table 13: Historical Sampling

Historical Data	
Sample Type	**Count**
Soil	981
Rock	511
Stream Sediment	241

Results for historical and recent Cu and Mo soil and rock samples are summarized in the figures below. Cu effectively highlights general areas of the porphyry centers. Mo in soil and rock is somewhat more restricted, but the patterns are similar to the Cu ones (Figure 12 and Figure 13). Zinc ("Zn") in soil and rock samples form an external halo surrounding the Cu and Mo anomalies. The combined Warintza Central-Warintza East area is characterized by a well-defined concentric zoning, with a central zone with Zn values lower than 200 part per million ("ppm") Zn in soils and a halo averaging 800 ppm Zn.

The soil sampling pattern for historic samples progressed from ridge soil sampling to a more detailed grid over the deposit. Surface sampling has effectively outlined outstanding drill targets at Warintza East, Warintza West, and Warintza South, which have been successfully tested.

A reinterpretation of the historical stream sediment data was carried out, which allowed delimiting of the Yawi anomaly with dimensions of 5 km x 2.5 km with anomalous values of 450 ppm Cu and 86 ppm Mo (Figure 14).

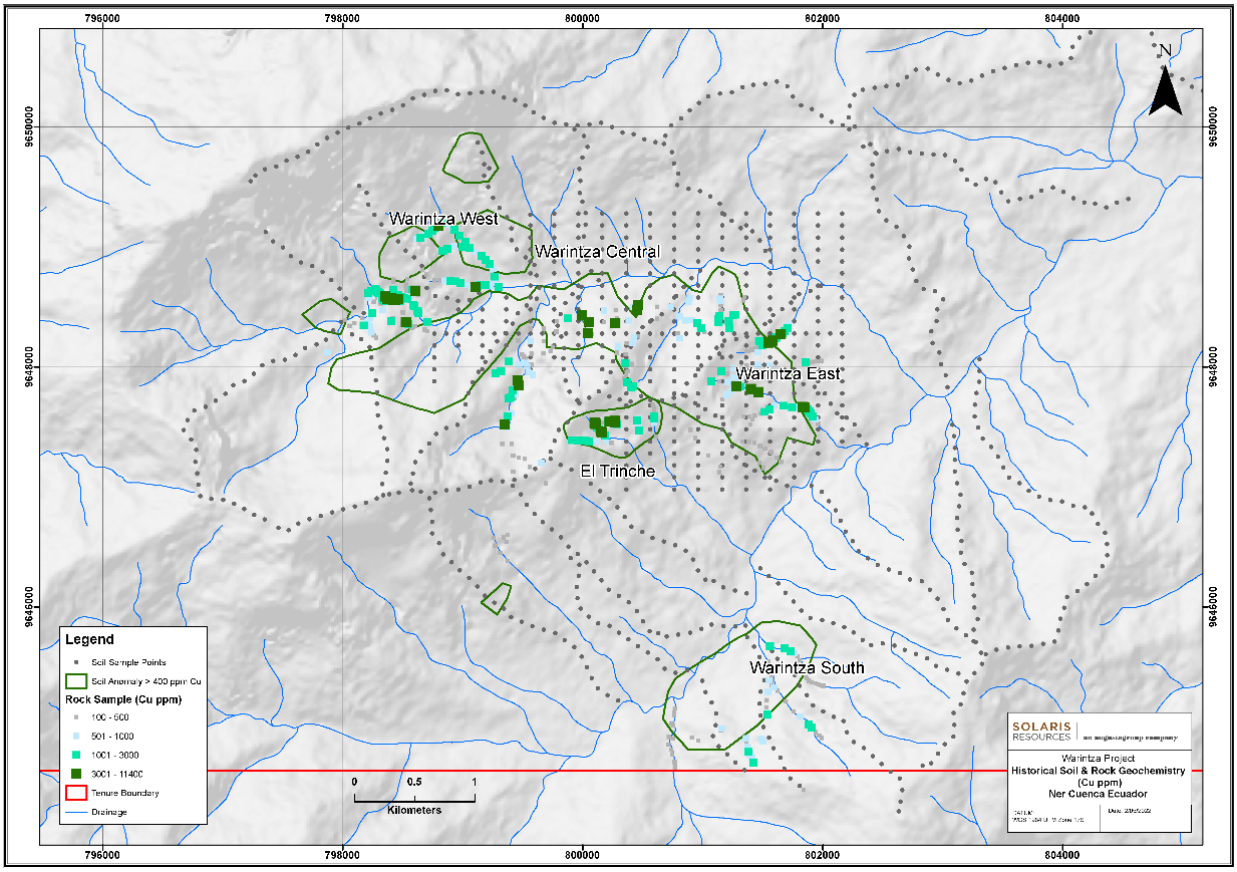

Figure 12: Historical Cu Soil and Rock Geochemistry Map of Warintza Cluster

Source: Solaris Resources Inc. (2022)

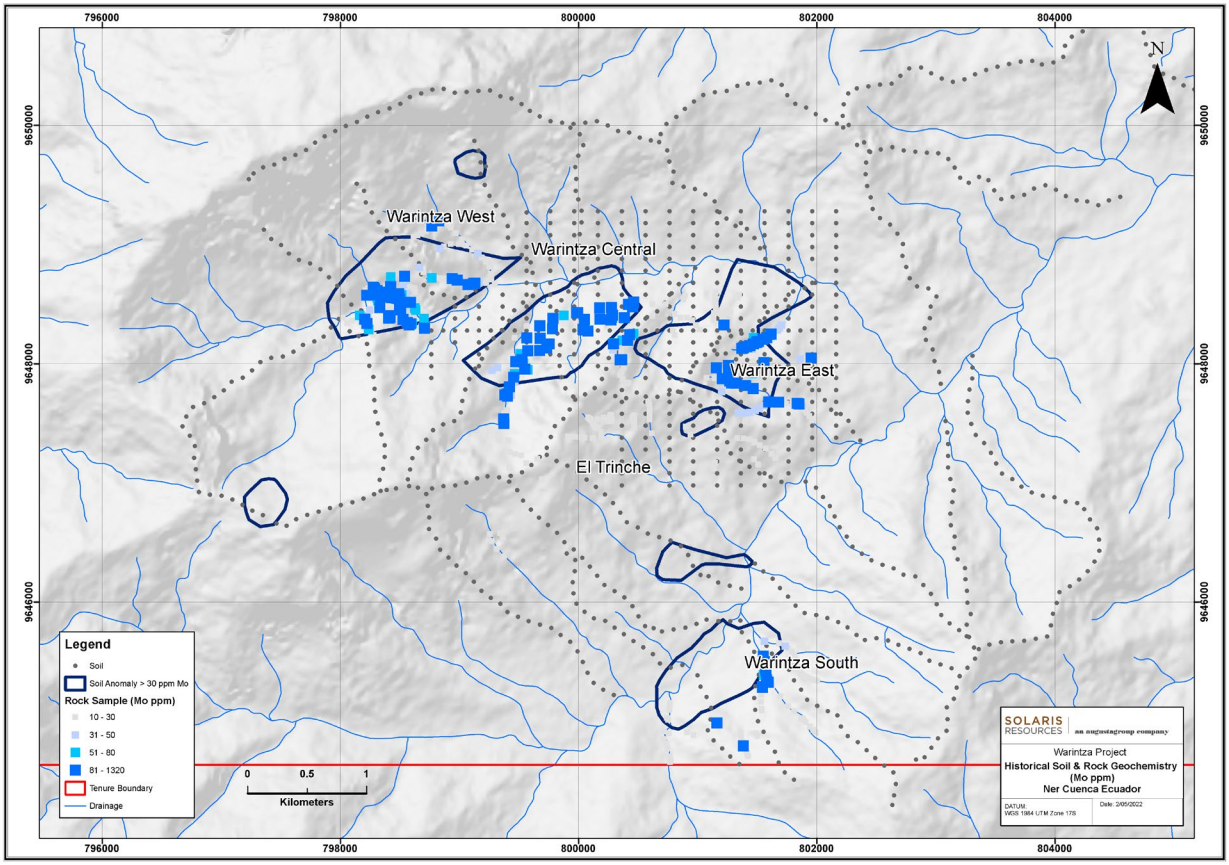

Figure 13: Historical Mo Soil and Rock Geochemistry Map of Warintza Cluster
Source: Solaris Resources Inc. (2022)

Currently, an extensive program of geological mapping and surface sampling is being conducted at the Warintza Property. Geological mapping is performed at a 10K scale, and rock samples are taken mainly from outcrops in creeks. Soil samples are collected at 100 m spacing in order to identify Cu-Mo porphyry centers and Au occurrences. Rock chip sampling is also performed where outcropping is altered and mineralized rocks are found. Soil sampling patterns differ from a regular grid to one that follows topographic contours in steep terrain. Surface samples collected in recent campaigns are summarized in Table 14.

Table 14: Recent Surface Sampling

Surface Sampling		
Sample Type	**Count**	**Analysis**
Soil	1200	Aqua regia – ICP MS
Stream Sediments	65	Aqua regia – ICP MS
Rock	497	4 Acids – ICP MS

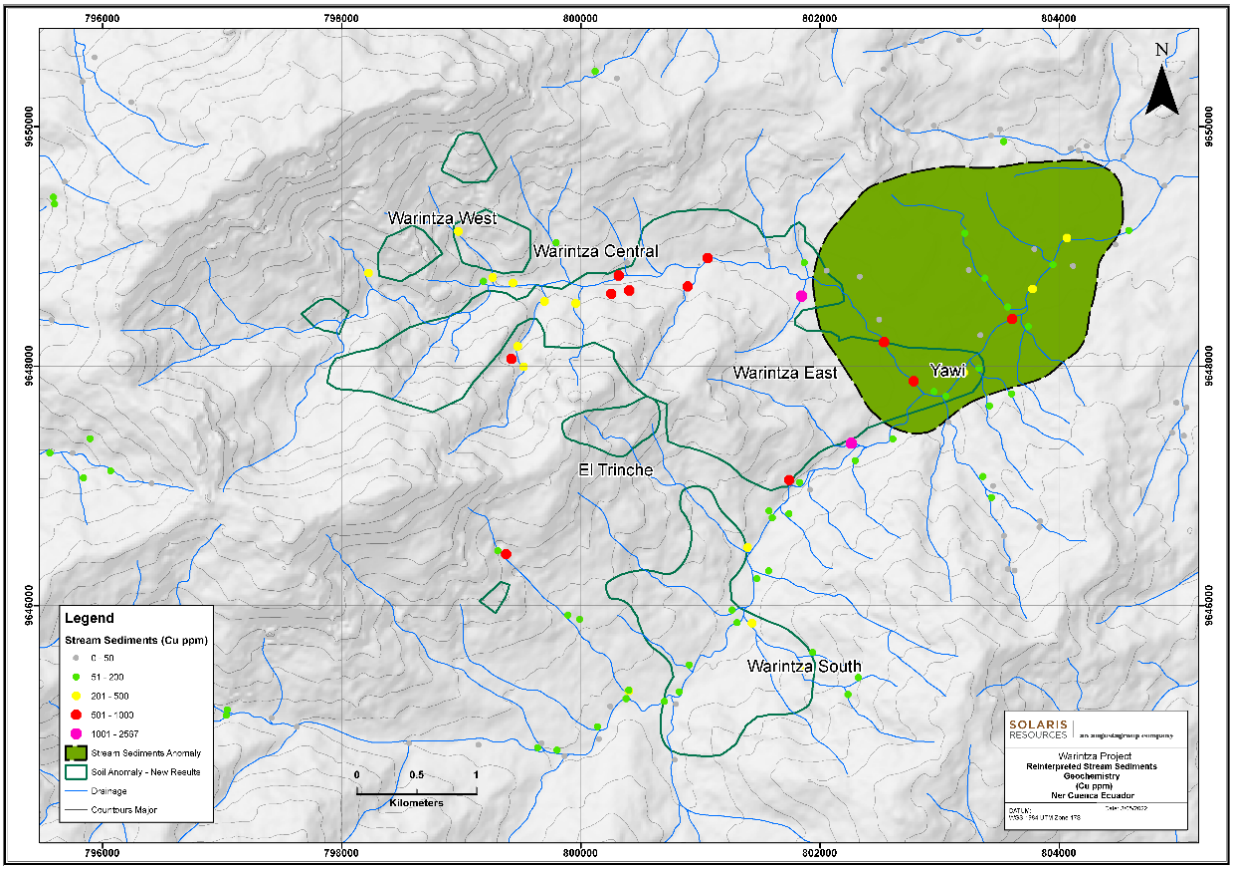

Figure 14: Yawi Reinterpreted Stream Sediments Copper Anomaly
Source: Solaris Resources Inc. (2021)

Recent soil sampling results expand Warintza East and Warintza South anomalies, see Figure 15 and Figure 16. Rock sampling in the Warintza East extension yielded Mo anomalous values between 10 and 50 ppm Mo. Rock samples within the Warintza South anomaly returned values between 400 ppm and 2900 ppm Cu, 15 to 180 ppm Mo ppm, and 0.5 to 2 ppm Au.

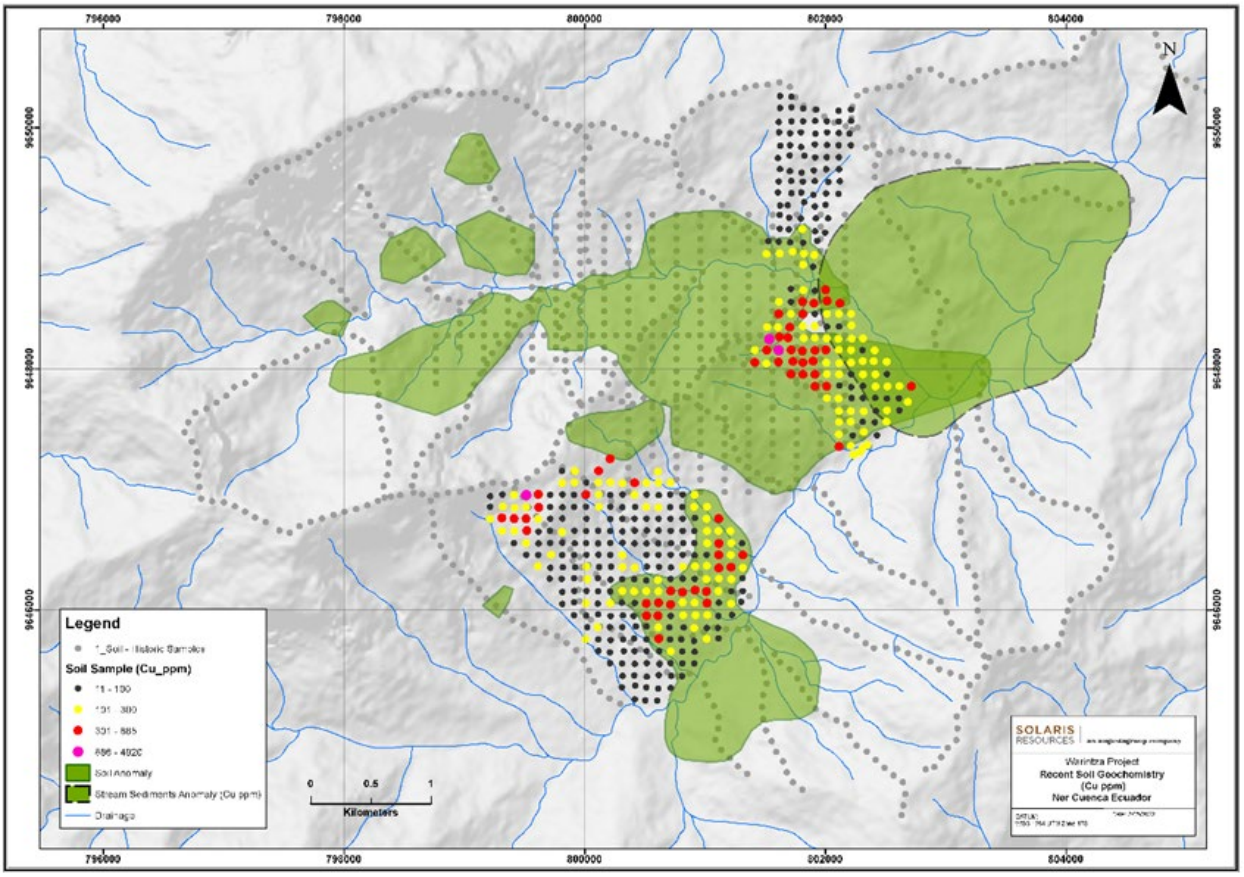

Figure 15: Warintza Soil and Stream Sediments Cu Anomalies
Source: Solaris Resources Inc. (2022)

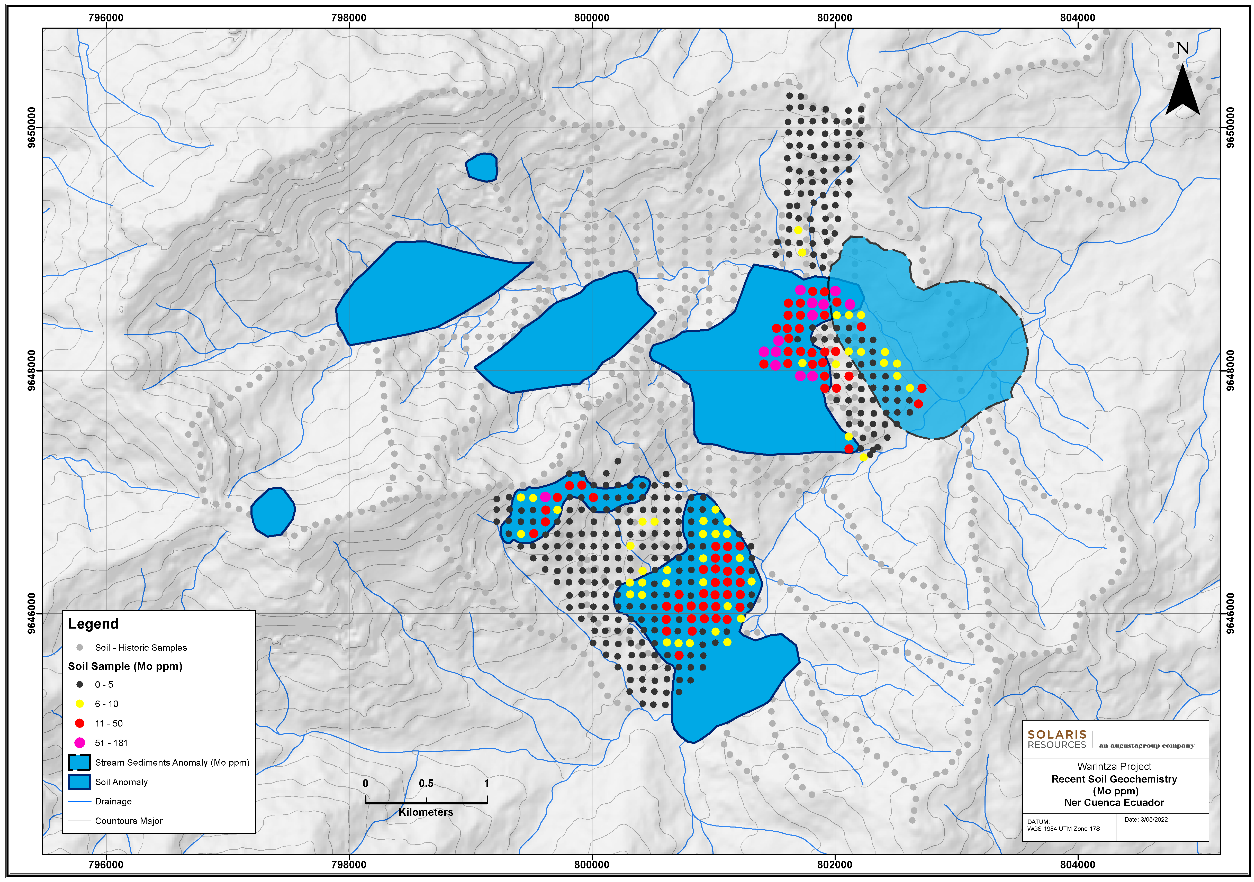

Figure 16: Warintza Soil and Stream Sediments Mo Anomalies
Source: Solaris Resources Inc. (2022)

At Caya 21 concession, a reinterpretation of the historical data was completed, and an anomaly of 5 km x 2.5 km was defined with Cu values ranging to 50 ppm, Mo values range from five to 260 ppm, and Au varies from 400 to 4,300 part per billion ("ppb").

Recent stream sediment sampling better defines the Caya anomaly with dimensions of 3 km x 2 km, average Cu values of 58 ppm, and Mo values of 3 ppm (Figure 17). Rock samples identified three anomalies named TG-01, TG-02, and TG-03, with Cu values ranging between 300 and 2,000 ppm and Mo values between 10 and 120 ppm (Figure 18).

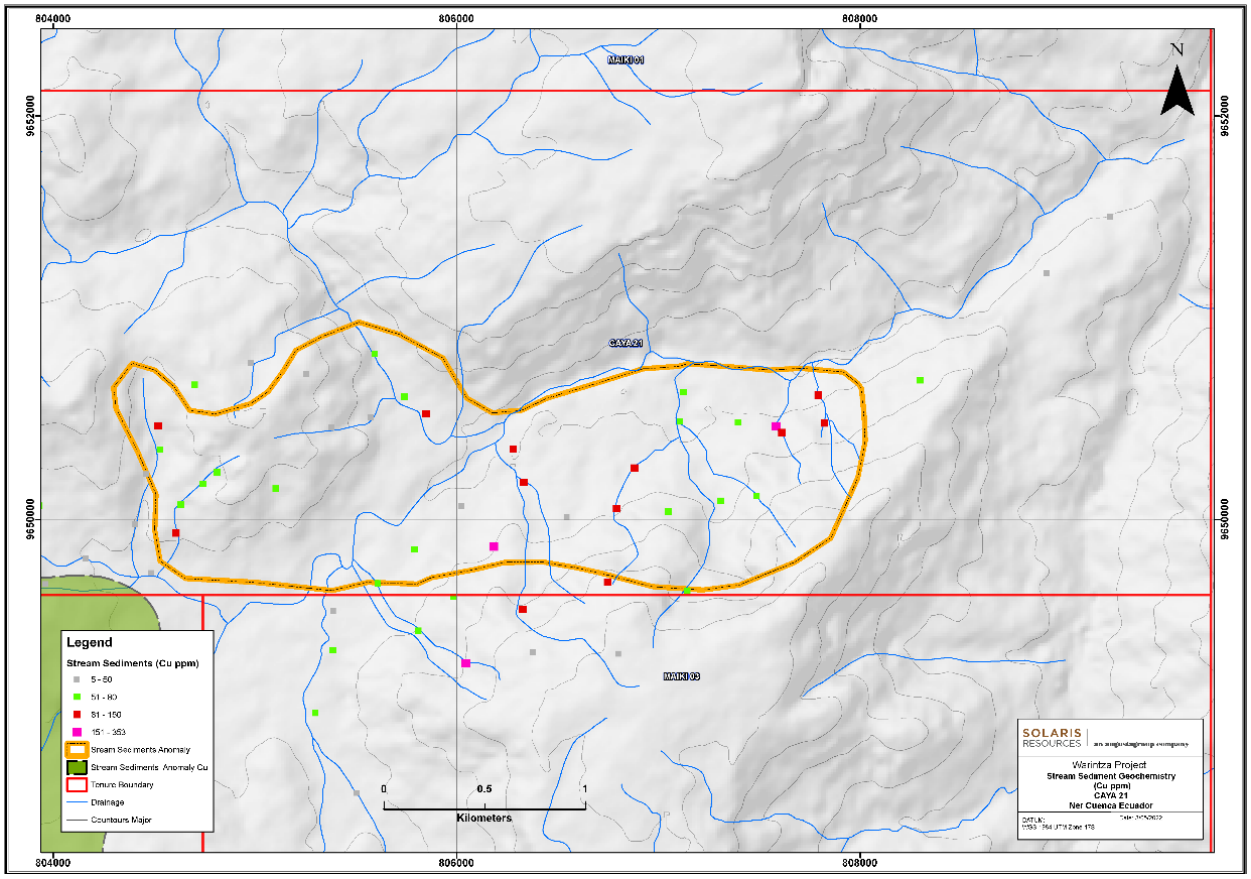

Figure 17: Caya 21 Stream Sediment Anomalies
Source: Solaris Resources Inc. (2021)

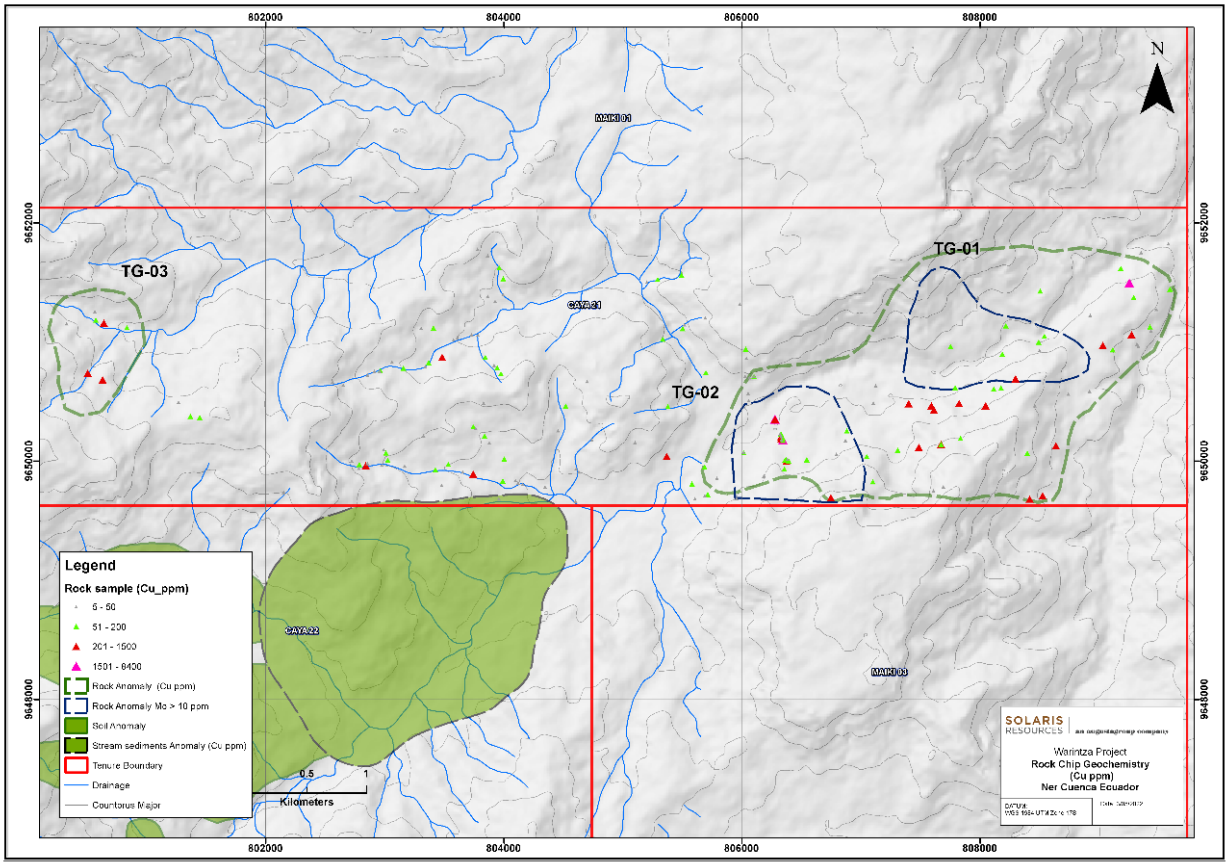

Figure 18: Cu Rock Samples Geochemistry
Source: Solaris Resources Inc. (2021)

9.3 Geophysical Surveys

A ZTEM AFMAG EM and magnetic survey was carried out by Geotech Ltd. between August-October 2020. This advanced airborne ZTEM survey covered approximately 1,666 line-km over the entire Warintza and area land package, totaling 268 km² (26,777 hectares).

In 2021, Solaris retained Condor Consulting Inc., recognized experts in the field of airborne EM, to perform detailed modelling and interpretation of the previously completed advanced airborne ZTEM survey.

Condor carried out a full 3D inversion of the EM and magnetic results using commercial and proprietary software, producing enhanced images based on a greatly expanded dataset, including a considerable amount of additional drilling since the prior interpretation and detailed geology, weathering, and density models for the Project.

In general, the refined high conductivity volumes capture mineralization closer to surface and correlate more closely to networked sulfide mineralization in stockwork veining, with the anomalies now starting at surface and better reflecting the vertical zonation of the Warintza porphyries from higher density stockwork veining to lower density veining and disseminated mineralization.

Figure 19 shows a view of the 3D ZTEM conductivity model and drilling. After drilling several of the target areas, it has been observed that portions of the higher-grade sulfides are conductive.

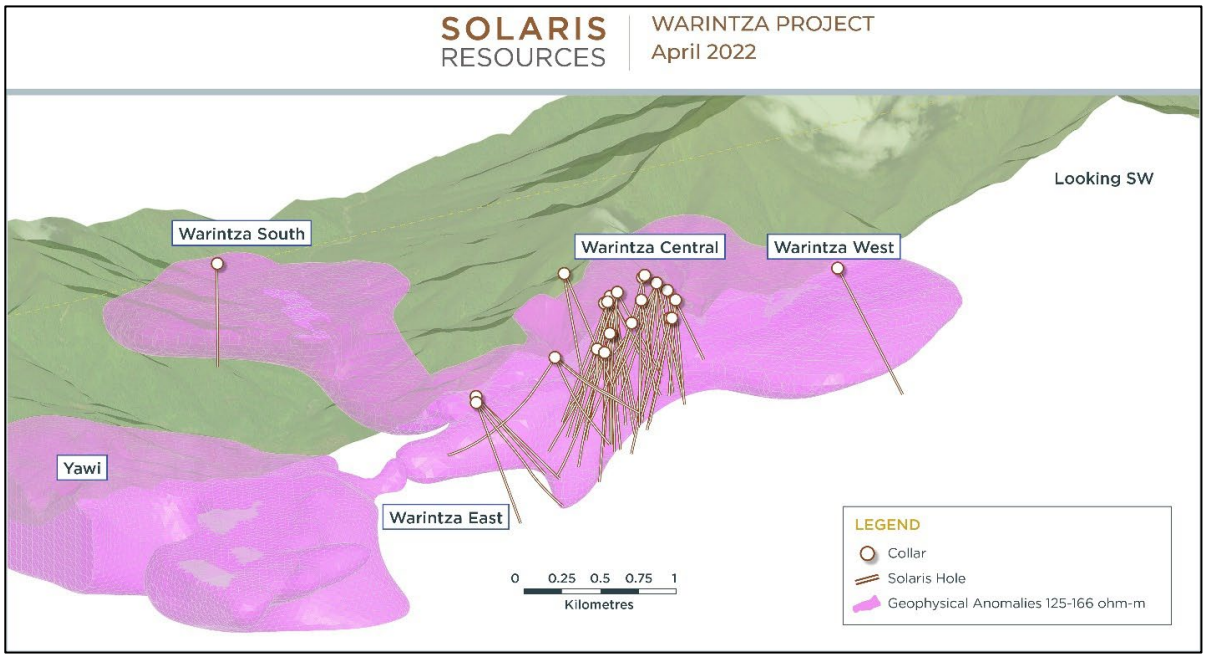

Figure 19: 3D ZTEM Conductivity Model Looking Southwest
Source: Solaris Resources Inc. (2022)

10.0 DRILLING

The Warintza Property was first drilled in two campaigns executed by Lowell and Corriente during 2000 and 2001. 33 diamond drill holes were completed at Warintza Central for a total of 6,530 m, see Table 15.

Solaris initiated a new drilling campaign in February 2020 which is still underway. Drill hole assays and data completed for this Report since February 2020 correspond to 58,011 m, for a total of 64,541 m.

Table 15: Summary of Drilled Meters by Year

Campaign	Number of Drillholes	Meters Drilled
2000	16	2,391
2001	17	4,139
2020	16	14,400
2021	50	43,611
Totals	**99**	**64,541**

Table 16: 2020 and 2021 Assay Results

Hole ID	From (m)	To (m)	Interval (m)	Cu (%)	Mo (%)	Au (g/t)	CuEq (%)
SLSE-08	8	544	536	0.35	0.02	0.04	0.45
Including	18	160	142	0.56	0.01	0.06	0.63
SLSE-07	632	1069	437	0.29	0.02	0.04	0.39
SLSE-06	0	484	484	0.33	0.02	0.04	0.43
SLSE-05	0	714	714	0.26	0.01	0.05	0.32
Including	446	714	268	0.42	0.02	0.08	0.54
SLSE-04	0	892	892	0.43	0.01	0.04	0.49
Including	276	892	616	0.54	0.02	0.04	0.64
SLSE-03	38	856	818	0.29	0.02	0.03	0.39
Including	276	602	326	0.48	0.03	0.05	0.63
SLS-54	0	1093	1093	0.45	0.02	0.04	0.55
Including	50	406	356	0.62	0.02	0.05	0.73
SLS-53	10	967	957	0.39	0.01	0.03	0.45
Including	16	192	176	0.65	0.03	0.04	0.79
SLS-52	42	1019	977	0.39	0.01	0.03	0.45
Including	96	578	482	0.55	0.01	0.03	0.61
SLS-51	36	1048	1012	0.38	0.01	0.06	0.45
Including	130	1048	918	0.41	0.01	0.05	0.47
SLS-50	336	458	122	0.14	0.04	0.03	0.32
SLS-49	50	867	817	0.50	0.02	0.04	0.60
Including	50	446	396	0.59	0.02	0.04	0.69
SLS-48	50	902	852	0.45	0.02	0.05	0.56
Including	50	150	100	1.39	0.03	0.20	1.61
SLS-47	48	859	811	0.41	0.02	0.05	0.52
Including	48	494	446	0.55	0.03	0.06	0.70
SLS-46	48	680	632	0.27	0.01	0.03	0.33
Including	48	216	168	0.61	0.02	0.04	0.71
SLS-45	44	608	564	0.37	0.01	0.03	0.43
Including	44	280	236	0.51	0.01	0.03	0.57
SLS-44	6	524	518	0.16	0.05	0.03	0.38

Including	44	376	332	0.18	0.06	0.03	0.44
SLS-43	138	350	212	0.17	0.03	0.03	0.31
SLS-42	52	958	906	0.42	0.02	0.06	0.53
Including	52	792	740	0.48	0.02	0.07	0.60
Including	52	692	640	0.51	0.02	0.07	0.63
SLS-41	0	592	592	0.42	0.02	0.06	0.53
Including	8	504	496	0.48	0.02	0.06	0.59
SLS-40	8	1056	1048	0.39	0.01	0.03	0.45
Including	50	432	382	0.56	0.02	0.04	0.66
SLS-39	28	943	915	0.49	0.01	0.04	0.55
Including	90	458	368	0.65	0.02	0.04	0.75
SLS-38	58	880	822	0.28	0.01	0.05	0.34
Including	58	302	244	0.58	0.02	0.06	0.69
SLS-37	28	896	868	0.39	0.05	0.05	0.62
SLS-36	2	1082	1080	0.33	0.01	0.04	0.39
Including	46	336	290	0.67	0.03	0.08	0.83
SLS-35	48	968	920	0.53	0.02	0.04	0.63
Including	50	376	326	0.69	0.02	0.05	0.80
SLS-34	52	712	660	0.36	0.02	0.06	0.47
Including	52	294	242	0.51	0.03	0.08	0.67
SLS-33	40	762	722	0.55	0.03	0.05	0.70
Including	46	472	426	0.71	0.03	0.06	0.86
SLSE-02	0	1160	1160	0.20	0.01	0.04	0.26
Including	0	320	320	0.39	0.02	0.04	0.49
SLS-32	0	618	618	0.38	0.02	0.05	0.49
Including	46	418	372	0.53	0.02	0.06	0.64
SLS-31	8	1008	1000	0.68	0.02	0.07	0.80
Including	44	812	768	0.75	0.03	0.08	0.91
SLS-30	2	374	372	0.57	0.06	0.06	0.84
Including	42	306	264	0.72	0.06	0.07	1.00
SLSE-02	0	320	320	0.39	0.02	0.04	0.49
Including	0	62	62	0.59	0.01	0.06	0.66
SLSE-01	0	1213	1213	0.21	0.01	0.03	0.27

Including	0	396	396	0.33	0.02	0.04	0.43
SLS-29	6	1190	1184	0.58	0.02	0.05	0.69
Including	48	528	480	0.69	0.03	0.04	0.83
SLS-28	6	638	632	0.51	0.04	0.06	0.70
Including	42	358	316	0.81	0.04	0.09	1.02
SLS-27	22	484	462	0.70	0.04	0.08	0.90
Including	36	408	372	0.81	0.04	0.09	1.02
SLS-26	2	1002	1000	0.51	0.02	0.04	0.61
Including	46	832	786	0.57	0.02	0.04	0.67
SLS-25	62	444	382	0.62	0.03	0.08	0.78
Including	62	292	230	0.87	0.04	0.10	1.08
SLS-24	10	962	952	0.53	0.02	0.04	0.63
Including	10	512	502	0.57	0.02	0.05	0.68
SLS-19	6	420	414	0.21	0.01	0.06	0.28
SLS-23	10	558	548	0.31	0.02	0.06	0.42
Including	10	362	352	0.34	0.02	0.06	0.45
SLS-22	86	324	238	0.52	0.03	0.06	0.67
Including	86	186	100	0.61	0.04	0.06	0.80
SLS-21	2	1031	1029	0.63	0.02	0.04	0.73
Including	2	422	420	0.72	0.02	0.05	0.83
SLS-20	18	706	688	0.35	0.04	0.05	0.54
Including	18	384	366	0.44	0.04	0.04	0.62
SLS-18	78	875	797	0.62	0.05	0.06	0.85
Including	80	450	370	0.71	0.05	0.07	0.95
SLS-17	12	506	494	0.39	0.02	0.06	0.50
SLS-16	20	978	958	0.63	0.03	0.06	0.78
Including	358	844	486	0.70	0.03	0.07	0.86
SLS-15	2	1231	1229	0.48	0.01	0.04	0.54
Including	2	1004	1002	0.52	0.01	0.04	0.58
Including	2	696	694	0.57	0.02	0.05	0.68
SLS-14	0	922	922	0.79	0.03	0.08	0.95
Including	34	884	850	0.82	0.03	0.08	0.98
Including	52	836	784	0.84	0.03	0.09	1.01

SLS-13	6	468	462	0.80	0.04	0.09	1.01
SLS-12	22	758	736	0.59	0.03	0.07	0.75
SLS-11	6	694	688	0.39	0.04	0.05	0.58
SLS-10	2	602	600	0.83	0.02	0.12	0.97
Including	56	602	546	0.88	0.03	0.12	1.06
SLS-09	122	220	98	0.60	0.02	0.04	0.70
Including	122	168	46	0.96	0.03	0.05	1.11
SLS-08	134	588	454	0.51	0.03	0.03	0.65
Including	134	274	140	0.90	0.03	0.05	1.05
SLS-07	0	1067	1067	0.49	0.02	0.04	0.59
Including	2	702	700	0.58	0.03	0.04	0.72
SLS-06	8	892	884	0.50	0.03	0.04	0.64
SLS-05	18	936	918	0.43	0.01	0.04	0.49
Including	18	324	306	0.52	0.02	0.04	0.62
SLS-04	0	1004	1004	0.59	0.03	0.05	0.74
Including	0	824	824	0.64	0.03	0.05	0.79
SLS-03	4	1014	1010	0.59	0.02	0.10	0.72
Including	4	892	888	0.61	0.02	0.10	0.74
Including	176	892	716	0.63	0.02	0.10	0.76
SLS-02	0	660	660	0.79	0.03	0.10	0.96
Including	48	656	608	0.79	0.03	0.10	0.96
SLS-01	1	568	567	0.80	0.04	0.10	1.01
Including	48	492	446	0.88	0.04	0.10	1.09
SLSN-02	0	200	200	0.43	0.02	0.10	0.56
SLSN-01	42	219	177	0.36	0.01	0.07	0.43
SLST-02	44	202	158	0.22	0.00	0.03	0.23
SLST-01	36	204	168	0.16	0.00	0.05	0.18

Notes to Table 16:

1. *Grades are uncut and true widths have not been determined.*
   Solaris defines copper equivalent calculation for reporting purposes only. Copper-equivalence calculated as: CuEq formula: CuEq (%) = Cu (%) + 4.0476 × Mo (%) + 0.487 × Au (g/t)., utilizing metal prices of US$3.50/lb Cu, US$15.00/lb Mo, and US$1,500/oz Au and assumes recoveries of 90% Cu, 85% Mo, and 70% Au, based on preliminary metallurgical test work.

Table 17: 2020 and 2021 Collar Locations

Hole ID	Easting	Northing	Elevation (m)	Depth (m)	Azimuth (degrees)	Dip (degrees)
SLSE-08	801485	9648192	1170	959	305	-70
SLSE-07	800749	9648146	1282	1069	84	-50
SLSE-06	801485	9648192	1170	1078	285	-55
SLSE-05	800749	9648146	1282	737	330	-65
SLSE-04	800749	9648146	1282	893	257	-45
SLSE-03	800749	9648146	1282	909	270	-45
SLS-54	800383	9648303	1412	1093	160	-74
SLS-53	800126	9648032	1566	967	170	-82
SLS-52	800258	9648097	1559	1019	110	-75
SLS-51	799873	9648008	1632	1048	85	-70
SLS-50	799870	9648315	1414	768	80	-75
SLS-49	800383	9648303	1412	867	135	-73
SLS-48	800178	9648285	1439	1056	180	-60
SLS-47	799968	9648102	1510	859	135	-72
SLS-46	800126	9648032	1566	882	125	-70
SLS-45	800258	9648097	1559	969	117	-70
SLS-44	799968	9648102	1510	676	0	-75
SLS-43	799870	9648315	1414	761	110	-75
SLS-42	800383	9648303	1412	1061	55	-80
SLS-41	799765	9648033	1571	792	115	-70
SLS-40	800124	9648044	1568	1056	105	-75
SLS-39	800253	9648105	1576	943	145	-80
SLS-38	800383	9648303	1412	923	90	-56
SLS-37	799968	9648102	1510	929	0	-90
SLS-38	800383	9648303	1412	923	90	-56
SLS-37	799968	9648102	1510	928	0	-90
SLS-36	799765	9648033	1571	1088	97	-60
SLS-35	800124	9648044	1568	995	78	-60
SLS-34	800383	9648303	1412	1057	78	-60
SLS-33	799873	9648008	1632	764	0	-80

SLSE-02	801485	9648192	1170	1191	275	-50
SLS-32	800383	9648303	1422	831	0	-89
SLS-31	799765	9648033	1571	1025	97	-80
SLS-30	799667	9648029	1499	552	0	-65
SLSE-01	801485	9648192	1170	1213	260	-45
SLS-29	800124	9648035	1580	1190	80	-72
SLS-28	799765	9648033	1571	570	50	-75
SLS-27	799667	9648029	1499	588	45	-70
SLS-26	800191	9648059	1580	1032	70	-60
SLS-25	799676	9648117	1443	513	220	-70
SLS-24	800124	9648035	1580	962	90	-75
SLS-23	799765	9648033	1571	570	270	-60
SLS-22	799676	9648117	1443	562	270	-60
SLS-21	800191	9648059	1580	1031	70	-70
SLS-20	800124	9648035	1580	816	0	-75
SLS-19	799667	9648029	1449	588	235	-80
SLS-18	799676	9648117	1443	875	100	-70
SLS-17	799765	9648033	1571	788	180	-80
SLS-16	800124	9648035	1580	1033	272	-77
SLS-15	800191	9648059	1580	1231	222	-80
SLS-14	799765	9648033	1571	1020	85	-80
SLS-13	799667	9648029	1499	468	0	-80
SLS-12	800124	9648035	1568	782	265	-62
SLS-11	800191	9648059	1570	860	280	-65
SLS-10	799765	9648033	1571	690	293	-77
SLS-09	800266	9648209	1493	500	0	-89
SLS-08	800253	9648105	1576	824	14	-80
SLS-07	800191	9648065	1580	1067	52	-80
SLS-06	800124	9648035	1580	1069	45	-79
SLS-05	800124	9648035	1580	1063	265	-81
SLS-04	800191	9648059	1580	1150	0	-88
SLS-03	800191	9648059	1570	1090	289	-79
SLS-02	799765	9648033	1571	744	0	-90

SLS-01	799765	9648033	1571	805	351	-80
SLSN-02	800509	9648410	1328	201	0	-90
SLSN-01	800555	9648384	1360	219	0	-90
SLST-02	800203	9647530	1596	835	12	-59
SLST-01	800203	9647530	1596	861	335	-63

Notes to Table 17:

1. *The coordinates are in WGS84 17S Datum.*

10.1 Drilling Procedures

The current drilling program executed by Solaris uses Kluane Drilling, man-portable, hydraulic rigs. The historical campaigns were carried out between February to April 2000 and from July to August 2001, starting with a core diameter of NTW (2.21" diameter), but in some cases, BTW (1.66" diameter) was used. In the current drilling program executed by Solaris, core diameters start with HTW (2.80" diameter) down to 500 m depth, NTW to approximately 900 m depth, and finally with BTW for greater depths.

Down hole surveys are made using equipment such as Ez TrackTM, Devishot, and Gyro, which are operated by the drilling company. Measurements are taken every 50 m in all drill holes. The Rocktest company performs quality control of the previous measurements using Gyro GT3 equipment, performing measurements every 20 m on descent and every 10 m on ascent in approximately 70% of the drill holes.

The drilling grid has an average spacing of 150 m. However, in an effort to minimize environmental disturbance and maximize efficiencies, several holes were drilled in different directions from the same platforms.

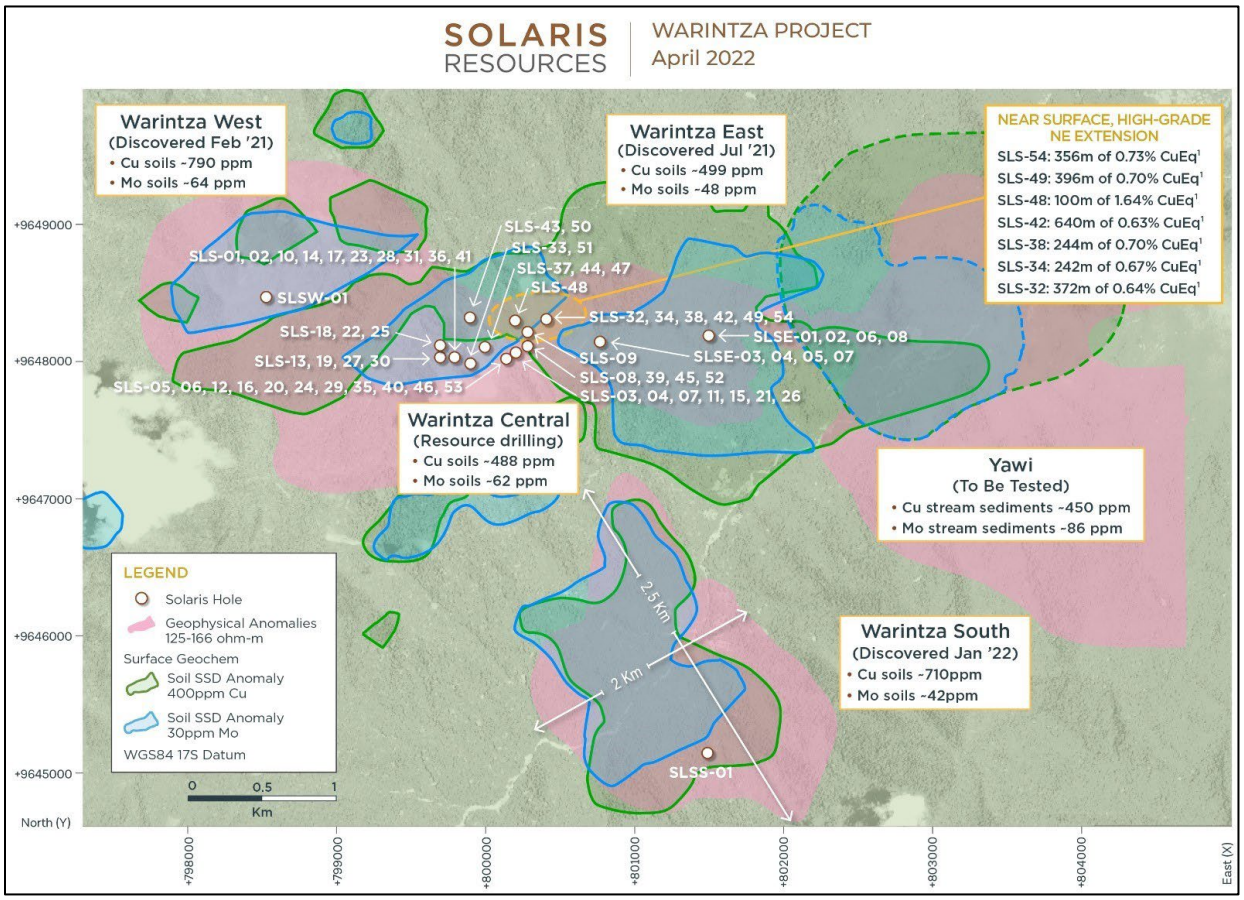

Figure 20: Drilling Completed with Select Grade Intercepts
Source: Solaris Resources Inc. (2022)

10.2 Core Handling Procedures

Core is placed in the core boxes and each box is labeled with the drill hole ID and box number. In addition, a core meterage control, basic geotechnical survey, and geological "quicklog" are performed at a station near each platform. Core boxes are packed with plastic film and moved to a loading platform to later be transferred by helicopter and truck to the Solaris core shed facilities in Quito.

At the core shed, the following processes are completed:

1. Control of drilling interval measurements
2. Core is marked every 2 m for sampling
3. Photographic record of the core complete with drilling intervals and sampling intervals is done
4. Core photos are uploaded onto the Imago software data-room

5. Structural logging using IQ Logger and Class structural logging system

6. Point load tests with PLT-measuring equipment every 10 m

7. Geotechnical logging of recovery parameters, RQD, number of fractures, geotechnical intervals, IRS, GSI, and others

8. Sampling of half core for assays

9. Geological mapping using the Anaconda mapping system, including lithology, primary and secondary alteration minerals, mineral species in mineralized zones, vein description, and density, etc.

Core is stored in racks at the core, and the geotechnical data is collected in detail as described above.

Samples for specific gravity are selected and cut at 10 to 15 cm samples every 20 m, considering that the core is sufficiently resistant to the cutting process. SG samples are sent to the Bureau Veritas laboratory in Lima, where the paraffin-coated, water-immersion method is used to measure SG.

11.0 SAMPLE PREPARATION, ANALYSES, AND SECURITY

Corriente Resources Inc. explored Warintza Central, drilling in 33 diamond drill holes (6,502.37 m)[1] in two campaigns from February-April 2000 (16 DDH) and July-August 2001 (17 DDH). The total samples taken were 2,142.

During 2020 and 2021, Lowell drilled a total of 58,011.17 m in 66 drill holes. The total number of samples taken was 28,915.

The QP reviewed Lowell's exploration work at the Project site, as well as all other installations where sample preparation and storage are completed both in Macas and Quito (Ecuador, see Figure 21).

Additionally, the QP visited ALS' sample preparation laboratory in Quito in late November 2021 and the assaying laboratory in Lima (Perú) in February 2022.

[1] One drill hole (W-02) was only sampled to 75 m depth, although it was drilled to 102.62 m.

Figure 21: Warintza Project, Central Core Shed Facilities in Quito, Ecuador
Source: GSI (2021)

11.1 Sample Preparation and Analyses

11.1.1 2000-2001 Drilling Campaign

Diamond drill core was sampled at regular one-meter intervals that do not honor lithological contacts. The splitting of the core was performed using a diamond bladed core saw at the exploration camp. Broken or soft core was sampled using a scoop to divide half the contents of the core box. The one-meter samples were bagged and labeled with sample IDs. The Bondar-Clegg preparation facility in Quito crushed and pulverised each sample before sending a 100 g pulp to North Vancouver, Canada. Using instructions from Lowell, the one-meter samples submitted were composited into larger samples designed to honor the mineralized zones (Table 18). The compositing length procedure was rigorously adhered to resulting in composites that mixed material types. The analytical results correspond to the composited intervals. Each hole has a record of the original one-meter samples taken and the relative composite assignment. It is unclear at which stage the composites are combined, but based on the description, it seems to be between crushing and pulverization.

The Bondar-Clegg preparation facility received core samples and prepared 2,142 pulps to ship for analysis (Table 19). Pulps were generated by first crushing core to -10 mesh that were then split in quarters up to a maximum weight of 250 g. One quarter split was pulverised to -150 mesh (106 micron), of which 100 g were shipped to the analytical lab for Au and multi-element analysis. Au was determined from a 30 g aliquot by fire assay with AAS finish. Cu, Mo, Zn, lead ("Pb"), and silver ("Ag") were determined by an ore grade method, using a three-acid digest and AAS finish (Vaca and León, 2001). Ag and Pb were only analyzed in the first campaign and results are available for 775 samples.

Table 18: Sample Composite Lengths Applied to Sample Based on Mineralized Zone Character
Source: Equity (2019)

Sample Composite Length (m)	Material Type	Note
5	Leached	2 m in W1 and W2
2	Secondary	
3	Primary	

Table 19: Table of Assays and QA/QC Samples Submitted
Source: Equity (2019)

Campaign	Year	# Samples Analyzed	# Reference Material	QA (%)	# Pulp Duplicates	QC (%)
1	2000	775.00	-	-	-	-
2	2001	1,367.00	65	5	65	5
Total		2,142.00	65	3	65	3

11.1.2 2020-2021 Drilling Campaign

Drill holes were sampled initially on a 2 m interval in mineralization and 5 m intervals in waste/barren rock. Currently, sampling is done at a fixed 2 m length.

Core is sawed in half for most of the competent rock. If necessary, a guillotine is used in softer areas, such as oxidized intervals. Core is cut following an axis line drawn by the geologist. According to protocol, the sample is always taken from the right side of the core.

Field duplicates are cut in half, obtaining a quarter core. A record is created with the sampling sequence, technical person in charge, bag number, codes, quality assurance/quality control ("QA/QC"), weight, and number of total samples of the bag. The sealed samples are placed inside the bags (usually three samples per bag) and sealed with disposable plastic ties (Figure 22).

The main laboratory of the Warintza Project is ALS Chemex, a commercial laboratory that has ISO/IEC 17025:2017 certification (Accredited Laboratory No. 670) valid from March 2010 to March 2026. The certification includes all the facilities that Lowell uses for the treatment of the samples. The certifying body is the Standards Council of Canada ("SCC"). Sample preparation (Table 20) is performed at ALS Quito, Ecuador. The analytical determinations are made in ALS Lima, Peru, from the pulps sent internally by the laboratory in Ecuador.

Table 20: Sample Preparation Protocol from ALS Chemex Quito
Source: GSI (2022)

ALS_Method Code	Sample Preparation Package - PREP-31 - Description
LOG-22	Sample is logged in tracking system and a bar code label is attached
DRY-21	Drying of excessively wet samples in drying ovens. This is the default drying procedure for most rock chip and drill samples (maximum 120ºC)
CRU-31	Fine crushing of rock chip and drill samples to better than 70 % of the sample passing 2 mm (Tyler 9 mesh, US Std. No.10)
SPL-21	Split sample using riffle splitter (250 g)
PUL-31	A sample split of up to 250 g is pulverized to better than 85 % of the sample passing 75 microns (Tyler 200 mesh, US Std. No. 200)

The analysis suite in ore grade corresponds to the determination of Au, Mo, Ag, Pb, Zn, and total Cu, Sequential Cu, Cyanide-soluble Cu; all these determinations by atomic absorption for the samples every 2 m of the drillings, while a suite of trace elements, by ICP, is requested for all samples, only for the first drill hole within the same platform. GeoSystems visited the ALS facilities in both countries to review the treatment of the Warintza samples, finding everything in accordance with Lowell's and ALS' protocols.

Figure 22: Laboratory Sample Reception and Preparation - ALS Quito, Ecuador
Sample Weighing and Internal Code Assignment
Source: GSI (2021)

The secondary laboratory of the Warintza Project is Bureau Veritas ("BV"), based in Quito, Ecuador, and Lima, Peru. It is a commercial laboratory that has ISO/IEC 17025:2017 accreditation (Certificate Number: 2185.02) valid from July 2021 to April 2023. The accrediting entity is A2LA for the Ecuador headquarters, while INACAL accredited the services of Bureau Veritas (former Inspectorate Services Perú S.A.C) in Lima, Peru, valid from June 2019 to June 2023.

Lowell has a pulp sampling procedure to select intervals to be sent for grade control. These pulps are separated based on the results obtained by ALS and for this purpose are chosen as follows: 1% low-grade

samples (<0.25% Cu), 2% medium-grade samples (0.25-0.6% Cu), and 3% of high-grade samples (>0.6% Cu). The master fraction envelopes returned by ALS are picked, and the samples are changed to a new envelope with new numerical encoding. The secondary laboratory facilities were not visited by the QP. The shipment of pulp from the Lowell facilities in Ecuador to the BV laboratory in Lima is made through the headquarters that BV has in Quito.

11.2 Sample Security

11.2.1 2000-2001 Drilling Campaign

The sample shipment was packed to the Warintza airstrip along footpaths. The shipments were flown via chartered aircraft to Macas and carried by commercial transport directly to the preparation facility in Quito (Vaca and León, 2001).

11.2.2 2020-2021 Drilling Campaign

Core boxes (pallets) from the Warintza Project are transported by helicopter (Figure 23) from the drill platforms to Patuca (Morona-Santiago). Then, the samples are transported by truck (Figure 24) to the Quito logging facility for processing. The core samples are then transported to the ALS laboratory in Quito for crushing and pulverizing (Figure 25).

Figure 23: Sample Boxes Waiting to be Picked Up from Drilling Platform by Helicopter
Source: GSI (2021)

Figure 24: Samples in Patuca for Transport to Quito-Core Shed Facilities
Source: GSI (2021)

Figure 25: Samples Arrival to the ALS Laboratory - Quito, Ecuador
Source: GSI (2021)

The laboratory sends the pulps through courier service to ALS Lima, Peru, where all the analytical determinations are made. The chain of custody from the moment the samples leave the Warintza Project until their analysis in the ALS laboratory was reviewed by the QP during its visit in November 2021 to Ecuador and in February 2022 to Peru. The documentation of each drilling is correctly managed and stored by the Lowell team. The chain of custody was also validated in the primary laboratory. No deviations were found that affect the quality and integrity of the samples during the different transfers.

In summary, the QP has verified the chain of custody of the samples from the field to the ALS main laboratory and is satisfied that the procedures in place are safe and guarantee sample provenance.

11.3 Quality Control and Quality Assurance Program

The QA/QC program implemented to date for the Warintza Project exceeds the recommended 15-20% percentage of control samples (29%). The results of the program are acceptable and sufficient to guarantee the reliability of the grades of the deposit.

Table 21: Summary of the QA/QC Program for Warintza
Source: GSI (2022)

Campaign	Drill Holes	Meter	# Core Sample	# QA/QC Sample	% QA/QC
2000-2001	33	6,502.37	2,142	130	6.1
2020-2021	66	58,011.17	28,915	8,879	30.7
Total	**99**	**64,513.54**	**31,057**	**9,009**	**29.0**

11.3.1 2000-2001 Drilling Campaign

The first drill campaign did not include a QA/QC monitoring program. The second drill program utilized a QA/QC monitoring program that included the use of reference materials and pulp duplicates with a one in 20 insertion rate for each type. There is no documentation stating which stage of the sample stream the QA/QC samples were inserted and by which party, either Lowell or Bondar-Clegg personnel. The QA/QC sample ID numbers are consistent with the sample ID series used to create the composites for analysis.

The reference materials were identified using the fifth digit of the sample ID. The duplicates were identified with a '1' in the final character and correspond with the parent sample with the same sample ID but with a final character of '0' (Ronning and Ristorcelli, 2018). Quality assurance for Cu was monitored with three different internal Billiton reference materials that had been round-robin tested at five laboratories. Reference materials to evaluate the accuracy of Mo or Au analyses were not used. 12 pulps of each type were submitted to five laboratories, including Bondar-Clegg, Chemex, Loring Labs, SGS, and CIMM. The internal reference materials utilized by Billiton have no background information available to the current Authors, with the descriptions compiled from Ronning and Ristorcelli (2018). The source material, homogenization method, analytical method, and locations of the laboratories used to create the reference materials are unknown.

The reference material performance is good with all reference materials passing within three standard deviations except one. The 1.5% failure rate is within acceptable range. There is a slight positive bias of the Cu analyses that should be monitored in future drill programs. This could result from a mismatch of the analytical method where there is incongruence between the digest used for core versus the round-robin analysis, or this could be intra lab drift.

There were 65 pulp duplicates inserted during the second drill campaign. The pulp duplicates have very good agreement for Cu and Mo as expected with intra lab pulp duplicates that monitor the analytical reproducibility. Cu has an average relative standard deviation of two, which suggests very good precision

of the paired results. The average relative standard deviation for Mo pairs is five, which suggests the agreement is acceptable.

11.3.2 2020-2021 Drilling Campaign

In the Warintza Project, Lowell determined by protocol the minimum insertion of 20% of control samples for the QA/QC with its main laboratory (ALS), with the following characteristics:

1. Field Duplicate ("FD"), which is a quarter core
2. Pulp Blank ("PB"): sterile commercial material (quartz), certified, with fine granulometry
3. Coarse Blank ("CB"): sterile commercial material (quartz), with coarse granulometry
4. Certified Reference Material-High grade ("CRM")
5. Certified Reference Material-Low grade (CRM)

This 2020-2021 program used a total of 7,217 control samples for the elements Au, Cu, and Mo. The blank and CRM commercial material were procured from Target Rock Perú.

The program is completed with a check of 6% of samples (pulps) for each drill hole that are sent to a secondary laboratory, Bureau Veritas. For the 2020-2021 program, 1,662 pulps were selected, with results to date of 663 samples. Pulps are selected from cores, duplicates, reference materials, and ALS-inserted blanks.

The QA/QC program for this 2020-2021 campaign contains 31% of control samples, 25% insertions rate for the primary ALS laboratory, plus 6% checks with the secondary laboratory, BV.

The details of sample preparation, insertion of sample types, control, and follow-up forms, etc., are detailed in the Core Sampling and Pulp Sampling procedures.

Lowell controls the results of the QA/QC program on a monthly basis, issuing a report for each drill hole and producing a bi-monthly report with results for all drill holes within a given date range. Lowell's internal calculations and graphs are performed following a protocol executed by an external manager, who is also responsible for inserting the samples.

The QP reviewed Warintza's global QA/QC database and performed QA calculations for the entire 2020-2021 program. Inconsistencies in the CRM and BK type assignment, as well as erroneous original vs. duplicate sample numbering, were corrected in the database for both ALS and BV samples.

The acceptance criteria used in the Warintza QA/QC program are presented in Table 22, Table 23, and Table 24. In the case of MPRD, only 10% of the population is expected to be above the proposed limits.

Table 22: Acceptance Criteria for Duplicates (Precision)

QA/QC Sample Type	Elements	ER	MPRD	
		Error %	Error %	Warning %
FD	Au /Cu /Mo	30	30	20
SL	Au	15	15	10
	Cu / Mo	10	10	5

ER = Global Relative Error / MPRD = Mean Paired Relative Difference

Table 23: Acceptance Criteria for CRMs (Accuracy)

±SD	Bias (%)	RSD (%)
Acceptable (<1SD-2SD)	Good (<5%)	Acceptable (<6%)
Warning (2SD-3SD)	Acceptable (5%-10%)	
Error (>3SD)	Unacceptable (>10%)	Unacceptable (>6%)

SD = standard deviation / RSD = Relative standard deviation

Table 24: Acceptance Criteria for Blanks (Contamination)

Error	Warning	Acceptable
>10DL	>5DL	<5DL

DL= lower detection limit

All out-of-range controls are reviewed with the laboratory involved, meetings are held to agree on corrective measures for nearby samples within the batch, and the agreed methodology is documented with internal reports.

For field duplicates, the QP evaluated the QA/QC after filtering the database using the five times the detection limit criterion (5 * DL).

Blanks

No contamination was detected in any of the laboratories (sample preparation and assaying) for Cu, Mo, and Au, including the secondary BV laboratory. These blanks are not blind to the laboratory since they are quartz.

Only in the case of Au, ALS Chemex had an error rate of 0.2%, corresponding to five samples out of 2,044 assayed blanks. Figure 26 shows graphically the results of the contamination checks.

The conclusion is that there does not appear to be any contamination that can impact the mineral resource estimate.

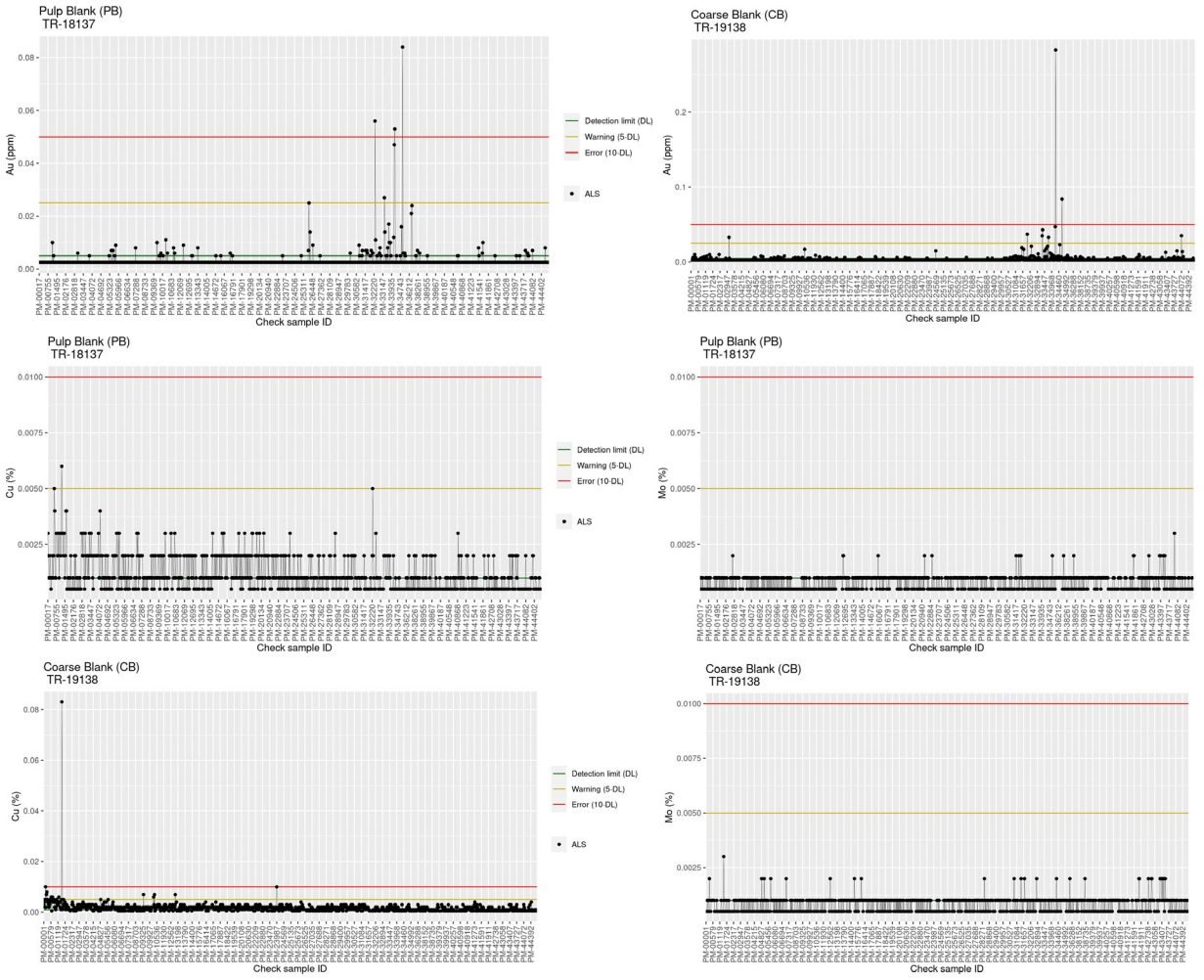

Figure 26: ALS Chemex Contamination Chart Control for Au, Cu and Mo

(PB=pulp blank, CB= coarse blank)

CRMs

Only a brief summary of the control work related to CRMs is presented here. The reader is referred to the references for more detailed information.

Control charts in terms of Standard Deviations (SD) are shown in Figure 27 for ALS and in Figure 28 for Bureau Veritas.

With respect to ALS, there are two reference materials (CRM) that exceed 10% of samples with greater than 3 SD, STRT-03 for Cu (high grade), and PORF-08 for Mo (low Mo). The PORF-08 presents a relative standard deviation RSD >10% in ALS and >6% in BV.

In the ALS laboratory, a high variability of STRT-03 for Au (high-grade Au CRM) is also observed with 8% samples >3SD and RSD>8%. This behavior of STRT-03 was also observed in the Bureau Veritas results with 54% of samples for Cu >3SD. In general, the bias does not exceed the absolute value of 5% in all the CRMs analyzed, both in ALS and in BV, so the results are accepted as good.

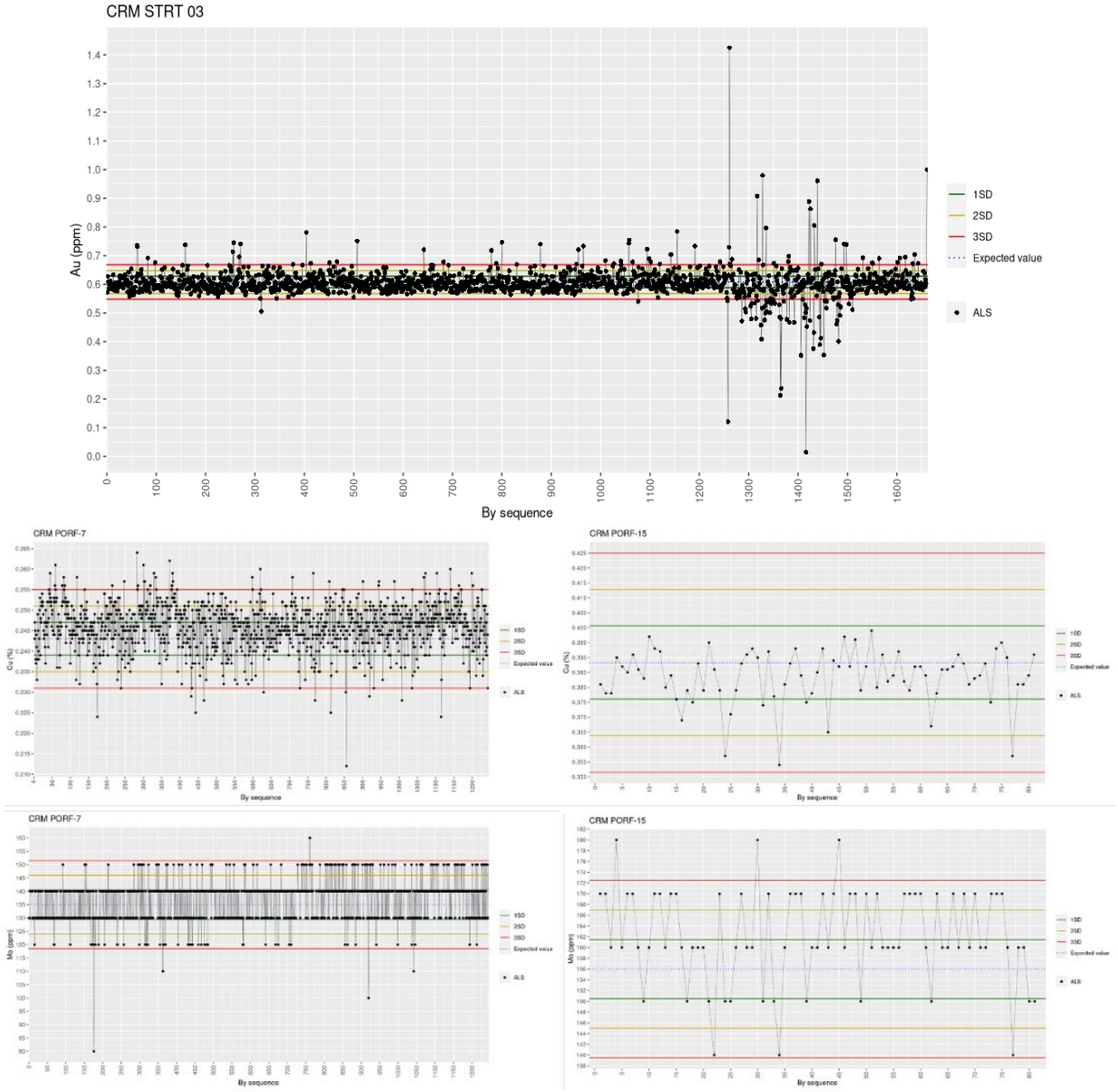

Figure 27: Control Charts of Reference Materials for Au, Cu, and Mo - ALS Chemex Laboratory

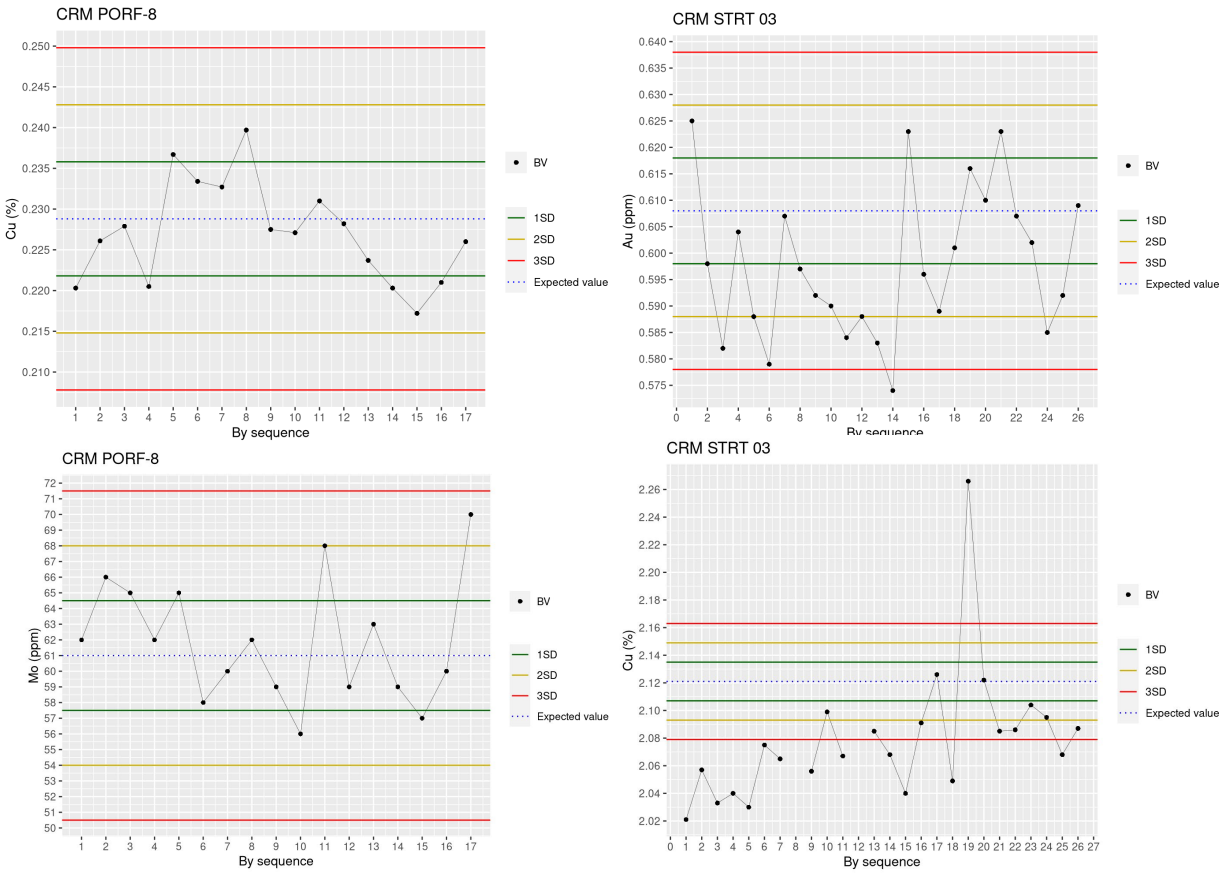

Figure 28: Control Charts of Reference Materials for Au, Cu, and Mo - Bureau Veritas Laboratory

For both ALS and BV laboratories, global bias is good at less than 5%. The difference for all CRMs between their expected values compared to the measured averages is less than 5% (Table 25). In general, ALS values tend to be slightly higher than Mo CRMs, while BV generally obtains lower values for both Cu and Mo.

Table 25: Differences Between Reference Materials Expected, Measured Value and Overall Bias Condition

Primary Lab (ALS)						
CRM / Elements	**Cu_%**			**Mo_ppm**		
	Measured	Expected	Diff (%)	Measured	Expected	Diff (%)
PORF-7	0.246	0.243	-1.15	136.38	135	-1.02
PORF-8	0.233	0.229	-1.66	63.38	61	-3.9
STRT 03	2.070	2.121	2.43	-		
PORF-15	0.384	0.388	1.20	162.35	156	-4.07
PORF-17	0.967	0.981	1.45	250	248	-0.81
Global stats	*Cu_%*			*Mo_ppm*		
Global bias (%)	2.16			1.69		
Coeff. of determination (%)	100			99.98		

Secondary Lab (BV)						
CRM / Elements	**Cu_%**			**Mo_ppm**		
	Measured	Expected	Diff (%)	Measured	Expected	Diff (%)
PORF-7	0.241	0.243	0.76	130.00	135	3.7
PORF-8	0.227	0.229	0.78	61.82	61	-1.35
STRT 03	2.080	2.121	1.94	-		
Global stats	*Cu_%*			*Mo_ppm*		
Global bias (%)	1.91			2.85		
Coeff. of determination (%)	100			99.96		

Notes: Overall bias condition is Good (<5%). Tolerance (Diff. ±5%)

Duplicate Samples

The precision of the field duplicate (quarter core) is acceptable based on the overall relative error for Au (24%) and Cu (16%). The population with relative differences between the MPRD means less than 30%, is 75% for Au, and 86% for Cu.

Low precision is observed in Mo field duplicates with an overall relative error of 39% and only 48% of the population with MPRD less than 30%. The linear correlation coefficient between the original sample and the field duplicate are Au=0.77, Cu=0.95, and Mo=0.72.

The precision of pulp duplicates is acceptable considering that the relative errors obtained are Au 16%, and both Cu and Mo, 12%. BV has 60% of the population, with MPRD less than 15%. ALS has 94% of the population for Cu and 73% of the population for Mo, with an MPRD less than 10%.

The linear correlation coefficients between the original samples analyzed by ALS and the pulp duplicates analyzed by BV are Au=0.99, Cu=0.98, and Mo=0.99.

The accuracy of Mo results improves significantly when pulp duplicates are analyzed. No evidence was found to indicate that the analytical technique was not adequate, a validation of the concentrations with different methods was performed (ASA vs ICP), and no differences greater than 20% were observed between the methods. The QP believes that the lack of precision of Mo is a consequence of the use of quarter cores.

Control charts, including scatterplots, Q-Q plots, AMPRD vs % population, and MPRD vs mean grade, can be seen in Figure 29 (Au), Figure 30 (Cu), and Figure 31 (Mo) for field duplicates checked in the ALS laboratory. Figure 32, Figure 33, and Figure 34 present the corresponding plots for BV results (pulp duplicates).

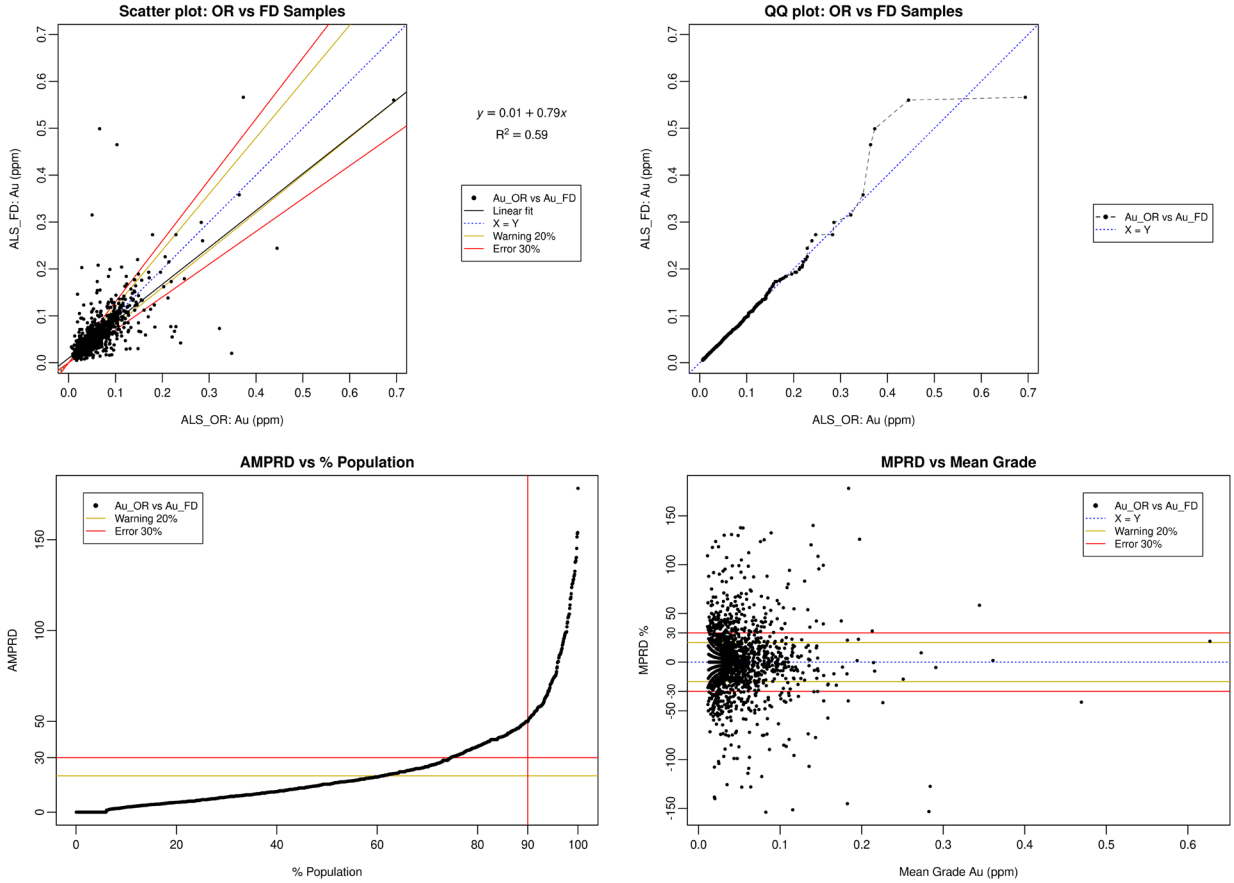

Figure 29: Field Duplicate Control Charts Au – ALS Chemex Laboratory

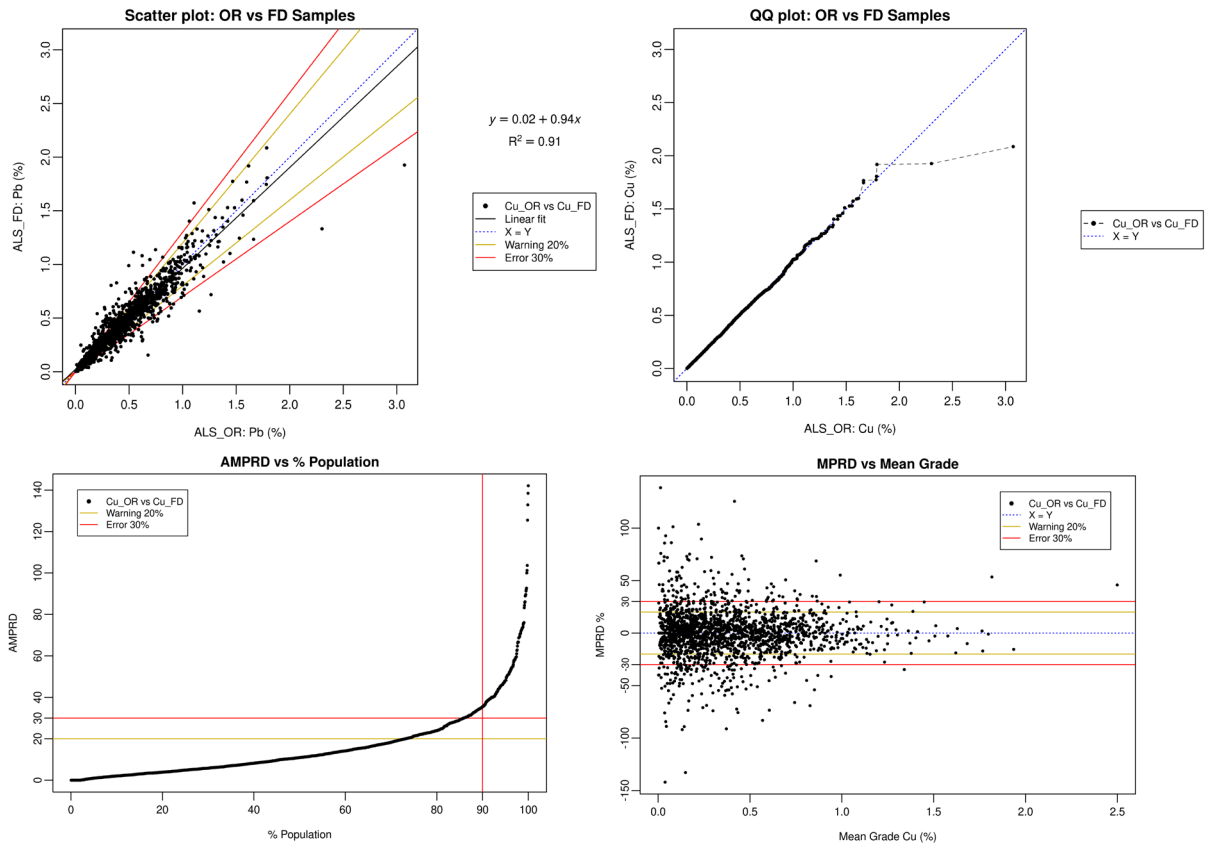

Figure 30: Field Duplicate Control Charts Cu – ALS Chemex Laboratory

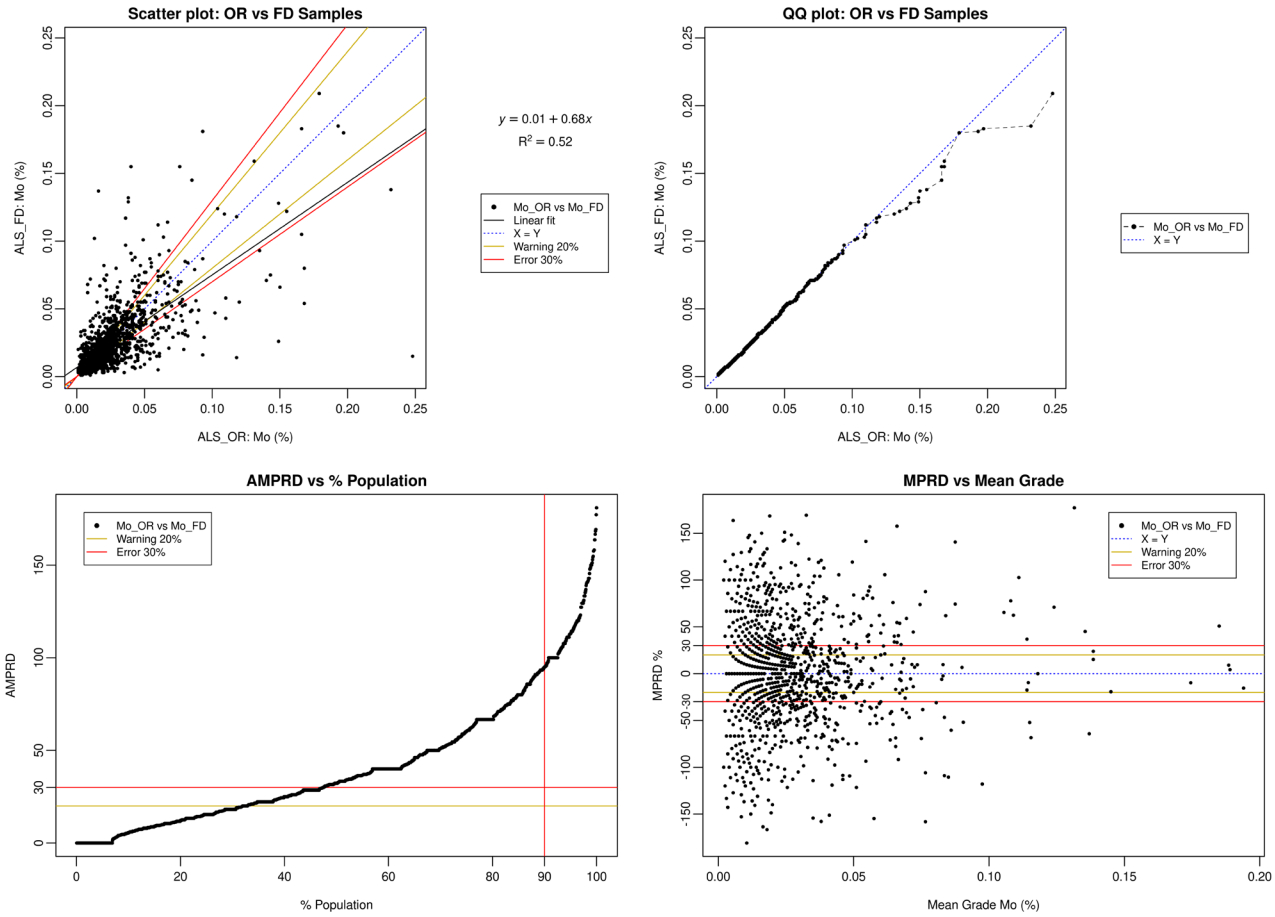

Figure 31: Field Duplicate Control Charts Mo – ALS Chemex Laboratory

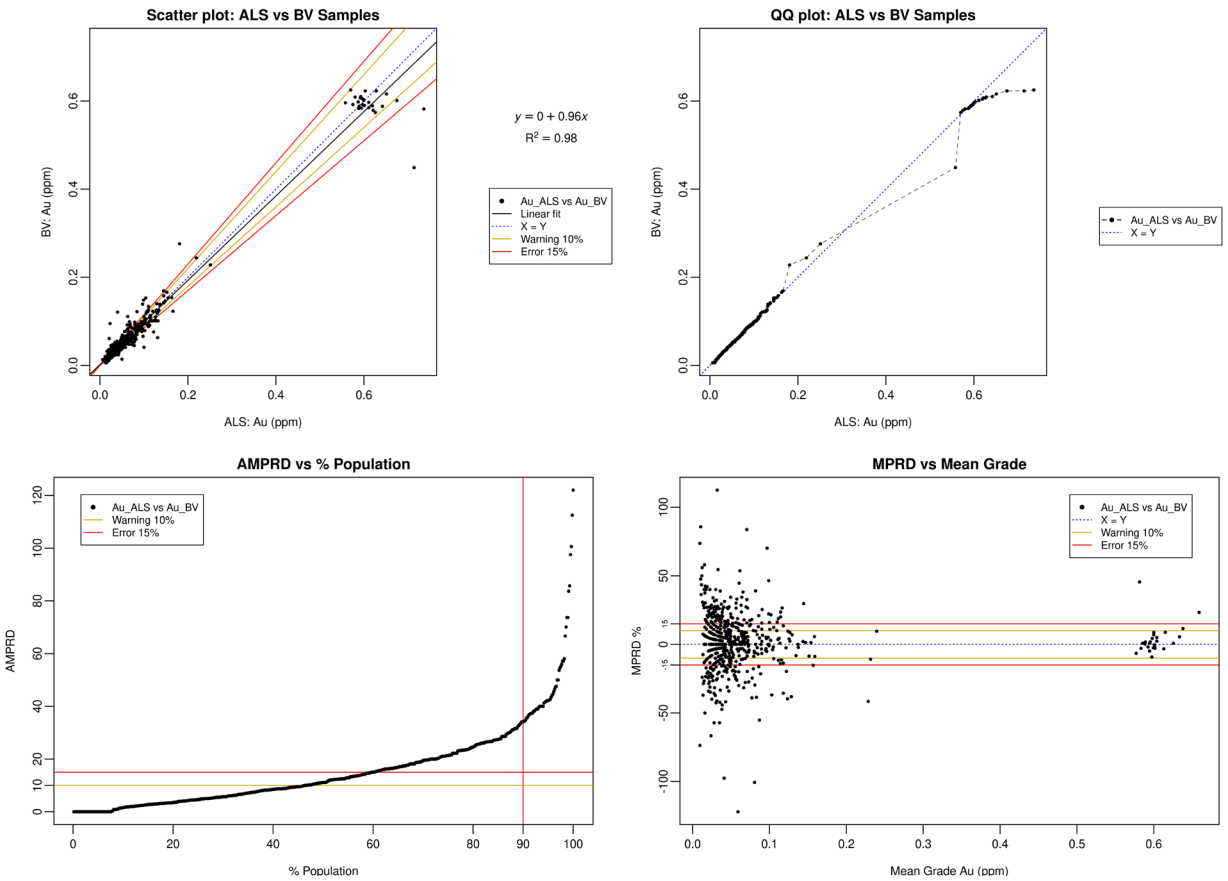

Figure 32: Pulp Duplicate Control Charts Au – Bureau Veritas Laboratory

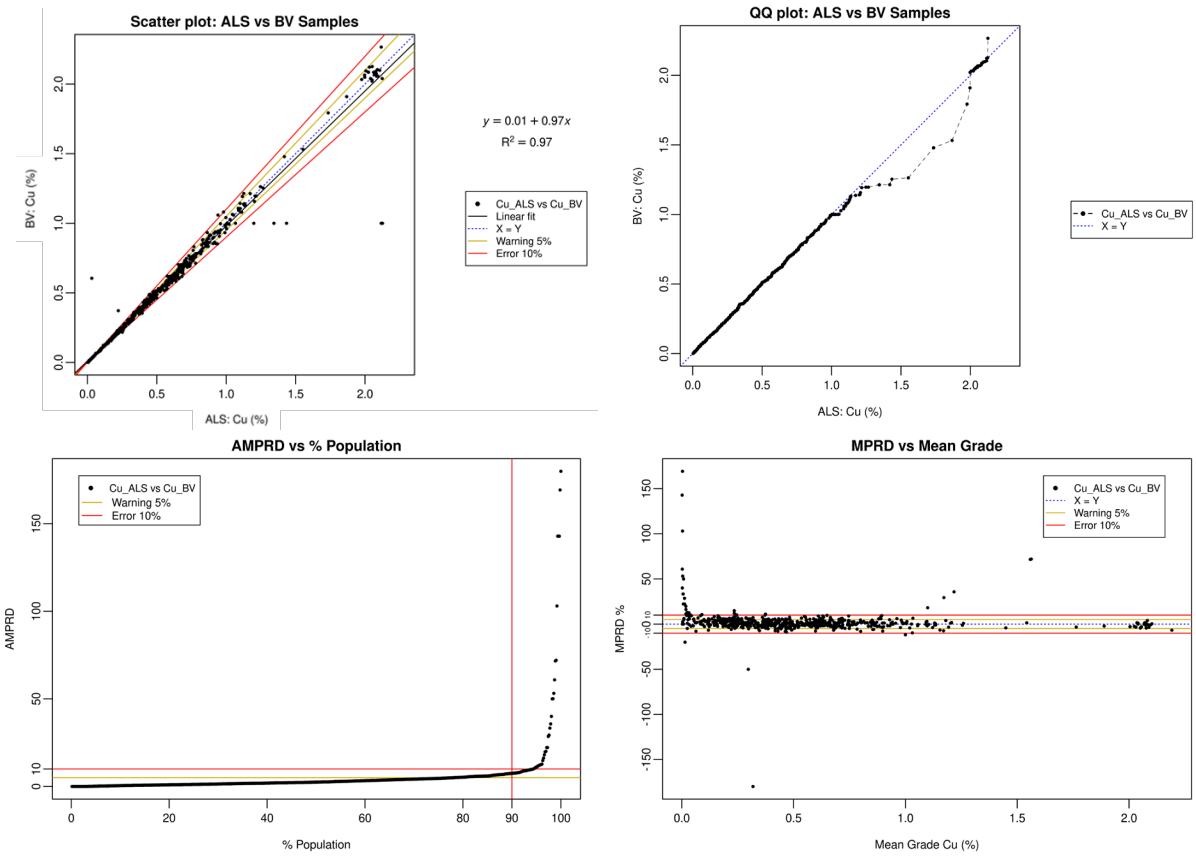

Figure 33: Pulp Duplicate Control Charts Cu – Bureau Veritas Laboratory

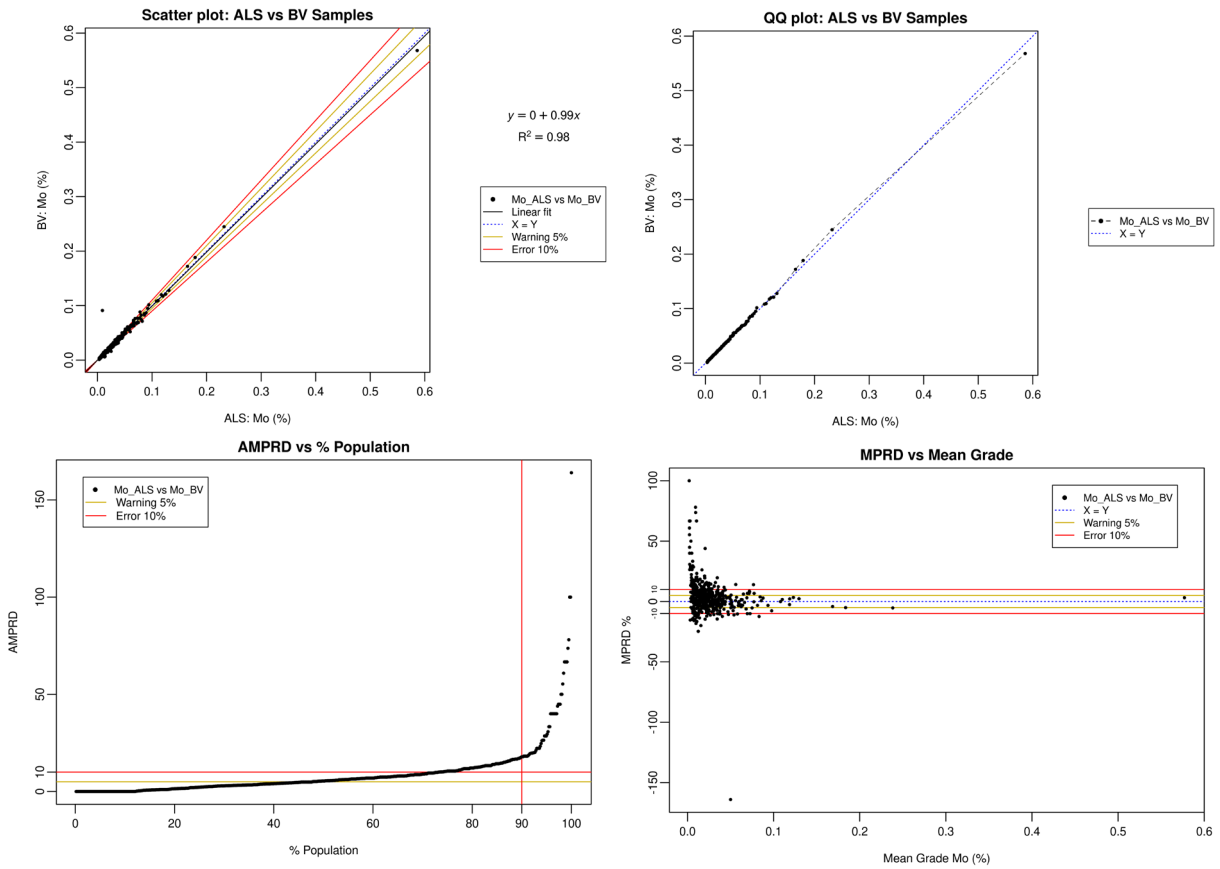

Figure 34: Pulp Duplicate Control Charts Mo – Bureau Veritas Laboratory

11.4 Data Adequacy

11.4.1 2000-2001 Drilling Campaign

In the QP's opinion, the sample preparation, security, and analytical procedures were adequate for the purpose of resource estimation, and the quality assurance and quality control program included regular insertion of reference materials and pulp duplicates into the sample stream. The reference materials were monitored for Cu and had acceptable performance. The reproducibility of the duplicates indicated acceptable analytical precision.

11.4.2 2020-2021 Drilling Campaign

In the QP's opinion, sample preparation, safety, and analytical procedures are adequate for resource estimation. The QP reviewed the QA/QC protocols, monthly and bi-monthly reports, and the database used in this resource estimate. Also, the QP determined, during its visit to ALS Quito, that the QA/QC samples are not blind for the laboratory.

The QP performed its own global QA/QC calculations, some of which have been presented in this report, concluding that they are satisfactory. The QP considers that the reference materials for Au, Cu, and Mo have an acceptable performance; there is little or no cross-contamination in the preparation and analysis processes, and the reproducibility of the field and pulp duplicates indicate an acceptable analytical precision, mainly for Au and Cu, much lower for Mo.

The analytical precision between the ALS and BV laboratories is acceptable. The overall number of check samples employed in the program exceeds the industry standards.

Additionally, two independent consulting companies (Wood PLC and Analytical Solutions) reviewed Warintza's QA/QC program between June and August 2021. The QP agrees with their recommendations with regards to field duplicates, which should be eliminated from the program and replaced with coarse duplicates (after the first stage of size reduction). This is because the style of mineralization introduces a bias mainly related to the style and shape of the Mo veinlets. This causes poor repeatability, in particular, of the Mo results.

11.5 Author's Opinion

It is the opinion of this Author that the sample preparation, security, and analytical procedures used provide reasonable support for the reliability of the sample database for the Warintza deposits under investigation such that it supports mineral resource estimation without limitation on confidence classification.

12.0 DATA VERIFICATION

During 2020 and 2021, Lowell drilled over 58,000 m in 66 drill holes. The total number of samples was 28,915. The QP reviewed Lowell's work in the Warintza Project area and throughout the Quito and Lima facilities.

The QP also audited 30% of Lowell's global database, which includes the 33 old and 66 recent holes. The geological databases (lithology, alteration, and mineralization), Collar, survey, assay, density, PLT, RQD, were delivered in CSV format, exported from Datamine's Fusion X system.

Lowell has well-documented protocols for activities from drilling, sample processing, and shipping to the laboratory. The QP reviewed over 10 different procedures related to sample transport and storage, obtaining geotechnical, geological, physical, geochemical parameters, QA/QC protocols, database administration, and others.

12.1 Drill Hole Location Verification

12.1.1 2020-2021 Drilling Campaign

Lowell conducted a new, detailed topographic survey of the old drill hole collars. The QP checked 30% of the topography certificates against the Collar database and 30% of the gyroscope survey reports. Minor inconsistencies (less than 1% of the total data) were found and corrected, mainly referring to the final depth of the drill holes, which is acceptable.

The QP flew over the Warintza platforms by helicopter and spent one day at the Piunts camp and the PE-01 platform in Warintza East to control the drilling activities and check the SLSE-08 coordinates. At the time of the visit, Kluane Drilling Ltd's drilling and sampling were observed (Figure 35). The planned coordinates were compared with a handheld GPS. No significant differences were found.

Figure 35: Drilling Platform PE-01, Drill Hole SLSE-08

12.2 Geological Data Verification and Interpretation

12.2.1 2000-2001 Drilling Campaign

Geological data from drill core logs and historical surface maps were used to build a new 3D geological model. In general, there is good section-to-section and section-to-surface map correlation of geology, indicating that both the drill hole database and surface mapping has good integrity. Core recovery averaged 94%. There is no relationship between recovery and Cu or Mo grade. While on the May site visit, Cu was verified at an outcrop exposure located approximately 80 m west of drill hole W12. The rock sample database includes two samples from this area that returned elevated Cu. This large creek exposure

is cut by abundant quartz veins and pyrite veins with secondary chalcocite consistent with the supergene enriched zone of the Warintza Central deposit.

12.2.2 2020-2021 Drilling Campaign

Lowell uses the Anaconda method to describe Warintza's geology, which consists of a detailed description of lithology, alteration, mineralization styles, type of veinlets, percentages of minerals, visual estimation of grades, among others. The descriptions are made digitally with Excel forms that contain validated fields.

Lowell also re-logged the old drill holes (W1-W33) using the same methodology. This information was reviewed by the QP in Quito. The QP also visited the PE-01 platform and reviewed the geological monitoring activities, presence of mineralization, and sample packing process for samples from drill hole SLSE-08 (Figure 36).

Figure 36: Meterage Control and Geology, Drill Hole SLSE-08

Working protocols, registries, digitization, and information storage were reviewed at the Piunts camp. The documentation is stored on a Google drive, which is backed up from the offices in Peru through a local server.

12.3 Assay Verification

12.3.1 2000-2001 Drilling Campaign

The following checks were completed, and in some cases, corrections were made to ensure that no sample composite interval exceeds the total depth of its hole. Values below the detection limit were converted

into a one-half the analytical method detection limit. 15% of the compiled assay values were checked against assay files provided directly by ALS. No differences in the values were identified. The QA/QC data was compiled and charted to validate the results and is here considered sufficient for an early-stage project.

10 core samples were collected during the 2019 site visit and compared with historical results for the same core depth intervals. Seven of 10 Cu and Mo re-assays were ~10% lower than the original analyses, whereas duplication of Au assays was somewhat better. Correlation between original analyses and 2019 re-assays is strong for Cu (0.98), Mo (0.95), and Au (0.99). Results of the 2019 re-assay program are less precise than the re-assay program published by Ronning and Ristorcelli (2018), which generally show a <10% difference but are nonetheless considered satisfactory.

12.3.2 2020-2021 Drilling Campaign

The QP reviewed 30% of the assay intervals for Au, Cu, Mo, Ag, Pb, and Zn grades. A first check was carried out against laboratory certificates in CSV and PDF format, both from ALS Chemex and Bureau Veritas. No significant differences were observed, although there are inconsistencies with the values of soluble Cu obtained through the sequential Cu method. Lowell does not use soluble Cu values when the sum of sequential Cu differs with the total Cu value by 30% or more.

A second check was carried out on the drill cores through a visual control of the presence of mineralization and estimation of the metal content versus chemical analysis.

Sampling intervals and detection limits of all techniques were also checked, and some inconsistencies were detected and corrected in the scripts that convert the lower detection limit to half its value. The database follows this methodology (DL/2), which Lowell has well documented in its procedures.

Additionally, six pulp samples (Figure 37) were taken from two drill holes for an independent analysis for Cu. The samples were sent by the QP to the ALS Chemex laboratory in Ireland. The results show a correlation of 0.999, and the grade differences are within ±2% (Table 26).

Figure 37: Pulp Samples Selected for Independent Re-Assaying
Drill Hole SLS-02: Samples PM-00606, PM-00701, PM00851
Drill Hole SLS-34: Samples PM-23428, PM-23472, PM-23569

Table 26: Comparison of Re-Assays (Ck) to Original (Or) Assay Data

#	HoleID	From	To	Or_code	Certif_Or	Cu_AA_pct	GSI_code	Certif_Ck	Cu-OG62_%	ABS_Dif	%_Dif
1	SLS-02	264	266	PM-00606	QI20168947	0.965	GSI-04	SV21313027	0.967	0.002	**0**
2	SLS-02	416	418	PM-00701	QI20178297	1.026	GSI-06	SV21313027	1.010	-0.016	**-2**
3	SLS-02	654	656	PM-00851	QI20187897	0.683	GSI-02	SV21313027	0.671	-0.012	**-2**
4	SLS-34	64	66	PM-23428	QI21226087	0.602	GSI-01	SV21313027	0.615	0.013	**2**
5	SLS-34	134	136	PM-23472	QI21226087	0.789	GSI-03	SV21313027	0.785	-0.004	**-1**
6	SLS-34	290	292	PM-23569	QI21227312	0.481	GSI-05	SV21313027	0.488	0.007	**1**

12.4 Data Adequacy

12.4.1 2020-2021 Drilling Campaign

The data from the 2020-2021 drilling campaign is considered by the Author to be adequate for the purpose of resource estimation. Data collection methodologies are well documented through protocols. All stages of the drilling process, core processing, and QA/QC are completed following such protocols.

The QP has reviewed the accuracy of drill hole collars and sample locations, down-hole deviation, the accuracy and internal consistency of lithological and alteration data, and the accuracy and precision of analytical information. The verification activities included a search for factual errors, completeness of the lithological and assay data, and suitability of the primary data. As part of the database verification activities, the assay information and certificates obtained directly from the analytical laboratory have been examined as well.

In addition, six pulp samples have been chosen and sent for re-assaying, confirming the grades observed in the database within a reasonable degree of accuracy.

The QP's inspections included reviews of the geological and sample information that are used in the preparation of the mineral resource estimate. The QP is confident that the available information and sample density allow preparation of a reasonable estimate of the geometries, tonnage, and grade continuity of the mineralization in accordance with the level of confidence established by the mineral resource categories in the CIM Definition Standards. The database fairly represents the primary information and is suitable to support estimation of a mineral resource.

13.0 MINERAL PROCESSING AND METALLURGICAL TESTING

13.1 Resource Development, Inc., Test Work

In 2002, Corriente commissioned Resource Development Inc. ("RDI") to do preliminary metallurgical testing of three samples of material, one of which was from Warintza Central (Resource Development Inc., 2002). The RDI draft report does not describe the samples, nor their sources, in detail. It does state that "Approximately 75 kg of each sample consisting of analytical rejects of RC cuttings were received for the study." There has been no RC drilling at Warintza, so that description cannot be correct for the sample from Warintza. It is likely that the samples consisted of coarse reject material from the analytical laboratory's preparation facility. The Warintza sample contained only 0.028% acid soluble Cu.

The discussion that follows in the remainder of this section is adapted and abridged from RDI (2002). Whereas the RDI discussion dealt with samples from three projects, only the results for the Warintza sample are used herein. In descriptions of procedures, the plural term ("samples") refers to all the samples, and the singular refers only to the Warintza sample.

The primary objectives of the RDI study were to determine the hardness of the samples, the recoverability of Cu and Au into a Cu concentrate, and the grade of the concentrate. The scope of the test program included sample preparation and head analyses of the samples, Bond's ball mill work index determination, rougher flotation tests at three grind sizes, and a cleaner test on each sample to access product quality.

The Warintza sample contained 437 ppm Mo, but no work was done to assess the recoverability of the Mo.

The samples were crushed to -10 mesh, blended and split into 2 kg charges for flotation test work. A 2 kg charge was pulverized and split for chemical analyses and x-ray fluorescence ("XRF") analyses. The head grade analyses of the Warintza sample for Cu, Au, and Ag are shown in Table 27.

Table 27: Head Grades of Warintza Metallurgical Sample

Cu, %	0.732
Cu (acid soluble), %	0.028
Au, g Au/tonne	0.21
Ag, g Ag/tonne	3.09
Notes: Adapted from part of Table 1 of RDI (2002)	

The samples that RDI received for metallurgical testing were not suitable for Bond's ball mill work index determinations as they were too finely crushed. RDI did receive a separate sample of drill core from another of Corriente's porphyry deposits. Using a Bond's work index determined for that material, RDI used an indirect method to calculate Bond's work indexes for the Warintza and other samples. The results for Warintza appear in Table 28. RDI classified the material as "moderately hard."

Table 28: Calculated Bond's Work Index for Warintza Sample

XF, µm (80% passing feed size)	1382
XP, µm (80% passing product size)	133
Work Index	17.54
Notes: Adapted from part of Table 4 of RDI (2002)	

A series of laboratory grind tests were undertaken to establish the time required to obtain targeted grinds of P80 (80% passing) of 65, 100, and 150 mesh for each sample. In each case, approximately 2 kg of material were ground in a laboratory rod mill at 50% solids for 10, 20, 30, and 45 minutes. The ground material was then de-slimed on a 400-mesh screen, and the products were dried. The plus 400 mesh fraction was dry screened from 20 to 400 mesh. The screen fractions were weighed, and the particle size distribution was determined. The grind time requirements for the Warintza sample appear in Table 29.

Table 29: Grind Time Requirements for Targeted Grind Size

Mesh Size	Grind Time, Minutes
P80 = 65 mesh	20
P80 = 100 mesh	27
P80 = 150 mesh	45
Notes: Adapted from part of Table 5 of RDI (2002)	

Following the grind studies, bench-scale rougher flotation tests were performed at three grind sizes: P80 of 65, 100, and 150 mesh. A simple reagent suite was employed, consisting of lime as a pH modifier, potassium amyl xanthate ("PAX") as a collector, and methyl isobutyl carbonyl ("MIBC") as a frother.

The test procedure consisted of grinding a 2 kg sample with 250 g/T lime in a laboratory rod mill at 50% solids for a known time to obtain the desired particle size. The ground pulp was transferred to a flotation cell, and the pH was adjusted with an additional 20 to 75 g/t lime to obtain a pH of ±8. Collector (60 g/T PAX) and frother (15 g/T MIBC) were added to the pulp and conditioned for one minute. Two concentrates were collected at cumulative times of one and four minutes. The flotation pulp was again conditioned for two minutes with additional collector (20 g/T PAX) and frother (5 g/T MIBC), and a third concentrate was collected at six minutes. The concentrates and flotation tailings were filtered, dried, pulverized, and submitted for Cu analyses. Au and Ag analyses were also obtained for the tailings. The test results for Warintza material are summarized in Table 30.

Table 30: Summary of Rougher Flotation Results

Grind, P80 mesh	Recovery (10 minutes)			Feed		Tailing	Rougher Flotation Conc. Grade, % Cu
	Wt., grams	Cu, %	Au, %	Calculated % Cu	Assayed g Au/T	Assayed g Au/T	
65	16.75	94.4	72.3	0.809	0.21	<0.07	4.56
100	13.84	94.2	71.3	0.804	0.21	<0.07	5.47
150	14.03	94.0	71.3	0.777	0.21	<0.07	5.21
Notes: Copied from part of Table 6 of RDI (2002)							

According to RDI (2002), the highlights of the test results were:

1. The Cu recoveries for Warintza material were in the 94% range in ten minutes of flotation.
2. The majority of the Cu (75% to 90%) floated in four minutes of flotation time.
3. The recovery of Cu was independent of the grind size within the range investigated.
4. The Au recoveries were calculated based on feed and flotation tailing assays.

The Au recovery from the Warintza sample was 71%. The Au may be associated with Cu minerals.

One open-circuit cleaner flotation test was performed on each sample to determine the quality of the possible product. No attempt was made to optimize the process conditions in the cleaner circuit. The test conditions for the cleaner flotation were selected based on RDI's previous experiences treating primary Cu ores.

The test procedure consisted of floating a rougher concentrate at a primary grind of P80 of 100 mesh with lime, PAX, and MIBC for ten minutes. The rougher concentrates were reground for 15 minutes in a laboratory ball mill. The pH of the ground pulp was adjusted to 10.5 with lime and conditioned for one minute with 10 g/T PAX and 5 g/T MIBC. The first cleaner concentrate was collected for four minutes. The first cleaner concentrate was re-cleaned in second-cleaner flotation at pH>10.5 and three timed concentrates collected for cumulative times of 0.5, 1, and 2.5 minutes. The products were analyzed for Cu, and the first second-cleaner concentrate was also analyzed for Au.

The product quality of the second-cleaner 0.5 minute and 2.5-minute concentrate products are shown in Table 31.

Table 31: Second-Cleaner Concentrate Product Quality

	0.5 Minute Product	2.5 Minute Product
Cu, %	15.1	11.93
g Au/T	1.23	
Notes: Adapted from part of Table 7 of RDI (2002).		

In commenting on the test results, RDI (2002) noted that:

1. Concentrate grades in the Warintza sample were postulated to have been lower than might have been achieved, due to the presence of pyrite, which also floats readily and may have gone into the concentrate with the Cu minerals. A higher flotation pH, greater than 11, may be required to depress the pyrite in the concentrate.

2. Additional testing may be required to optimize the regrind time and cleaner flotation process conditions to determine the quality of product that can be produced in the second cleaner concentrate.

RDI (2002) stated that, based on its experience of other similar primary Cu deposits, it is likely that a Cu concentrate assaying 24% to 28% Cu could be produced. RDI indicated a need for additional testing.

13.2 Current Testing

13.2.1 Mineralogy / Comminution Test Work Completed

Warintza has commissioned a preliminary metallurgical test work program with FLSmidth USA Inc. for the Warintza Project, utilizing core from the latest exploration drilling campaign. The test work program is in early stages, and only mineralogy and comminution test work are complete at the time of this report. The metallurgical flotation test work plan is outlined below and commenced in Q1 2022.

Mineralogy Report

Warintza submitted seven core samples to FLSmidth USA Inc. for a metallurgical test work program, which included mineralogy and liberation analysis, comminution test work, and flotation test work. The samples were combined into one master composite utilizing equal weight per sample to form the master composite.

The master composite went through a 25-minute grind cycle and resulting P80 of 138 microns. Polished sections were prepared from this sample for QEMSCAN analysis. Table 32 presents the QEMSCAN bulk mineralogy of the master composite sample. Gangue mineralogy matches well with the XRD data. Quartz and muscovite are in main gangue phases. K-feldspar, plagioclase, clays, and chlorite are the minor gangue phases detected. Traces of calcite, iron, oxides, biotite, rutile, and apatite are also present. Pyrite and chalcopyrite are the main sulfides. Traces of bornite, chalcocite, and covellite are present.

Table 32: QEMSCAN Bulk Mineralogy

	Master Comp
Minerals	Wt.%
Chalcopyrite	1.48
Bornite	0.05
Chalcocite	0.08
Covellite	0.07
Cu Carbonate	0.00
Chrysocolla	0.00
Cu/Chlorite	0.00
Cu/Biotite	0.00
Cu/Muscovite	0.01
Cu Bearing Clays	0.00
Cu Wad (SiMnFe)	0.00
Fe Oxide (Cu)	0.00
Other Cu	0.00
Molybdenite	0.07
Pyrite	6.21
Quartz	43.79
K_Feldspar	3.19
Plagioclase	2.35
Muscovite	33.03
Biotite	0.38
Chlorite	2.45
Smectite/Kaolinite	4.56
Calcite/Dolomite	0.56
Iron Oxide	0.18
Rutile/Ilmenite	0.34
Apatite	0.16
Gypsum	0.81
Other	0.22

Chalcopyrite is the main Cu bearing sulfide followed by chalcocite, covellite, and bornite. Traces of Cu bearing gangue phases are present, but the sum of all non-sulfide Cu represents less than 1% of the Cu in the sample. Table 33 and Figure 38 present the Cu deportment of the master composite.

Table 33: QEMSCAN Cu Deportment

	Master Comp
Minerals	Dist.%
Chalcopyrite	78.28
Bornite	5.08
Chalcocite	9.22
Covellite	6.78
Cu Carbonate	0.03
Chrysocolla	0.05
Cu/Chlorite	0.06
Cu/Biotite	0.00
Cu/Muscovite	0.20
Cu Bearing Clays	0.00
Cu Wad (SiMnFe)	0.00
Fe Oxide (Cu)	0.01
Other Cu	0.27

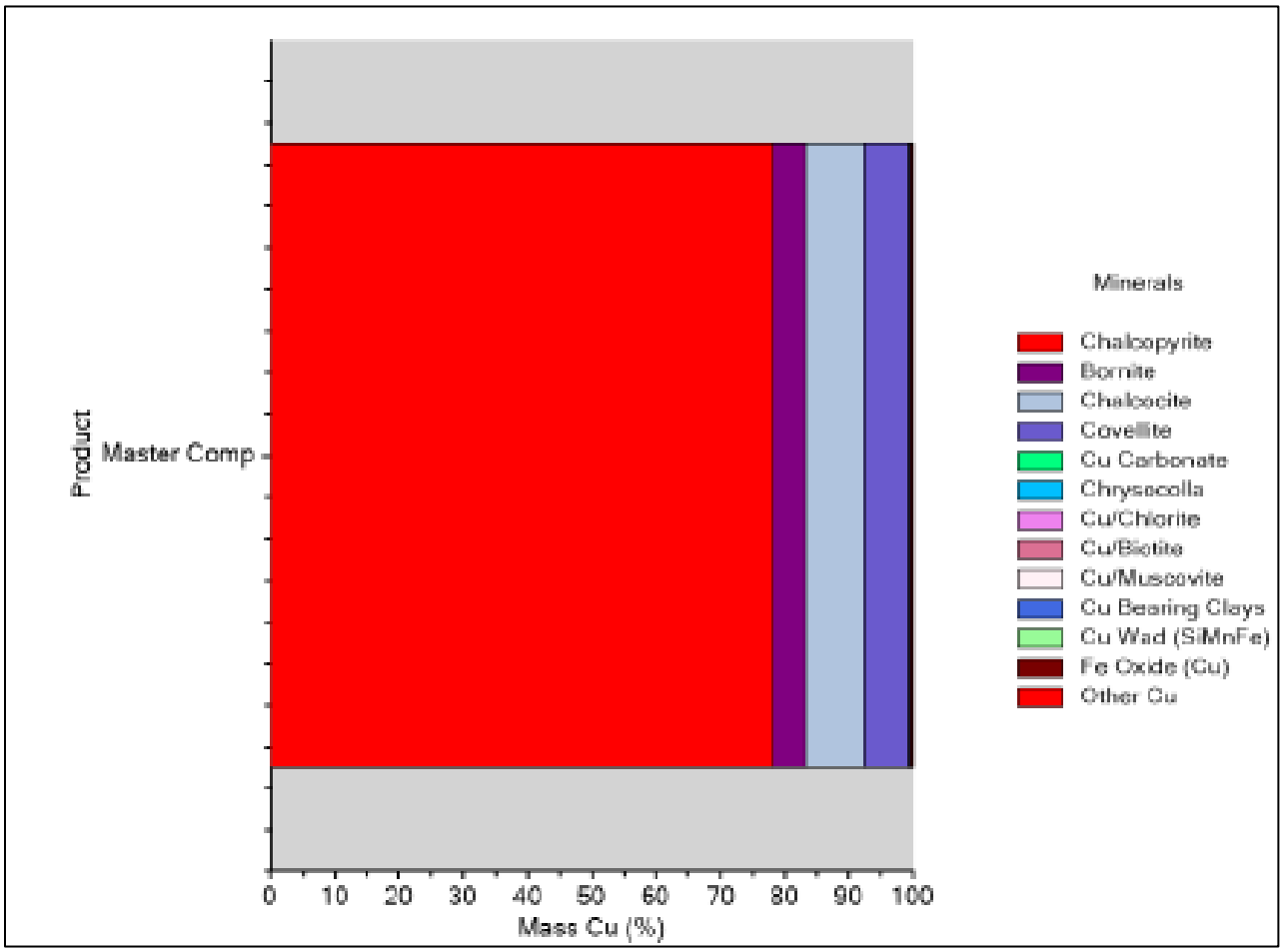

Figure 38: QEMSCAN Cu Deportment

Bright phase searches were conducted to prepare maps of particles containing sulfide minerals. These particles were separated into liberation classes for Cu sulfides (all Cu sulfides grouped together) and pyrite. Definitions for these classes are:

- Liberated – Surface area percent of mineral > 80%
- Middling – Surface area percent of mineral > 20%
- Locked – Surface area percent of mineral > 0%
- Encapsulated – Surface area percent of mineral = 0%
- Barren – No mineral interest present

The results of the liberation analysis separated into the liberation classes above can be found in Table 34. The particle sizes are electronic and not physical sized fractions. The data is not as robust as measurements on physically sized material due to the potential of stereological biases, but it provides a good rapid indication of the liberation and mineral grain sizes. The results illustrate that 73% of the Cu sulfides are liberated and 17% are in middling. This is a high level of liberation of Cu sulfides.

Table 34: Cu Sulfide Liberation (Distribution % of Cu Sulfides)

	Size (microns)							
Liberation Class	>150	>100	>75	>53	>20	>10	<10	Total
Lib	2.09	3.72	5.38	9.69	28.72	15.46	7.97	73.02
Mid	1.27	0.47	2.61	1.51	5.04	3.61	2.70	17.19
Locked	2.05	2.11	1.52	1.16	1.31	0.24	0.14	8.53
Encapsulated	0.28	0.29	0.25	0.17	0.21	0.05	0.01	1.25
Barren	0.00	0.00	0.00	0.00	0.00	0.00	0.00	0.00
Total	5.69	6.58	9.76	12.53	35.27	19.36	10.82	100.00

The liberation analysis for the distribution percent of pyrite in the Cu sulfide can be found in Table 35. Less than 0.5% of pyrite is contained in liberated and middling categories of Cu sulfides. There are no strong associations of pyrite and Cu sulfides that could lead to low concentrate grades.

Table 35: Cu Sulfide Liberation (Distribution % of Pyrite)

	Size (microns)							
Liberation Class	>150	>100	>75	>53	>20	>10	<10	Total
Lib	0.00	0.00	0.00	0.00	0.00	0.00	0.00	0.01
Mid	0.00	0.00	0.28	0.00	0.05	0.05	0.01	0.39
Locked	5.70	2.70	1.80	1.91	0.91	0.13	0.02	13.17
Encapsulated	1.33	1.40	0.00	0.28	0.17	0.00	0.00	3.17
Barren	18.53	17.47	9.86	12.85	17.54	5.06	1.98	83.27
Total	25.56	21.56	11.94	15.04	18.66	5.24	2.01	100.00

Approximately 99% of pyrite is liberated or in middling particles (Table 36). Pyrite is significantly coarser than the chalcopyrite. 47% of pyrite is in particles coarser than 100 microns while only 12% of Cu sulfides are on particles coarser than 100 microns.

Table 36: Pyrite Liberation (Distribution % of Pyrite)

	Size (microns)							
Py Liberation	>150	>100	>75	>53	>20	>10	<10	Total
Lib	21.59	19.07	10.47	13.93	17.90	4.75	1.71	89.43
Mid	3.67	2.07	1.35	0.92	0.66	0.46	0.28	9.40
Locked	0.29	0.35	0.09	0.18	0.09	0.03	0.01	1.04
Encapsulated	0.01	0.07	0.03	0.01	0.01	0.00	0.00	0.13
Barren	0.00	0.00	0.00	0.00	0.00	0.00	0.00	0.00
Total	25.56	21.56	11.94	15.04	18.66	5.24	2.01	100.00

Gangue mineralogy of all samples is dominated by quartz and muscovite. Clays are present in each sample but in amounts that should not cause concerns during grinding and flotation. Self-floating gangue minerals were not detected. The major sulfide minerals are chalcopyrite and pyrite. There is a presence of secondary Cu sulfide in the master composite but in low amounts (<0.1 wt%) The Cu sulfides are well liberated and do not show a high level of association with pyrite. It is expected that high concentrate grades should be achievable without high iron contamination from pyrite.

Assay Report

The master composite was assayed and measured by ICP-OES for all elements except for Au, which was measured via fire assay. Additional elements were assayed but not listed in the table because each element tested below the detection limit. Table 37 illustrates the assay results for each sample and master composite. Table 38 illustrates the detection limit for elements assayed and not listed.

Table 37: Head Assays for Samples and Master Composite

Sample	Au	Cu	Fe	Mo	$S_{(total)}$	$S^{=}$	Si
	ppm	wt.%	wt.%	wt.%	wt.%	wt.%	wt.%
P1	0.12	0.86	2.54	0.04	2.32	2.23	32.95
P2	0.09	0.66	4.32	0.02	5.47	3.46	22.60
P3	0.07	0.48	4.00	0.03	4.01	3.69	28.51
P4	0.03	0.33	4.24	0.02	4.91	4.33	22.95
P5	0.21	0.26	3.08	0.05	2.54	2.46	26.95
S1	0.08	0.54	3.88	0.02	4.95	4.33	22.64
S2	0.07	1.11	3.30	0.06	4.08	3.52	27.09
Master Composite	0.15	0.67	4.19	0.03	4.07	2.83	28.23

Table 38: Detection Limits for Elements Assayed and Not Listed

Element	Detection Limit, ppm
Ag	3.4
As	6.8
Bi	6.9
Pb	66
Zn	69

SMC and BWi Test work

The comminution test work included an SMC test and Bond ball mill work index on the master composite by SMC testing Pty Ltd. and JKTech. The SMC Test was conducted on the -31.5 mm/+26.5 mm size fraction of the master composite. Table 39 provides the summary results from the SMC test.

Table 39: Summarized SMC Test Results

Sample	A x b	T_a	SG	SCSE, kWh/m^3	DWi, kWh/m^3	M_{ia}, kWh/mt	M_{ih}, kWh/mt	M_{ic}, kWh/mt
Master Composite	36.8	0.35	2.7	10.26	7.36	21.0	15.8	8.2

- SCSE is the SAG Circuit Specific Energy
- M_{ia} is the work index for the grinding of coarser particle (> 750 µm) in tumbling mills (e.g., AG, SAG, rod and ball mills)
- M_{ih} is the work index for the grinding in High Pressure Grinding Rolls (HPGR)
- M_{ic} is for size reduction in conventional crushers

After completing the SMC Test, the entirety of the master composite sample was stage-crushed to 100%, passing 19.0 mm in preparation for the BWi test. After crushing, the material was thoroughly blended, and the BWi test was ran to specifications provided in the original test practices as outlined in Angove & Dunne (1997), Kaya & Thompson (2003), and Mosher & Tague. The BWi test feed sample was screened and stage-crushed to minus 3.35 mm (6 Mesh) as per test specification. The BWi results were run with a closing size of 150 microns. Several quality control measures, as well as rigorous closing criteria listed below, were followed.

1. Minimum of six cycles
2. Average grams per mill revolution less than 3% for last three cycles with inflection
3. Within five to 10 grams of undersize target weight
4. Circulating load ratio 2.47 or higher
5. Only last cycle wet screened for product P80 size (semi-log interpolated)

The BWi test results are summarized in Table **40**, while the scale ranges for the classification of the BWi are shown in Table **41**.

Table 40: Bond Ball Mill Work Index (BWi) Summarized Test Results

Sample	Feed % Passing Closing Size (150 µm)	F_{80}, µm	P_{80}, µm	Gbp	Bond Ball Mill Work Index		Classifi-cation
					kWh/short t	KwH/metric t	
Master Composite	18.6	2141.0	114.6	1.40	14.9	16.4	Medium-Hard

Table 41: Ball Mill Work Index (BWi) Hardness/Resistance to Breakage Classification Ranges

Classification	Units	Very Soft	Soft	Medium	Hard	Very Hard
BWi	kWh/short t	<7	7-9	10-14	15-20	>20

13.3 Planned Metallurgical Test Work Scope (New Sample)

Grind Studies

Master composite and variability samples to determine Laboratory grind times and curves on each sample to achieve the target P80. Three varying grind times will be used.

Floatation Testing:

One master composite:

- Reagent screening tests to select appropriate depressants and collectors.
- Primary grind evaluation to determine recovery vs. grind size.

- Cleaner floatation testing to determine appropriate regrind sizes and cleaner circuit configurations.

Eight variability samples for evaluation of optimized flotation kinetics.

Master Composite Rougher Kinetic Flotation Testing

Kinetic rougher floatation tests are planned to delineate a robust reagent scheme on the master composite. Depressants for non-sulfide gangue will be evaluated. Lime will be evaluated for pyrite depression. Collectors and xanthates will also be evaluated.

Reagent screening will be followed by a primary grind size floatation series at the selected reagent scheme. Three grind size rougher flotation tests with P80 values ranging between 53 um to 150 um will be conducted.

The rougher flotation tests will be conducted in kinetic format with four products (three concentrates and final tailings). Products will be assayed for Cu, Au, Mo, Ag, Fe, total sulfur (St), and sulfide sulfur.

A confirmation rougher test on the master composite will be conducted for product size by size analyses on the combined rougher concentrate and tailings. Mineralogical characterization of select floatation products may be beneficial and will be recommended.

Master Composite Cleaner Floatation Testing

A preliminary cleaner flotation test will be performed on rougher concentrate generated from 4 kg of ore to determine regrinding characteristics in the laboratory regrinds mills. Cleaner flotation is expected to be conducted through three stages of cleaning. Three grind size P80 values will be targeted: no regrind, 53, and 25 um.

All batch cleaner floatation tests will be conducted in open-circuit, and products will be assayed for Cu, Au, Ag, Mo, Fe, and S. Final concentrates will also be assayed for the 29 element ICP suite. Mineralogical characterization of select flotation products may be beneficial and will be recommended.

Individual Variability Rougher Kinetic Flotation Testing

The appropriate floatation parameters delineated from the master composite tests will be used in the test work on individual samples to determine ore variability. The rougher flotation tests to determine optimal parameters will be conducted in kinetic format with four products (three concentrates and final tailings). Products will be assayed for Cu, Au, Mo, Ag, Fe, Sulfide Total, and Sulfide Sulfur.

13.4 Sample Representativity

The test samples used in previous and in the current testing program are believed to be representative of the mineralization style and type present at Warintza.

At this stage of testing and development, there are no known elements or factors that can have a material impact on the potential economic extraction of the Warintza mineralization.

14.0 MINERAL RESOURCE ESTIMATES

14.1 Database

The Warintza exploration database consists of 99 inclined surface diamond drill holes for a total of over 64,500 m of drilling as shown in Table 42.

As shown in Figure 39, drill holes have varying orientations. Most drill holes are surveyed at 30 m intervals down the hole using a Reflex single shot camera. The sampling interval is mostly 2 m down the hole but with samples from older drill holes at 5 m, 1 m, and other lengths. There are 40,080 samples in the exploration drill hole database used for this Resource estimate.

Table 42: Summary Warintza Drill Database

Target	# Drill Holes	Meters Drilled	Years
Warintza Central	33	6,530	2000-2001
Warintza Central	56	48,265	2020-2021
Warintza East	8	8,050	2021
El Trinche	2	1,696	2021
Total	**99**	**64,541**	

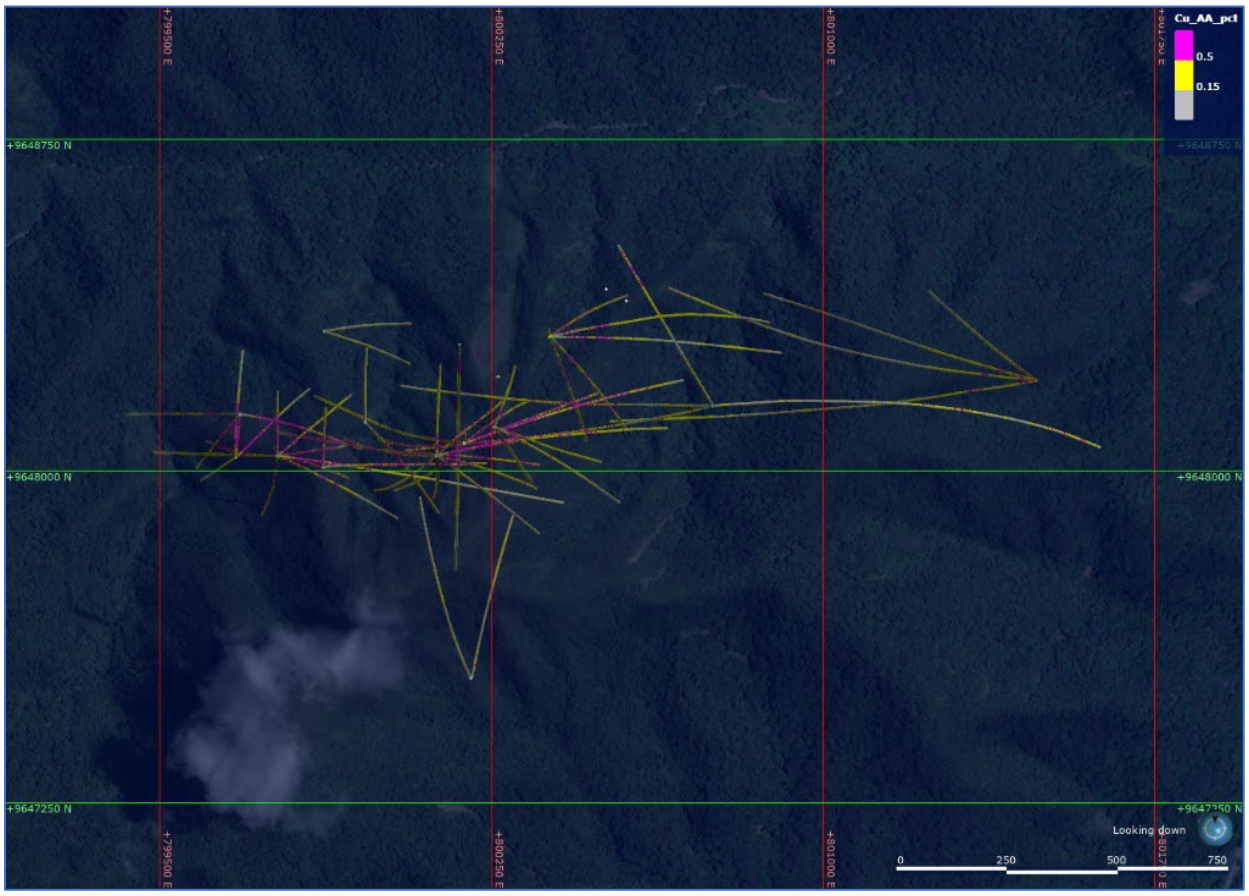

Figure 39: Plan View of Warintza Central, Warintza East, and El Trinche Drill Holes

There are also 1,620 in-situ density measurements collected using a wax-coat water immersion method or which 1,599 were used to estimate and assign densities to the block model as explained below.

The total Cu values obtained from the sequential Cu analysis was compared to the independent total Cu value. The percentage ratios of soluble Cu were estimated to correlate with the mineralogy of the enriched and primary species. It should be noted that there is no significant Cu oxide mineralization in Warintza, as described before. For this reason, the usefulness of the sequential Cu information is limited because it is expected that, based on current mineralogical information, all the mineralization within Warintza would be processed as sulphide mineralization. Therefore, sequential Cu assays aid in the definition of mineralization zones but otherwise do not have a direct impact on resource estimates or reporting.

Subsequently, the database in Leapfrog v.2021.2.4 was reviewed for an evaluation and confirmation of intervals, final depths, survey control, drilling intersections, and 3D geological model. The solids of mineralized zones (variable ZMIN) were also reviewed based on the grades of total Cu and soluble Cu. The minimum modelled thickness was also controlled, which is currently 5 m.

14.2 Exploratory Data Analysis

The Cu grade distribution in assays is, as expected, characteristic of a porphyry Cu-Mo-Au deposit. Figure 40, Figure 41, and Figure 42 show the global raw histogram and basic statistics for Cu, Mo, and Au grades, respectively.

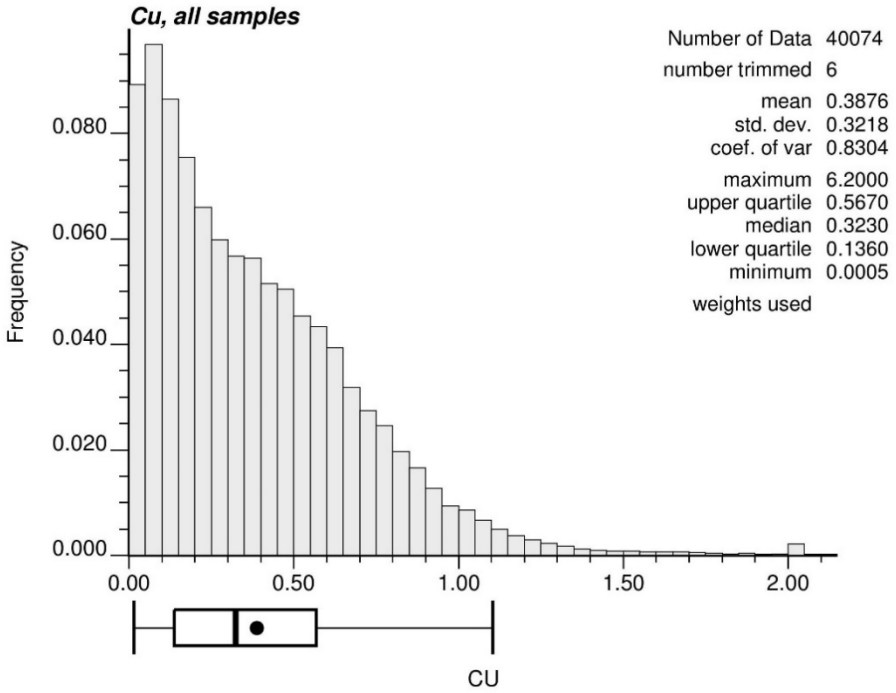

Figure 40: Warintza Global Histogram and Basic Statistics, Cu (%)

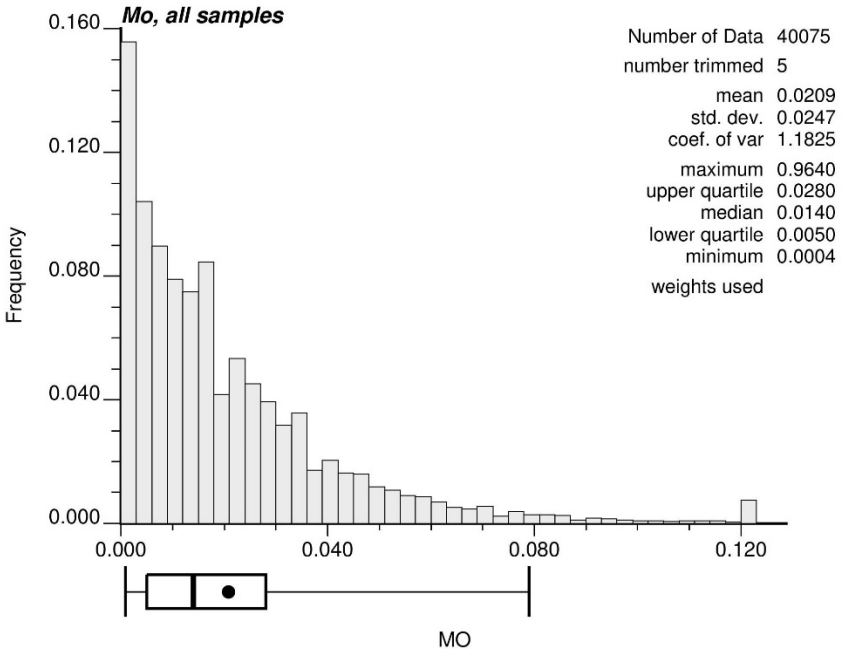

Figure 41: Warintza Global Histogram and Basic Statistics, Mo (%)

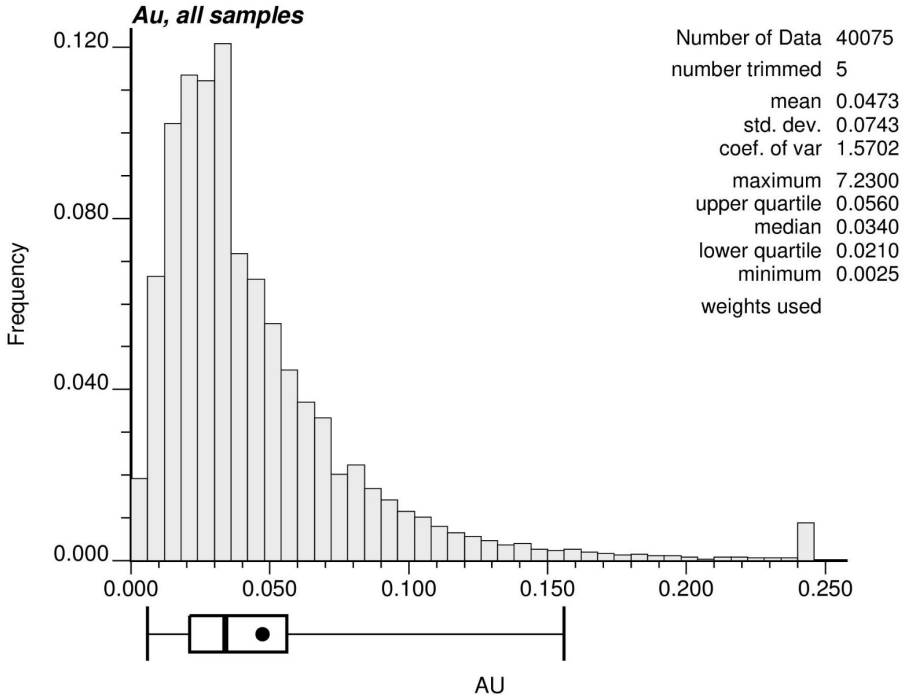

Figure 42: Warintza Global Histogram and Basic Statistics, Au (g/t)

14.2.1 In-situ Bulk Density

There are 1,390 values in the database for in-situ density. These samples have been obtained using the immersion method. A box plot of in-situ density values by lithology is presented in Figure 43.

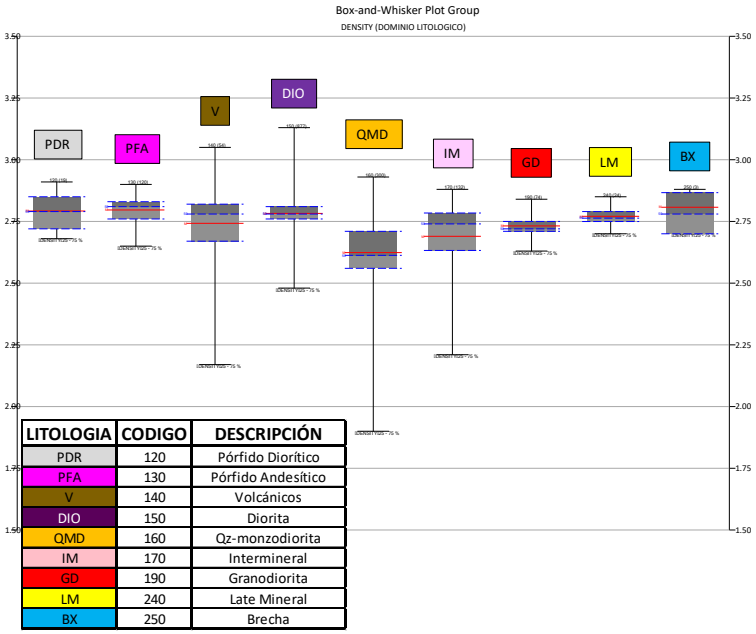

LITOLOGIA	CODIGO	DESCRIPCIÓN
PDR	120	Pórfido Diorítico
PFA	130	Pórfido Andesítico
V	140	Volcánicos
DIO	150	Diorita
QMD	160	Qz-monzodiorita
IM	170	Intermineral
GD	190	Granodiorita
LM	240	Late Mineral
BX	250	Brecha

Campaign	Number of Drillholes	Density Samples
2020	9	255
2021	44	1344
Totals	**53**	**1599**

Figure 43: Box and Whisker Plot, In-situ Bulk Density Values by Lithology

14.3 Geological Models and Estimation Domains

The Warintza geologic model is composed of models for three main geologic variables: lithology, alteration, and mineralization zones.

The logging from the drill hole intervals is pre-processed within the software Leapfrog to define the units to be modelled, using a 5 m minimum width for each unit and discarding those logged lithologies, alterations, and mineralization zones that have little or no volumetric representation.

This pre-processing of geologic codes results in the modelling codes shown in Table 43, Table 44, and Table 45 for lithology, alteration, and mineralization zones, respectively. Note that for each alphanumeric logging code, a numeric code has been assigned, which is used then for all further analysis in the drill hole data and block model.

Examples of working cross sections for lithology, alteration, and mineralization zones are shown in Figure 44, Figure 45, and Figure 46, respectively. While they do not correspond to the final model used, these are presented here as examples of the process undertaken to verify the logged drill hole information as it is updated from the field on a daily basis against the existing modelled geology.

The drill holes were backtagged (flagged) with the information from the three-dimensional models of lithology, alteration, and mineralization zone. This created in the database a new field with geologic codes, which was compared to the original logged information. The percent coincidence was obtained for each pairing of lithology, alteration, and minzone codes (original logged vs backtagged from interpreted models) and found the differences acceptable. The detailed information is available as backup.

In the modelling and definition of the estimation domains that follow, the backtagged codes were used to ensure consistency with the 3D geologic models.

Table 43: Lithology Codes Used in Modelling

LITHOLOGY	CODE	DESCRIPTION
PDR	120	Dioritic Porphyry
PFA	130	Andesitic Porphyry
V	140	Volcanics
DIO	150	Diorite
QMD	160	Qz-monzodiorite
IM	170	Inter-mineral
GD	190	Granodiorite
LM	240	Late Mineral
BX	250	Breccia

Table 44: Alteration Codes Used in Modelling

ALTERATION	CODE	DESCRIPTION
NA_CA	311	Calco-Sodic
POT_BT	321	Potassic_Biotite
SV	331	Green Sericite
PRO	351	Propilitic
QSER	361	Qz-Sericite
SE_ARC	381	Sericite-Clays

Table 45: Mineralization Zone Codes Used in Modelling

MINERALIZATION	CODE	DESCRIPTION
PY>CPY	410	Pyrite>Chalcopyrite
CPY>PY	420	Chalcopyrite>Pyrite
BL	430	Low Grade
ESE	440	Supergene Enrichment
PLIX	450	Partial Leached
LIX	460	Leached

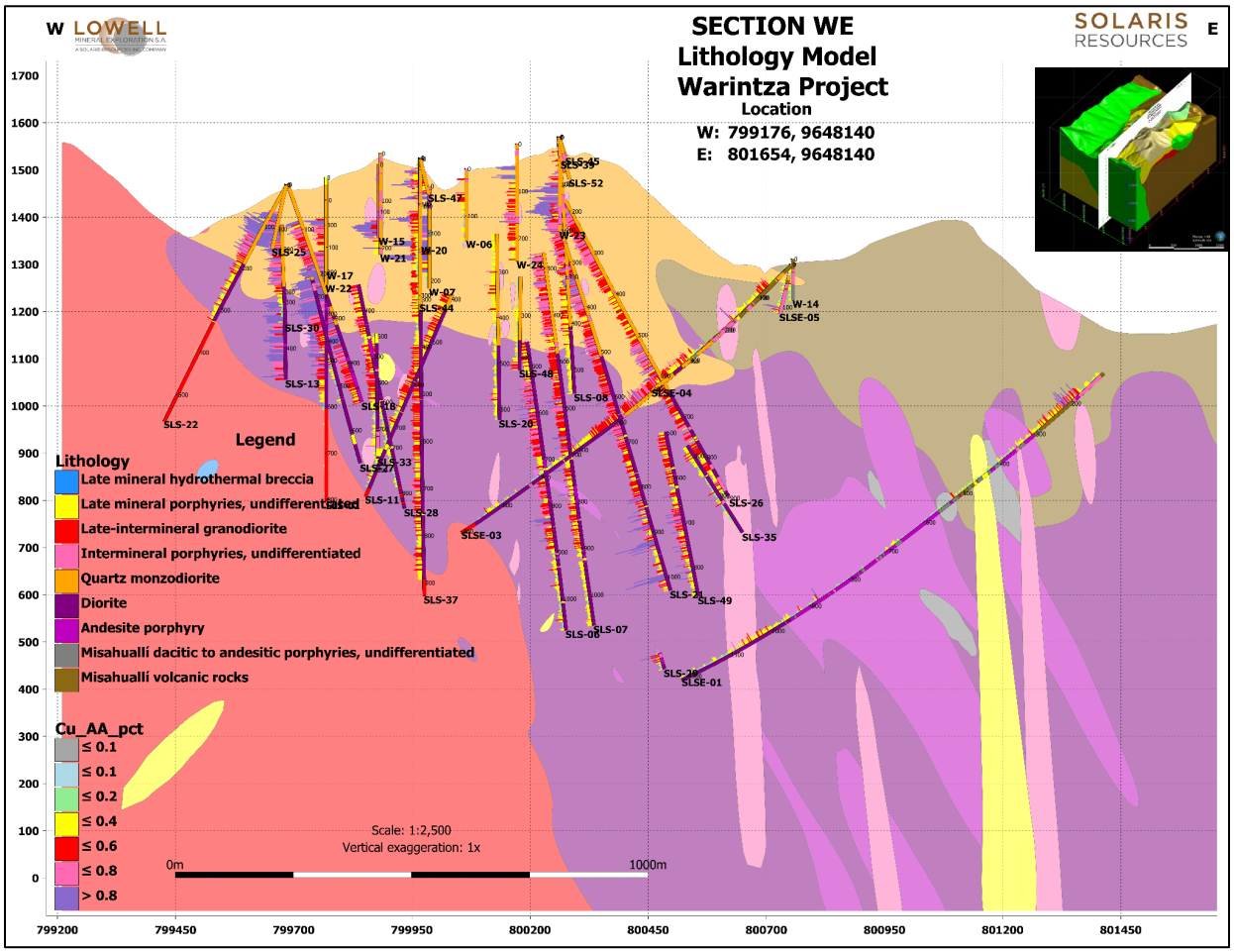

Figure 44: Warintza Cross Section, Interpreted Lithology, and Supporting Drill Data
Source: Solaris Resources Inc. (2022)

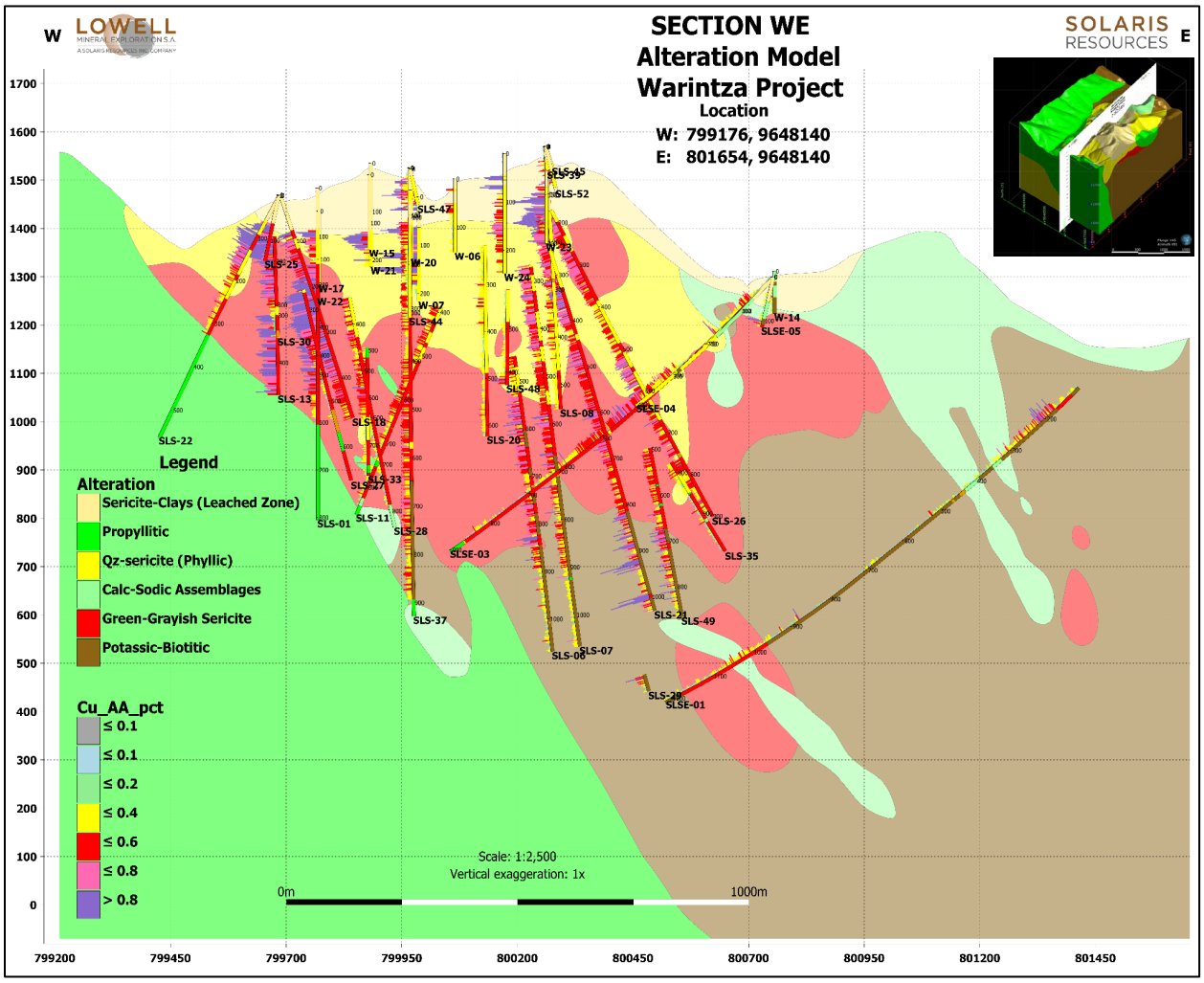

Figure 45: Warintza Cross Section, Interpreted Alteration, and Supporting Drill Data
Source: Solaris Resources Inc. (2022)

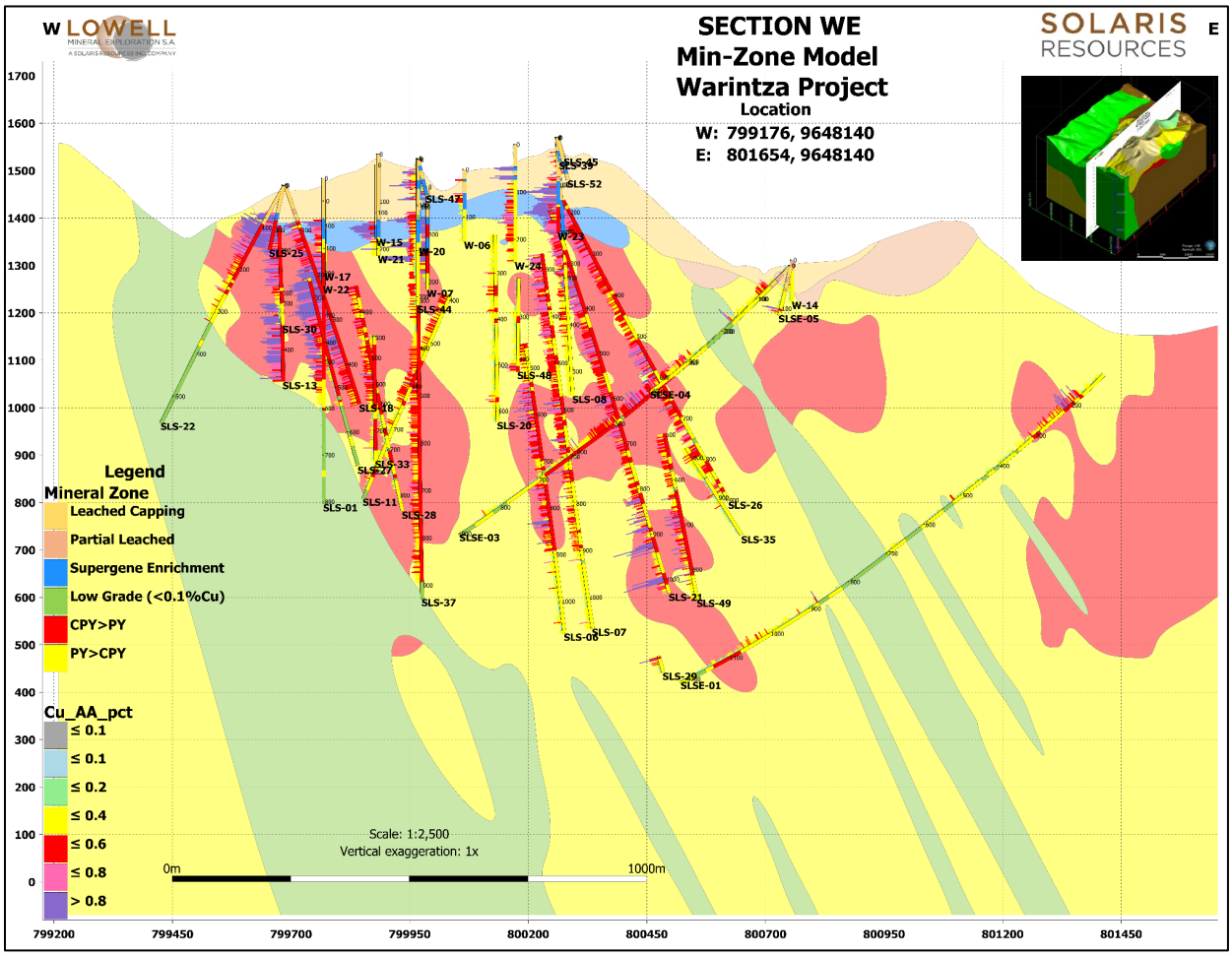

Figure 46: Warintza Cross Section, Interpreted Mineralization, and Supporting Drill Data
Source: Solaris Resources Inc. (2022)

The final models for lithology, alteration, and mineralization zones were obtained using the software Leapfrog and are discussed below.

Figure 47, Figure 48, and Figure 49 show a cross section from the final lithology model and the box and whisker plots for Cu, Mo, and Au for each of the modelled lithology codes, respectively. In these statistics, the backtagged codes were used, as explained above.

Note that, for Cu, the Quartz-monzodiorite (QMD), the Diorite (D), and the Volcanics (V) are the units with the highest grades, while the Granodiorite (GD) is the host, mostly barren rock.

Although with some specific differences, similar comments can be made for Mo and Au, although Au has, in relative terms, the highest grades in the Breccia (Bx), a smaller unit that has less Cu and Mo.

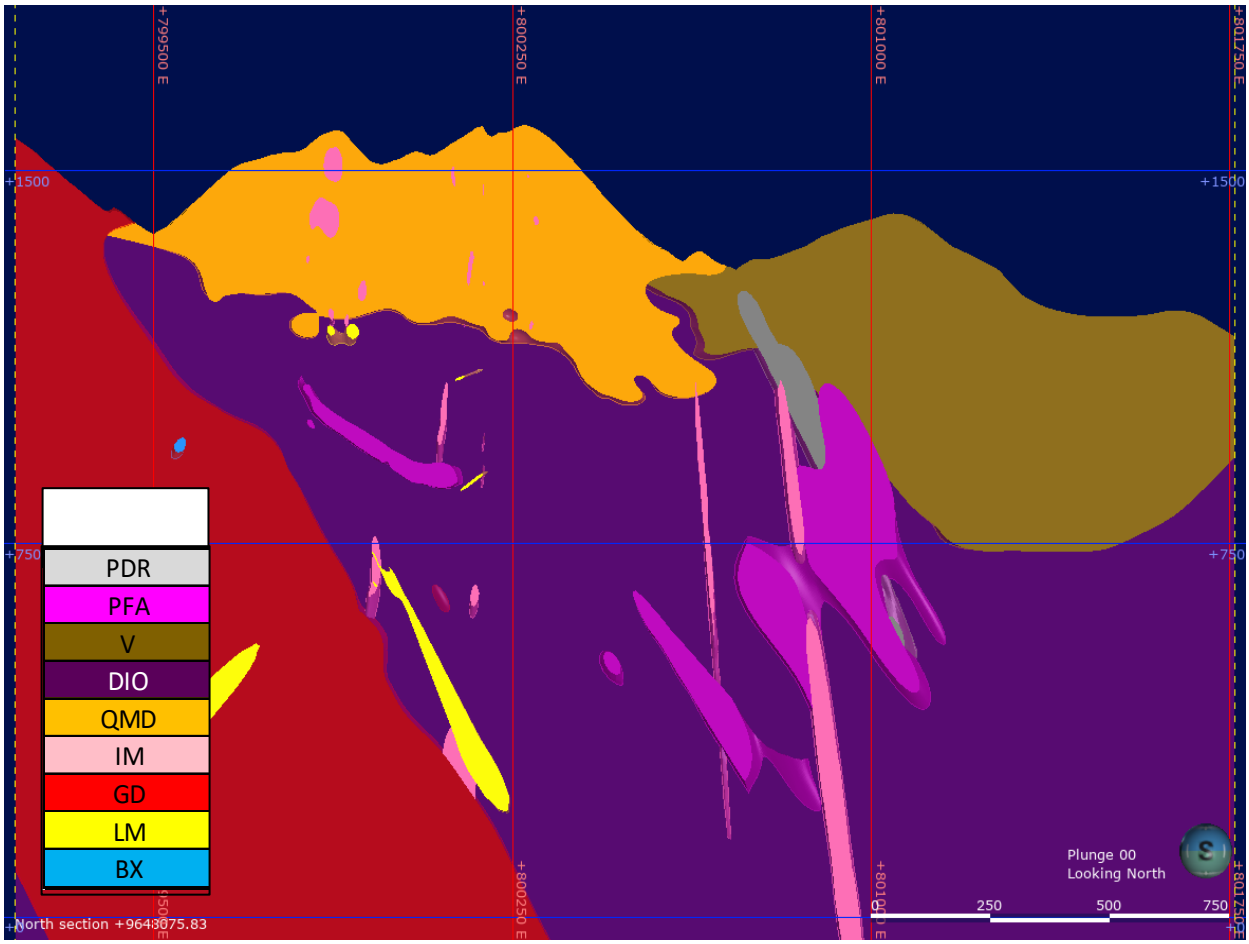

Figure 47: Cross Section Showing Lithology, Final Interpreted Model
The units shown are: Diorite (purple); Granodiorite (Red); Late-mineral dykes (yellow); Breccia (blue); Andesitic Porphyry (magenta); Volcanics (brown); Qz-monzodiorite (orange); and Inter-mineral dykes (pink)

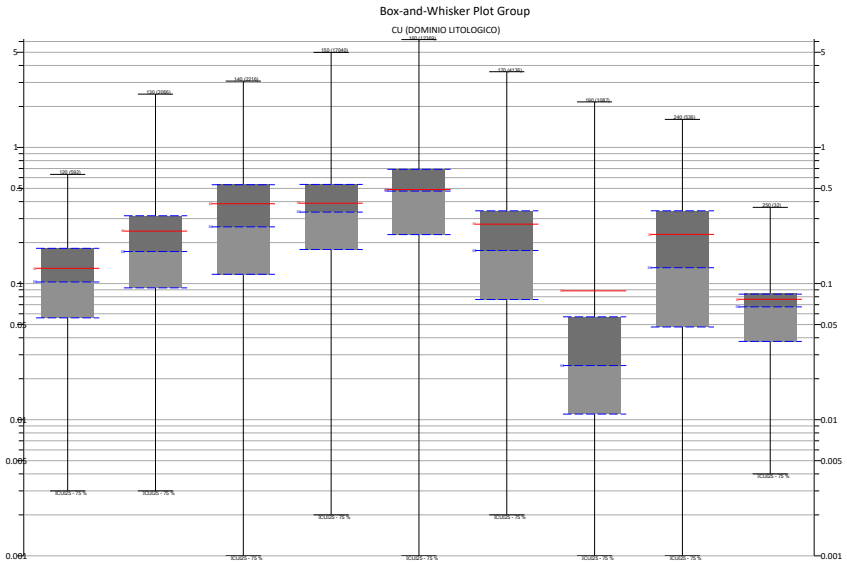

Figure 48: Box and Whisker Plot, Cu Grade by Lithology Codes

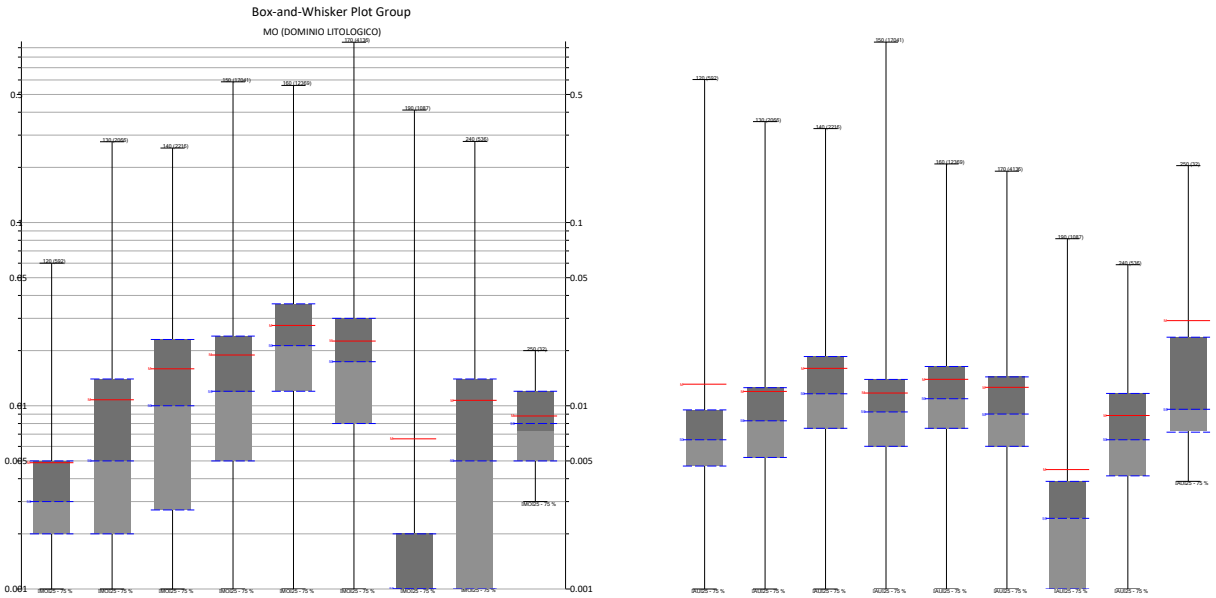

Figure 49: Box and Whisker Plots, Mo (L) and Au (R) Grades by Lithology Codes

The analysis of the relationship of grades and alteration is simpler since there are less alteration codes. Figure 50 shows a cross section of the final alteration model, while Figure 51 and Figure 52 show the box and whiskers plots for Cu, and Mo and Au, respectively.

As expected, propylitic alteration has a low or very low content of all three metals. In the case of Cu, the clay-sericite alteration is also low grade, but not so much for Mo and Au. With respect to the other alteration types, the controls are fairly subtle and highlight the importance of modelling the behavior of each in the context of (intersections with) lithologies and mineralization zones.

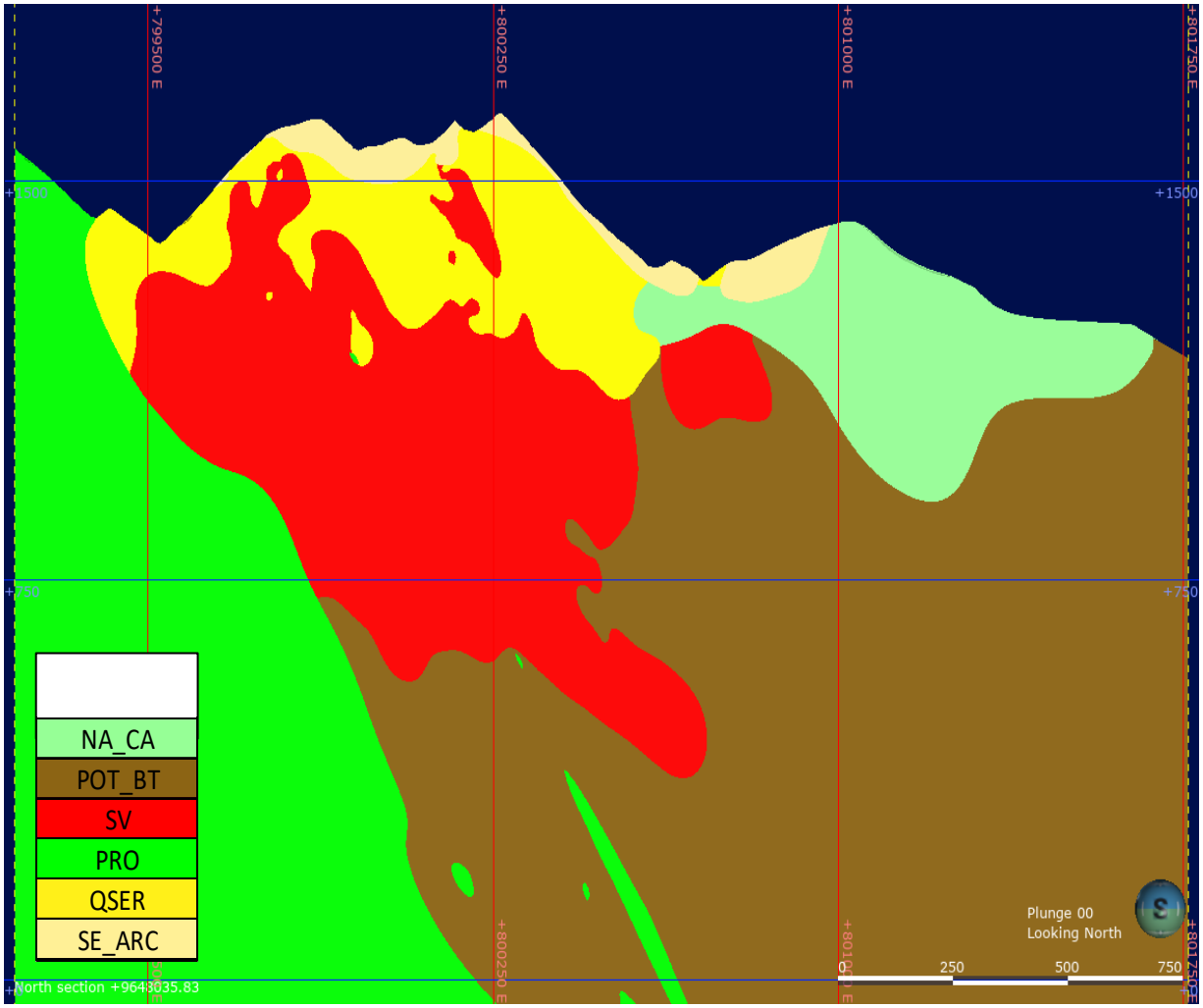

Figure 50: Cross Section Showing Alteration, Final Interpreted Model
The units shown are: Green Sericite (red); Propilitic (green); Potassic-Biotite (brown); Qz-sericite (yellow); Calco-sodic (light green); and Sericite-clays (light brown)

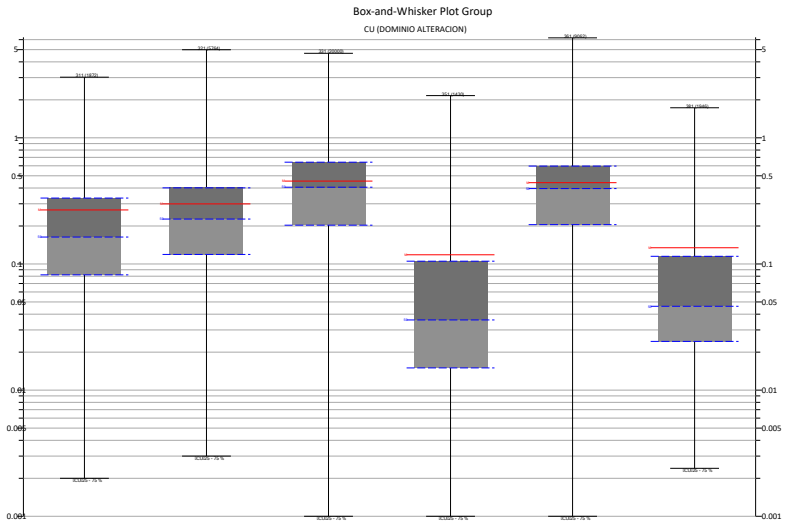

Figure 51: Box and Whisker Plot, Cu Grade by Alteration Codes

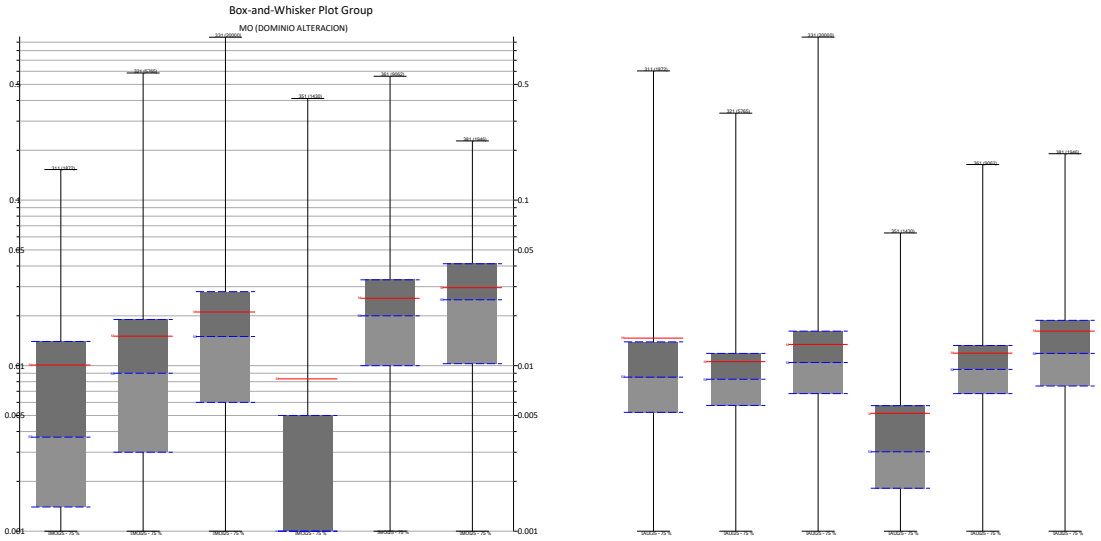

Figure 52: Box and Whisker Plots, Mo (L) and Au (R) Grades by Alteration Codes

The mineralization zone model (Minzone) is shown in Figure 53. Note that the highest-grade zones are near the surface (in blue, secondary enrichment zone) and in red, where chalcopyrite predominates over pyrite (Cpy > Py). This primary unit forms the core of Warintza Central and also appears in Warintza East.

The Cu, and Mo and Au grades are shown in the box and whiskers plots in Figure 54 and Figure 55, respectively. As expected, the supergene and the Cpy>Py units are the highest-grade units. Note also that

the supergene unit is a relatively low-enrichment zone, “immature” as described in Section 7. Still, it is volumetrically significant and contributes to an expected favourable mining scenario, being near surface.

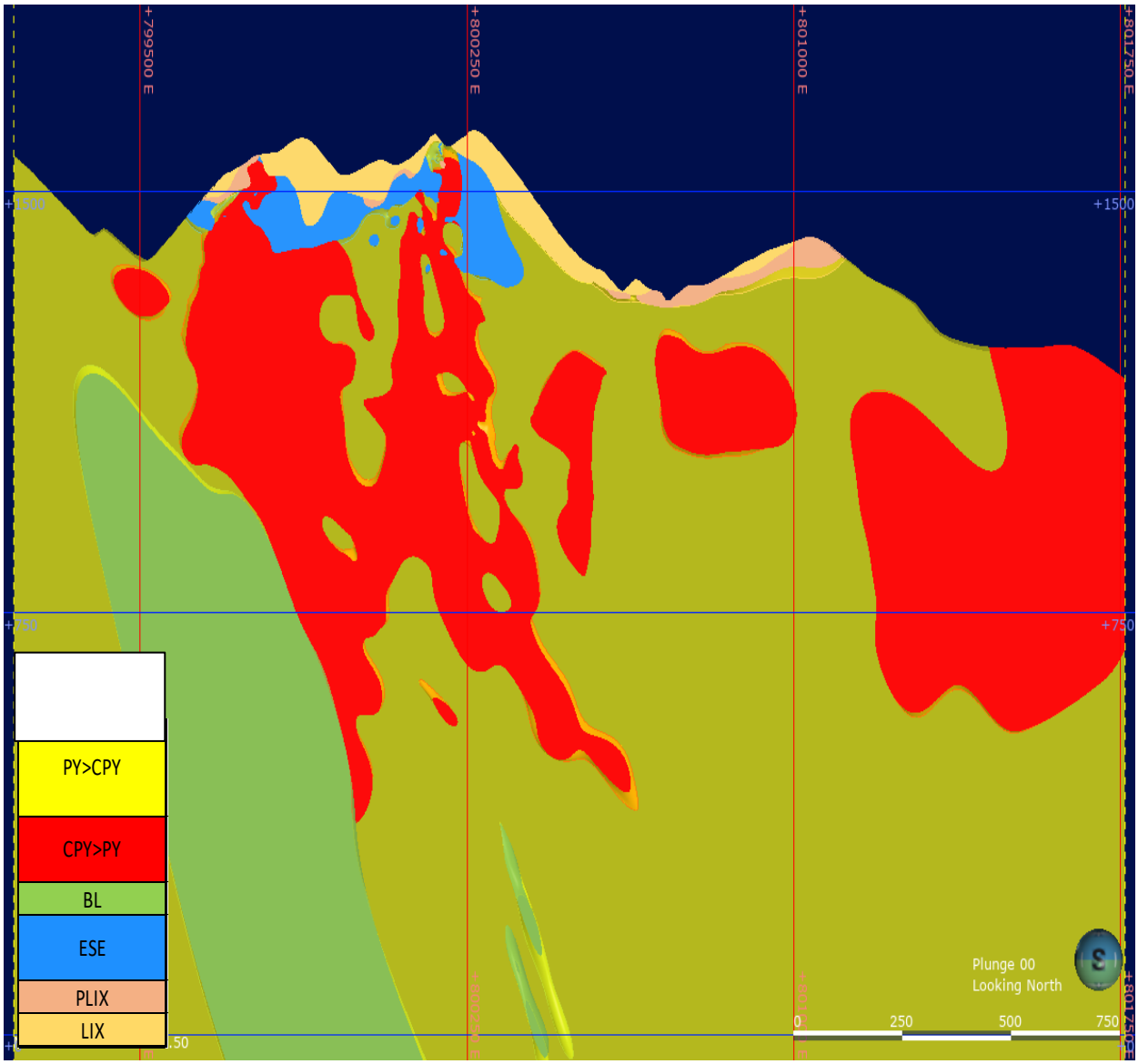

Figure 53: Cross Section Showing Mineralization Zones (Minzone),
Final Interpreted Model
The units shown are: Low Grade (green); Cpy>Py (red); Py>Cpy (mustard); Supergene enrichment (blue); Partial Leach (pink); and Leached (light brown)

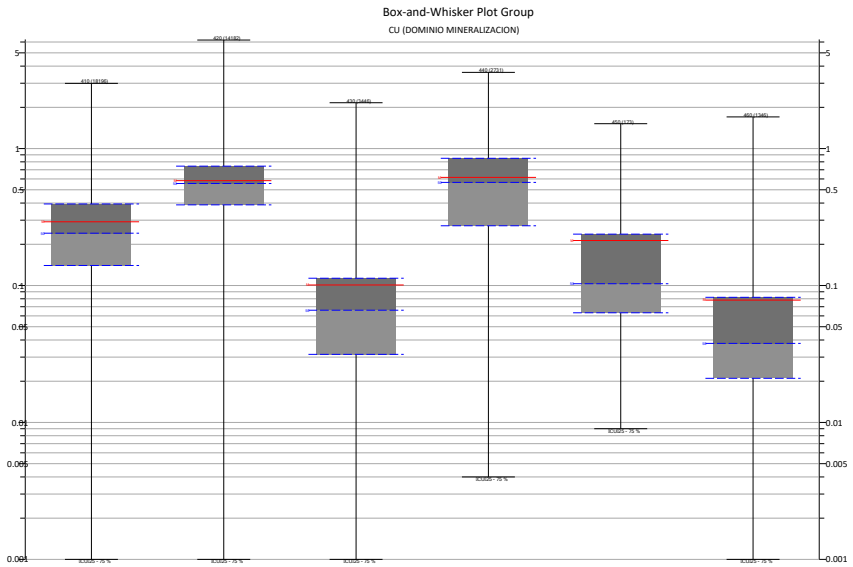

Figure 54: Box and Whisker Plot, Cu Grade by Minzone Codes

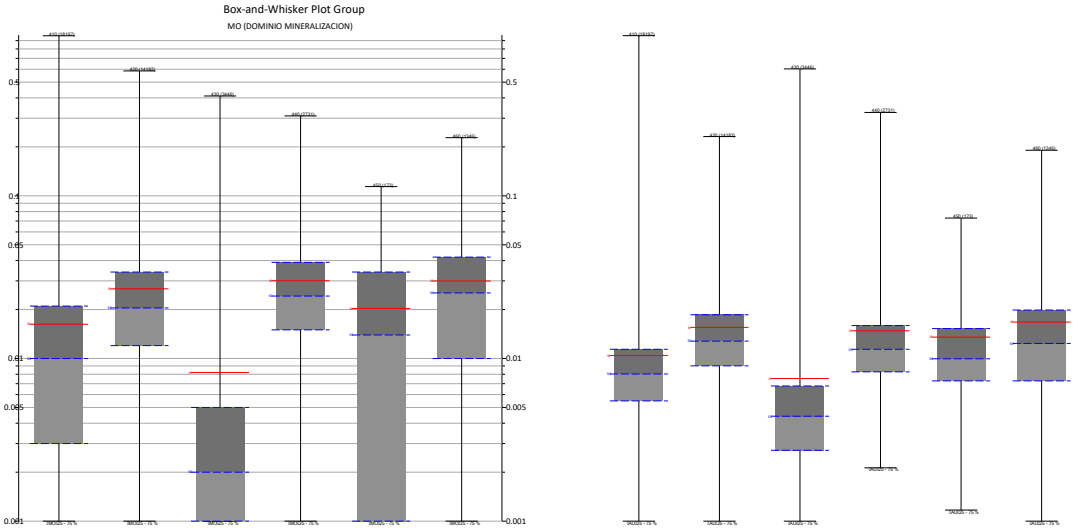

Figure 55: Box and Whisker Plots, Mo (L) and Au (R) Grades by Minzone Codes

14.3.1 Estimation Domain Definition

Estimation of grades proceeds within domains defined on the basis of geological and statistical considerations. The definition and modelling of these domains is an important step in mineral resource estimation.

Estimation domains are the geological equivalent to geostatistical stationary zones and are defined as a volume of rock with mineralization controls that result in approximately homogeneous distributions of mineralization. The spatial distributions of grade exhibit consistent statistical properties. This does not mean that the grades are constant within the domains; however, the geological and statistical properties of the grades facilitate its prediction.

The process of defining the estimation domains begin with a detailed statistical analysis of the grades within each lithology, alteration, and minzone unit separately. A similar process was followed for the in-situ density information. The workflow can be summarized as:

1. Development of the grade domains begins with geologic knowledge. The various logged codes are grouped and re-grouped based on a combination of data abundance, geologic knowledge, and sometimes statistical analysis. This results in the geologic variables that are modelled, as explained above.

2. Next, initial estimation domains based on all possible combinations of the geologic attributes are defined. These are all the possible intersections of each of the geologic variables in the model. In the case of Warintza, there are six different alteration codes, six different mineralization codes, and nine different lithology codes to consider for a theoretically possible 324 combination. However, data abundance and geologic considerations will filter out a large number of these. For Warintza, most initial combinations with less than 1% of the total number of intervals in the database were grouped with others according to geologic criteria.

3. The subsequent step is to statistically analyze the distribution of grades of the initial domains. The main purpose is to remove or group domains according to geologic considerations. The main statistical tools used is quantile-quantile (Q-Q) plots, which allow for a direct comparison of grade distributions within each proposed domain, although some specific histograms and probability plots were also used. The Q-Q plots, in combination with geologic criteria and abundance of information, allows to combine the initial domains.

4. This iterative process is repeated until a final set of domains that clearly separates different types of mineralization is found. While labor-intensive, this process ensures that the most important geologic and statistical aspects are combined into estimation domains that are the basis for the grade estimation that follows.

The examples shown below of two Q-Q plots for Cu used in the intermediate iterations illustrate a case where two distributions are considered similar, and, therefore, can be grouped as a single domain (Figure 56), and a case where the opposite occurs, the two distributions are clearly different and cannot be grouped (Figure 57).

The Q-Q plot is frequently used because it presents, in a graphical and most evident manner, the degree of similarity between two distributions. Still, in cases that are not as clear-cut as the one shown below, a degree of subjectivity is involved in the decision to group or not two sub-domains.

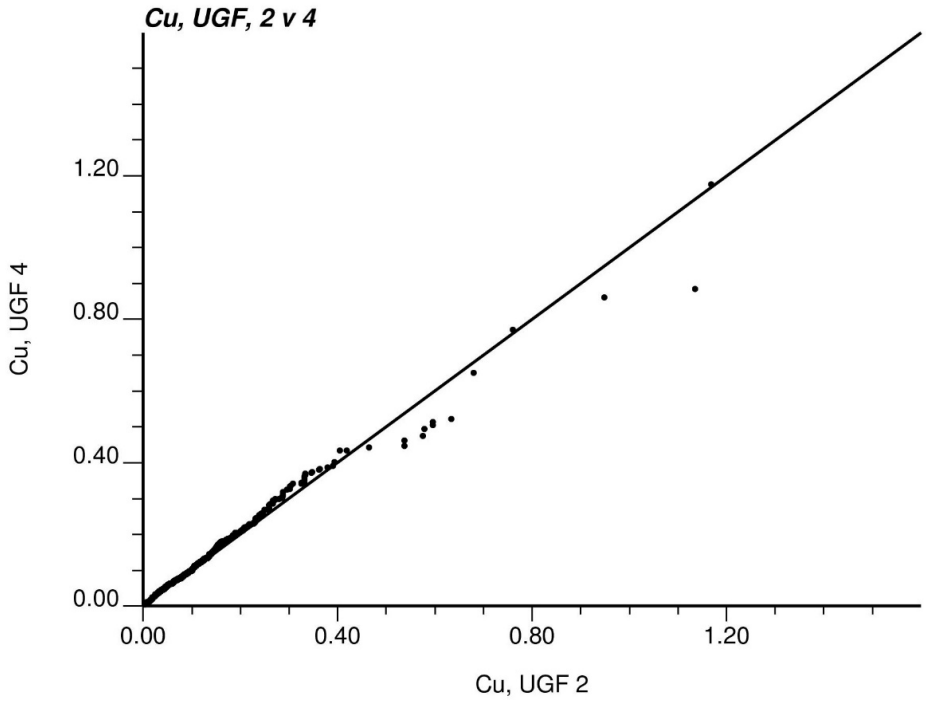

Figure 56: Q-Q Plot, Cu, Example of Two Preliminary Domains That Are Grouped

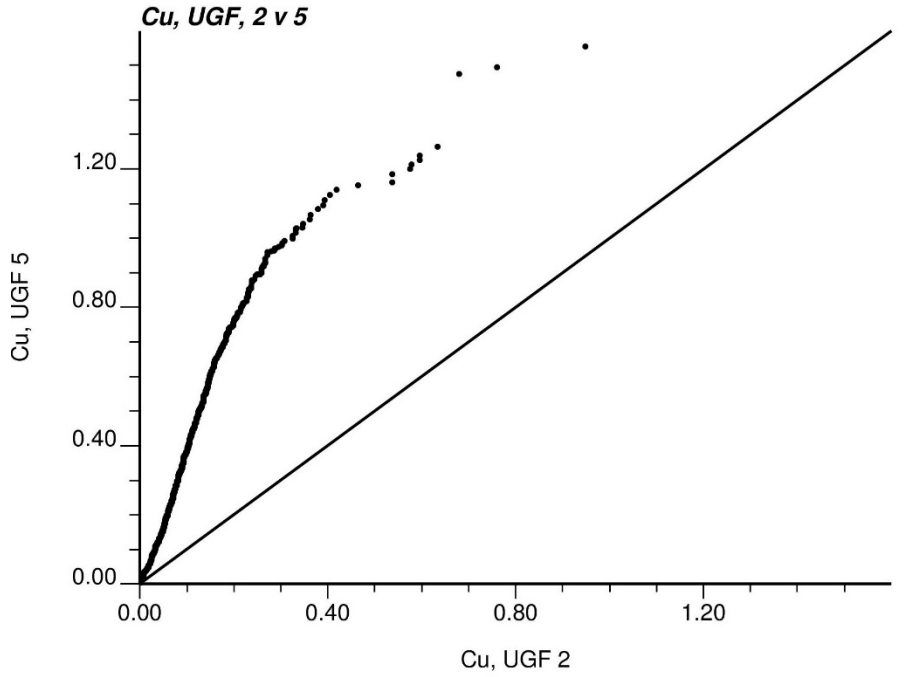

Figure 57: Q-Q Plot, Cu, Example of Two Preliminary Domains That Cannot Be Grouped

The process resulted in the definition of different estimation domains for Cu, Mo, Au, and in-situ density. While it is sometimes appropriate to use the same set of estimation domains for all estimated variables, in the case of Warintza, since the underlying geologic controls are different for Mo, Au, and the in-situ density variables, it is appropriate to define separate estimation domains.

The domains defined are shown in Figure 58 and Table 46 (Cu, 10 domains), Table 47 (Mo, seven domains), and Table 48 (Au, four domains). The corresponding box-and-whisker plots for the three metals are shown in Figure 59, Figure 60, and Figure 61 for Cu, Mo, and Au, respectively.

Note that, as expected, the low and high grades units are well differentiated, with, for example, the mostly barren Cu unit 10 capturing the Granodiorite lithology (GD). Domains 4, 6, and 8 capture the best combination of lithology, alteration, and minzone, and thus are higher grades than the other units. Similar analysis can be done for Mo and Au.

Overall, the domains defined are consistent with the known geology and discriminates well between volumes of different mineralization and corresponding grade ranges.

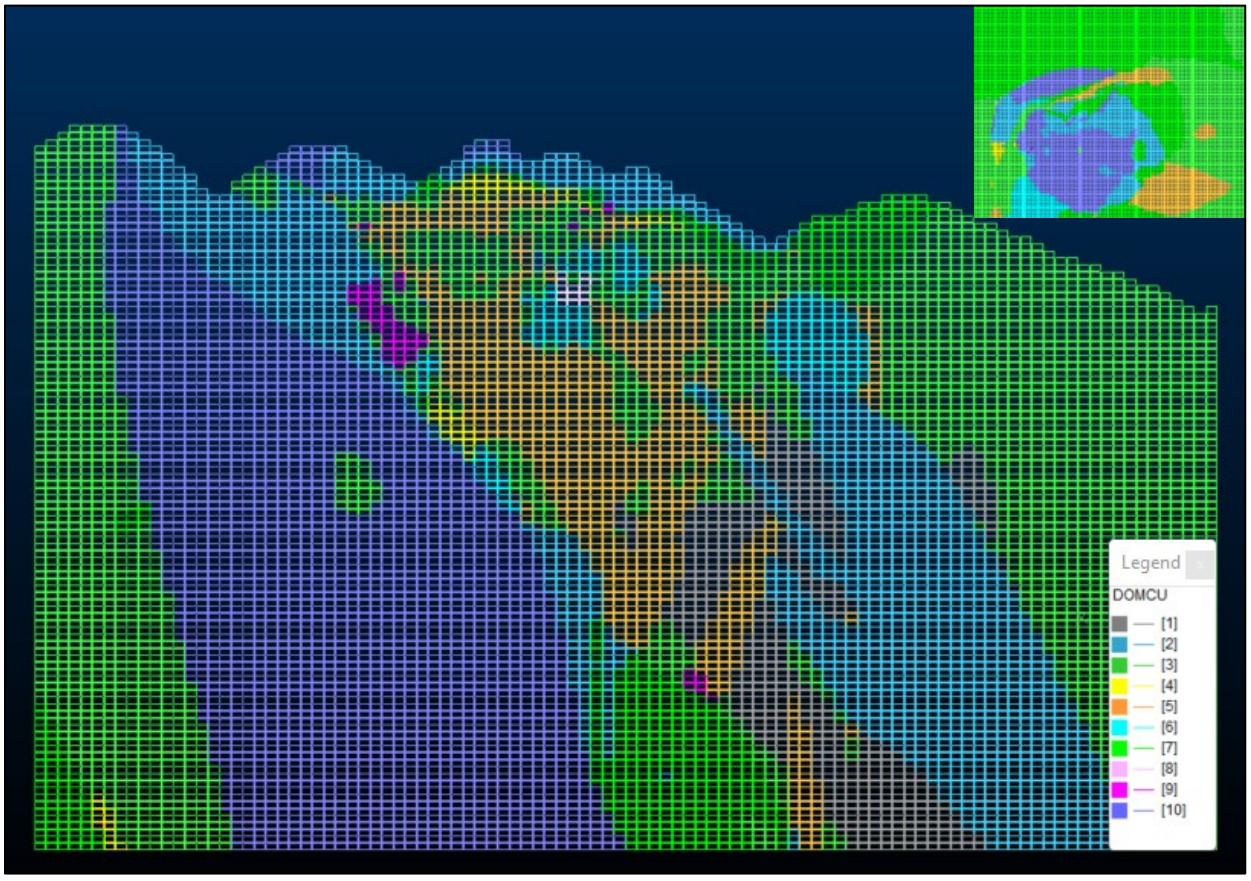

Figure 58: Cross Section Showing Cu Estimation Domains

Table 46: Warintza Cu Estimation Domains

Cu_DOMAIN	LITO	ALT	MINZONE	DESC.
1	120	311+321	410+420	
		331+361	410	
	130	311+321	410	
	240	311+321	410	
		351+381	420	
2	120	311+321	430	
	130	311+321	430	
		331+361		
	140+150	311+321	430	
		331+361	430	
		351+381	430+460	
	160	311+321	410	
		331+361	430+460	
		351+381	430+450	
	170	311+321+331+361	430	
		351+381	410+460	
	190	331+351+361+381	430	
			420	
	240	311+321+331+361	430	
	250	331+361	410	
3	130	311+321	420	
		331+361	410+420	
	140+150	311+321	410+420	
	160	331+361	410	
		351+381	440	
	170	331+361	420	
	190	351+381	410	
	240	331+361	420	Few Samples
		351+381	430+440	Few Samples
				Few Samples
4	140+150	311+321+331+361	440	

	160	331+361	440	
	170			
	190		410	Few Samples
	240	311+321	420	Few Samples
5	140+150	331+361	410	
	170	311+321+331+361	410	
	240	331+351+361+381	410	
6	140+150	331+361	420	
	160	351+381	410	
	170	311+321	440	
	190		410	
7	130	351+381	410+440+450	
	170		450	
8	160	331+351+361+381	420	
9	160	331+361	450	
	170	311+321	420	
		351+381	440	
10	160	351+381	460	
	190	311+321	430	
		351+381	430	
	240	351+381	460	

Table 47: Warintza Mo Estimation Domains

Mo_DOMAIN	LITO	ALT	MINZONE
1	120	311+331+361	410
		321	420+440
	130+240+250	311+331+361	410
		321	410+420+440
		351	410+420+430+440
		381	460
	140	311+321	410
	150+170	311	410
		381	430
	190	321+331+351+361	410
2	120+130+240+250	311+321	430
	150+170	311	430
		381	410
	160	311	410
3	120	321+331+361	410

	160	331+361	430
	190	351	420+430+440
4	130+240+250	331+361	420+440
	140	311+321+381	420+440+460
	150+170	311+321+331+361	420+440
	160	331+361	410+420+440+450+460
		381	410
	190	331+361	430
5	130+240+250	331+361	430
	140	331+361	410
		381	450
	150+170	321+331+361	410+430
		351	410
6	140	311+331+361	430
		381	410

	190	321	430
7	140	381	420+440
	150+170	351+381	420+430+440+450+460
	160	321	410
		351	430
		381	420+430+440+460

Table 48: Warintza Au Estimation Domains

Au_DOMAIN	LITO	ALT	MINZONE	DESC.
1	120	311+321+331+361	410+420	
	130+140+160+170	321		
	150	321 +331+351 +361		
	240+250	331+361		
		351	440+450+460	Few Samples
2	120	311 +321	430	
	130+140+160+170	311 +321+331+361	430	
		351	410+420	
			430	
		381	430	
	150	311	410+420	
	190	351	410+420	
	240+250	321	410+420	
			430	
		331+361	430	
		351	410+420	
		381	440+450+460	Few Samples
3	130+140+160+170	311	410+420	
			440+450+460	
		321	440+450+460	
		331+361+381	410+420+440+450+460	
	190	321+331+361	410+420	
	240+250	381	410+420	
4	150	321+331+351+361	430	
	190	321+331+351+361		
	240+250	311		

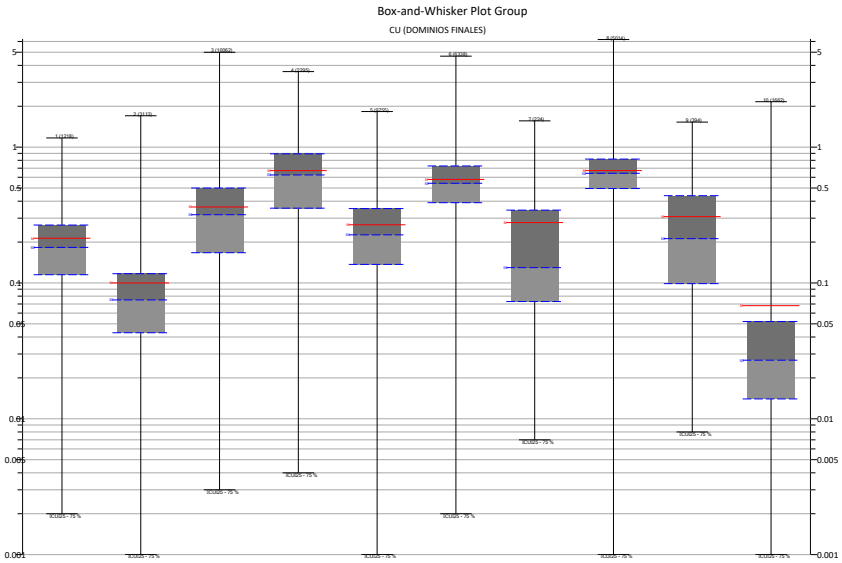

Figure 59: Box and Whisker Plots, Cu Grades by Cu Estimation Domains

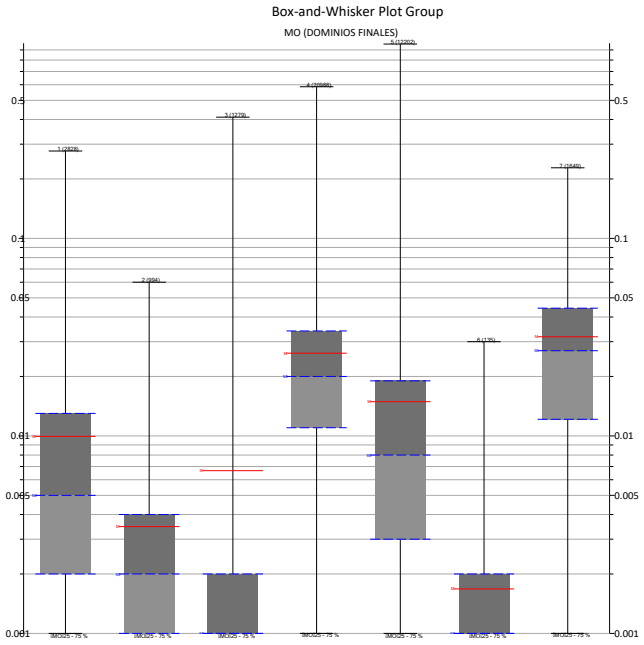

Figure 60: Box and Whisker Plots, Mo Grades by Mo Estimation Domains

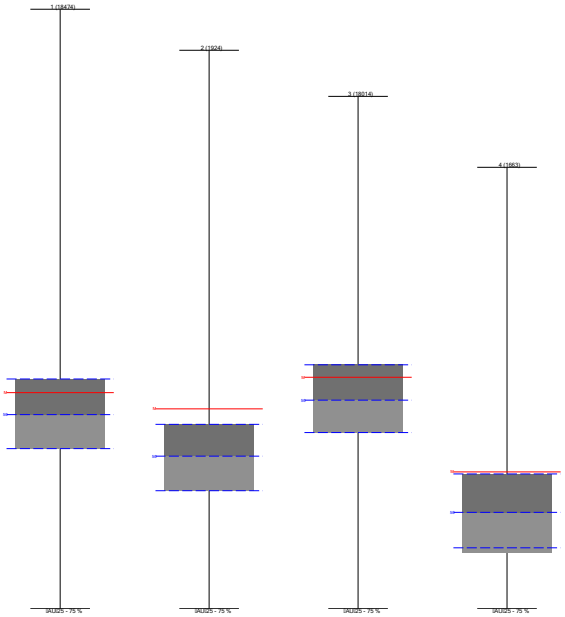

Figure 61: Box and Whisker Plots, Au Grades by Au Estimation Domains

14.3.2 In-situ Density Domains

The same process was applied to the density data combining the information available by lithology, alteration, and mineralization zone. This resulted in five domains being defined for in-situ density, which are shown in Table 49. Figure 62 shows the basic statistics (box and whisker plot) for each domain.

Note that, as expected, the lower density values are found in units closer to the surface, including the sericite-clay alteration and in the leached zone, at less than 2.5 m^3/t. At deeper levels of the deposit, density values are in the 2.7 to 2.75 m^3/t range, which is typical for the types of rocks found at Warintza.

Table 49: Warintza In-situ Density Estimation Domains

DENUG2	LITO	ALT	MINZONE	DESC.
1	120+130+140+150+240+250	311+331	410+420+430	
	120+130+140+150+240+250	321	410+420+430	
	120+130+140+150+240+250	351	410+420+430	
	120+130+140+150+240+250	361	410+420+430	
	120+130+140+150+240+250	381	410+420+430	
	190	311+331	410+420+430	
2	160	311+331	410+420+430	
	160	311+331	440+450	
	160	361	410+420+430	
	160	361	440+450	
	160	361	460	
	160	381	410+420+430	
3	160	381	440+450	
	170	311+331	440+450	
	170	361	440+450	
	170	381	460	
4	120+130+140+150+240+250	381	440+450	
	160	381	460	
	170	381	440+450	
5	170	311+331	410+420+430	
	170	321	410+420+430	
	170	351	410+420+430	
	170	361	410+420+430	
	190	321	410+420+430	
	190	351	410+420+430	

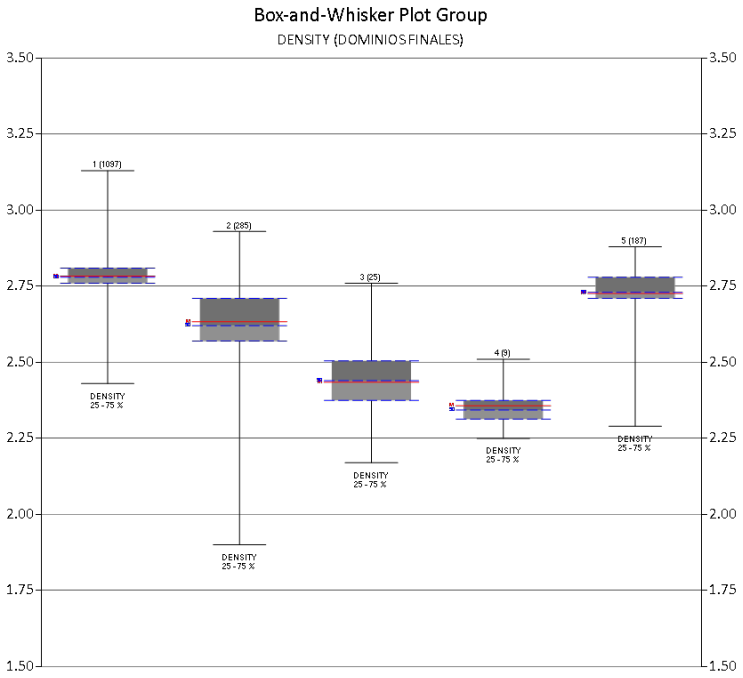

Figure 62: Box and Whisker Plots, Density Domains

14.4 Grade Capping

Extreme or unusual values (outliers) in grade distributions are grade that deviate from the general tendency of most other grades in the deposit and can be spatially and statistically isolated. In the discussion that follows, outliers are valid assayed samples, not a consequence of spurious or erroneous data collection, and are defined in terms of geological and statistical populations.

The determination of what values are considered outliers is subjective. Outlier values are commonly examined on a log-normal cumulative frequency plot on a domain basis. Breaks at the high end of the distribution may represent outlier populations. For example, Figure 63 shows the log-normal probability plot of Cu grade for estimation domain 6. In this case, for grades higher than 2.0%, the distribution appears to break up and exhibits a slight slope change, represented by about 0.2% of the total samples.

To limit the influence of the outlier data, all samples above the specified (capping) grade cut-off are reset to the top value defined. This is a fairly popular method in the industry to define outlier values, which is always a subjective decision.

Capping the grades removes metal from the sample distribution and limits the influence of the outliers. There may still be a region of high estimates around the outliers, yet there may be isolated high grades. The local estimates are checked on a case-by-case basis, always bearing in mind the impact of capping on the overall distribution for each domain.

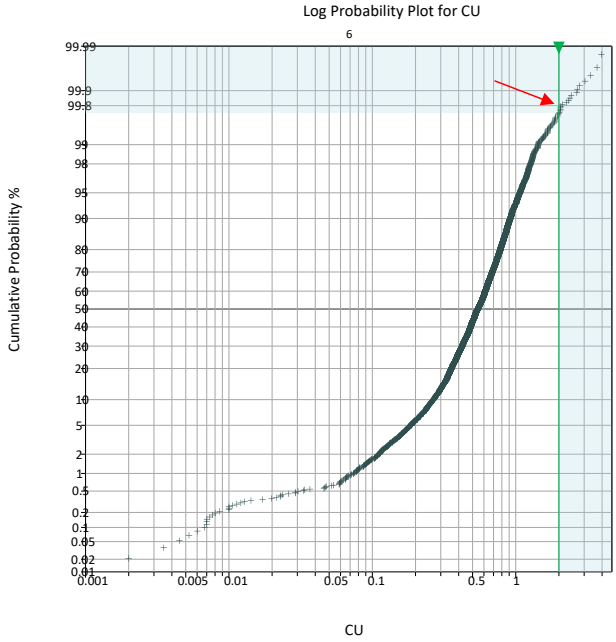

Figure 63: Probability Plot, Cu, Estimation Domain 6, Warintza

The summary of the capping analysis and as applied in the grade estimation process are shown in Table **50**, Table **51**, and Table 52 for Cu, Mo, and Au, respectively. These tables show the impact of capping on the original (assay) database for each domain. The number of samples being affected (reset to the capping value) is shown, as well as the relative percentage reduction in metal content, which considers sample length.

Table 50: Summary Capping by Domain, Cu

Copper						
Domain	**Outlier or Capping Value (%)**	**Number of Samples Above Capping Value**	**% Of Total Assays Intervals Impacted**	**Non-declustered Average Before Capping**	**Non-declustered Average After Capping**	**% Metal Reduction**
1	1.0	4	0.30%	0.216	0.216	0.20%
2	1.5	3	0.10%	0.104	0.104	0.10%
3	2.0	10	0.10%	0.369	0.368	0.30%
4	2.4	23	1.00%	0.670	0.667	0.40%
5	1.5	4	0.00%	0.266	0.266	0.10%
6	2.0	17	0.30%	0.582	0.580	0.30%
7	1.5	4	1.80%	0.294	0.293	0.30%
8	2.0	7	0.10%	0.668	0.666	0.50%
9	1.3	4	1.00%	0.317	0.315	0.40%
10	1.2	9	0.50%	0.079	0.078	1.50%

Table 51: Summary Capping by Domain, Mo

Molybdenum						
Domain	**Outlier or Capping Value (%)**	**Number of Samples Above Capping Value**	**% Of Total Assays Intervals Impacted**	**Non-declustered Average Before Capping**	**Non-declustered Average After Capping**	**% Metal Reduction**
1	0.090	4	0.10%	0.010	0.010	1.50%
2	0.050	3	0.30%	0.004	0.003	0.50%
3	0.110	5	0.40%	0.007	0.006	7.80%
4	0.300	21	0.10%	0.026	0.026	0.20%
5	0.300	2	0.00%	0.015	0.015	0.50%
6	0.005	2	1.50%	0.002	0.001	15.90%
7	0.130	7	0.40%	0.032	0.032	0.30%

Table 52: Summary Capping by Domain, Au

Gold						
Domain	**Outlier or Capping Value (%)**	**Number of Samples Above Capping Value**	**% Of Total Assays Intervals Impacted**	**Non-declustered Average Before Capping (g/t)**	**Non-declustered Average After Capping (g/t)**	**% Metal Reduction**
1	0.500	23	0.12%	0.044	0.043	2.20%
2	0.240	21	1.10%	0.036	0.028	21.60%
3	0.600	27	0.10%	0.054	0.054	1.10%
4	0.200	5	0.30%	0.015	0.014	6.50%

14.5 Composites

After applying the capping to the original samples, 2 m long composites were prepared from the original assay data, truncated at the contacts between domains.

No significant correlation between assayed Au grades and assay length is observed (Figure 64), so all resulting composites greater or equal to 0.40 m are used to estimate grades.

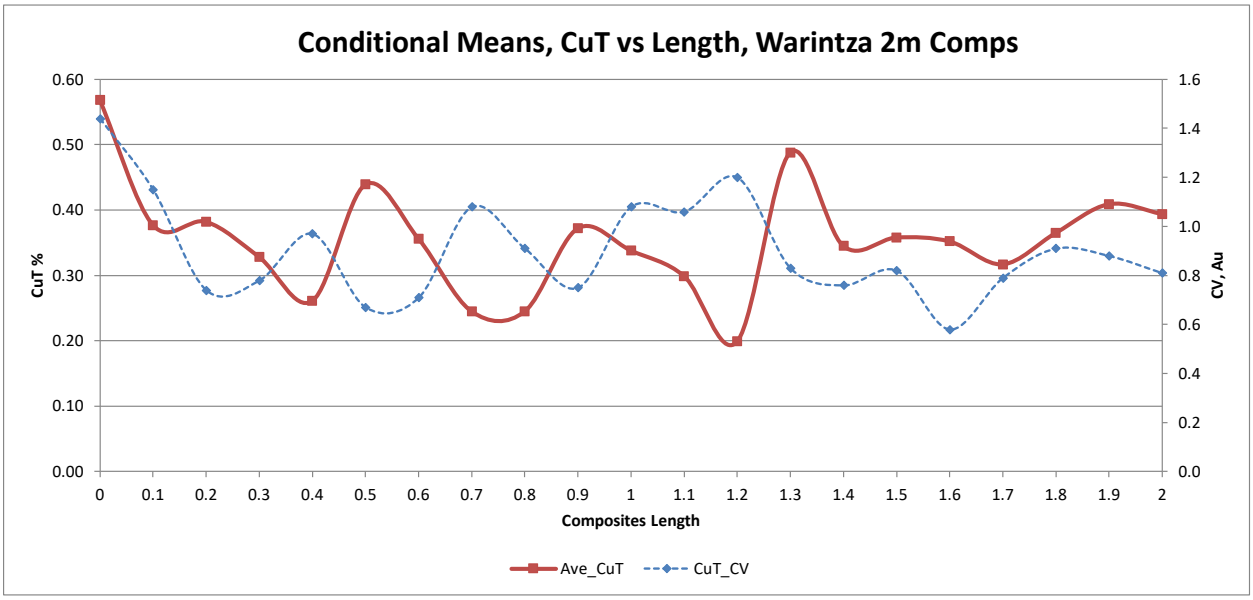

Figure 64: Conditional Cu Grade Means by Composite Length (Red)
Coefficient of Variation is in Light Blue (Second Y-Axis)

Given that composites are the same length as most of the samples, their basic statistics compared to the original samples do not change significantly. As examples,

Figure **65** shows the histogram and basic statistics for Cu, domain 4, 2 m composites. Figure 66 shows the corresponding probability plot.

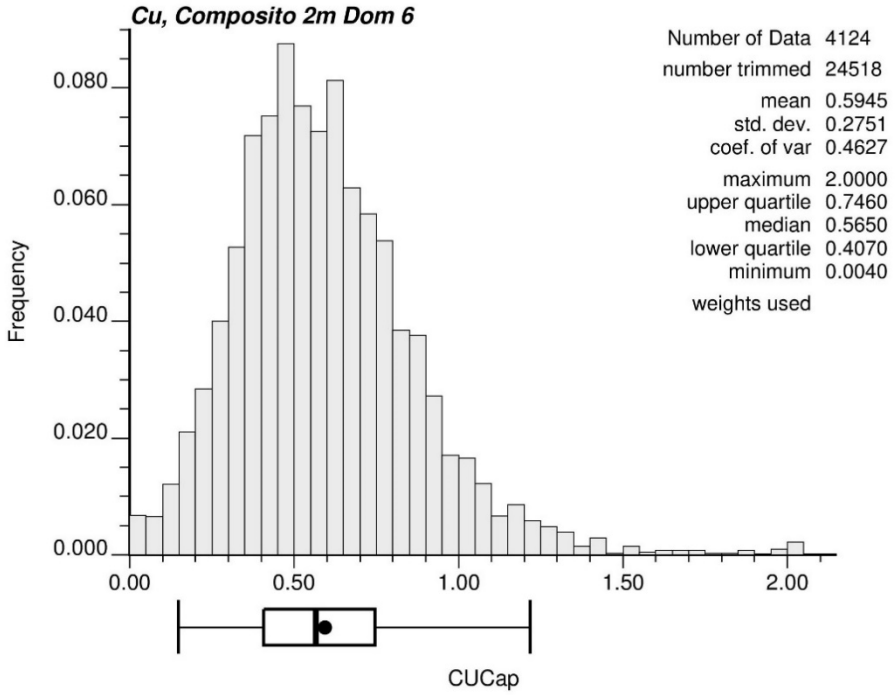

Figure 65: Histogram and Basic Statistics, Cu, Domain 6, 2 m Composites

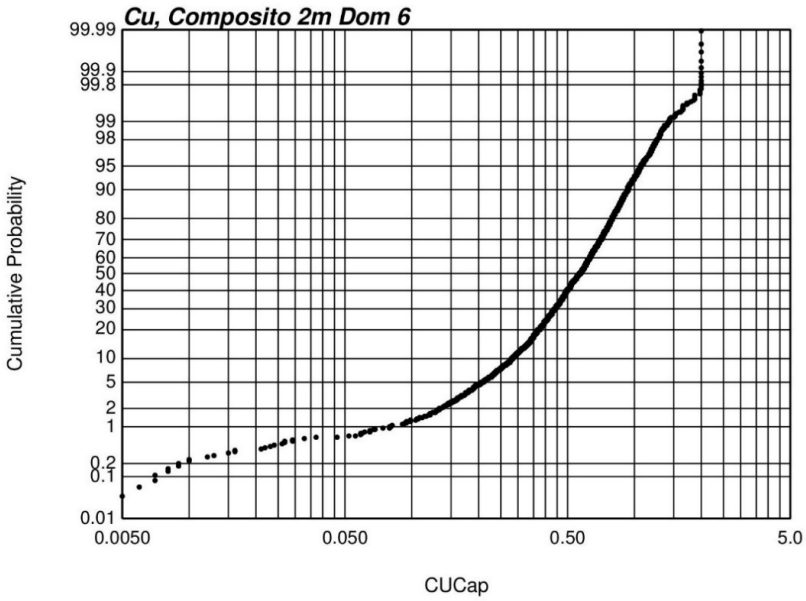

Figure 66: Probability Plot, Cu, Domain 6, 2 m Composites
Note the Effect of Capping at 2%

14.6 Spatial Clustering

Data are rarely collected randomly, and, in a spatial sense, each sampled interval does not represent the same volume across the deposit. In the case of Warintza, since multiple holes are drilled from a single platform, this effect is exacerbated, and the spatial aggregation of data can be significant, particularly for the upper intervals in the drill holes.

Therefore, there is a need to adjust the histograms and summary statistics to be representative of the entire volume of interest. Declustering techniques are, with the exception of kriging itself, geometric methods that assign each datum a weight based on closeness to surrounding data. These weights are greater than zero and sum to one. The composite distribution and all summary statistics are calculated with the weights to obtain more representative statistics.

The cell declustering method (Deutsch, 1989) was applied to the 2 m composite for all three metals and by domain. Figure 67 shows the declustered histogram and basic statistics of the composites for domain 6 and should be compared to

Figure **65**. Note how the average grade is slighter lower after declustering. This is typical in positively skewed distributions since most of the redundancy occurs in higher grade zones. Overall, and for this particular unit, the impact of clustering is considered minor.

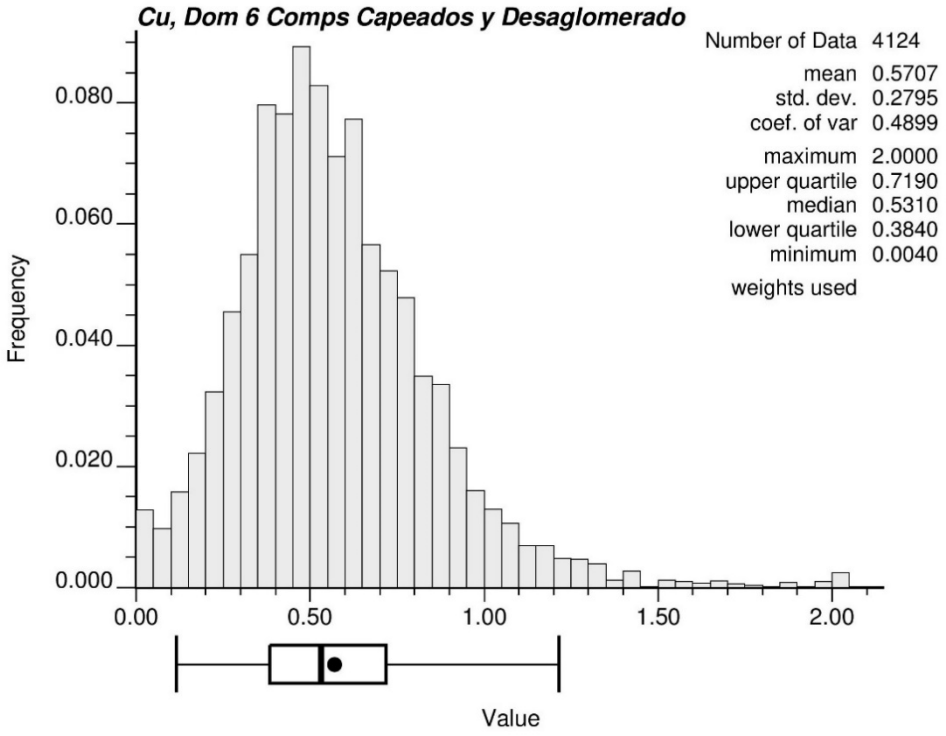

Figure 67: Declustered Histogram and Basic Statistics, Cu, Domain 6, 2 m Composites

14.7 Contact Analysis

The treatment and definition of boundaries have implications on resource estimation, such as dilution, lost ore, or a mixture of geological populations. The treatment of boundaries at the time as grade estimation is of practical importance. The terms hard and soft boundaries are used to describe whether the change in grade distribution across the contact is abrupt or not, respectively.

Conventional grade estimation usually treats the boundaries between geological units as hard boundaries, whereby no mixing occurs across the boundary. Soft boundaries allow grades from neighbouring domains to be used. Sometimes, soft and hard boundaries can be predicted or expected from geological knowledge but should always be confirmed with statistical contact analysis (Larrondo and Deutsch, 2004).

The behavior of grade distributions across contacts is analyzed by finding pairs of data in the two estimation domains of interest at pre-defined distances.

In this work, pairs within pre-specified distances were found using a three-dimensional search of nearby assay intervals belonging to a different unit, see Figure 68 as an example.

This process was completed exhaustively for all combinations of domains and for each metal, although there are instances where the domains have no contacts. The analysis of grade trends near contacts defines whether the grade estimation for any given unit should incorporate composites of a neighboring unit.

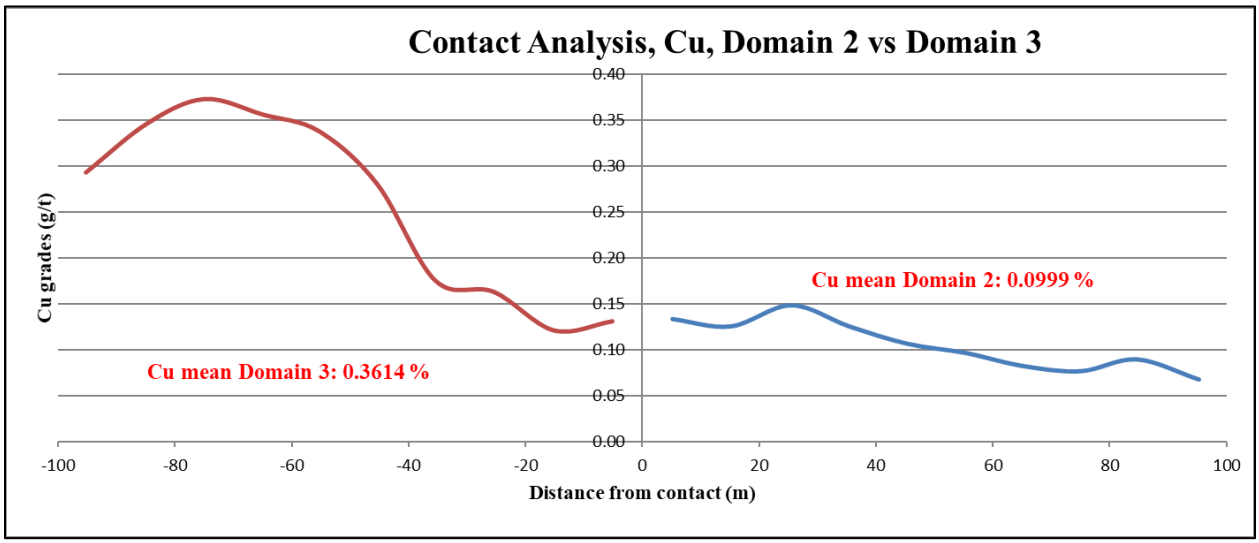

Figure 68: Contact Profiles, Cu, Domains 2-3 Contact

The summary of all possible contacts and the strategy they indicate should be implemented at the time Cu grade estimation is summarized as a contact matrix in Figure 69. The hard contacts (no data sharing) are represented by cells shaded in red (3); the semi-soft contacts are represented in green (2) and indicate that composites from both domains should be shared in the first estimation (shortest) pass only; the soft contacts are highlighted in yellow (1) and indicate that composites should be shared in the first two passes. There are no cases when composites are shared across contacts in all three-grade estimation passes.

The corresponding contact matrices for Mo and Au are shown in Figure 70 and Figure 71, respectively.

	1	2	3	4	5	6	7	8	9	10
1	0				2					
2	3	0	2				2		2	2
3	3	3	0		1	2				
4	3	3	3	0						
5	2	3	1	3	0					
6	3	3	2	3	3	0		2		
7	3	2	3	3	3	3	0			
8	3	3	3	3	3	2	3	0		
9	3	2	3	3	3	3	3	3	0	
10	3	2	3	3	3	3	3	3	3	0

Figure 69: Contact Matrix, Cu
In Red, Hard Contacts (No Sharing); In Green, Semi-Soft Contact (Share Only in The First Pass);
In Yellow, Soft Contact (Share in Estimation Passes 1 and 2)

	1	2	3	4	5	6	7
1	0					2	
2	3	0					
3	3	3	0				
4	3	3	3	0	1		
5	3	3	3	1	0	2	
6	2	3	3	3	2	0	
7	3	3	3	3	3	3	0

Figure 70: Contact Matrix, Mo
In Red, Hard Contacts (No Sharing); In Green, Semi-Soft Contact (Share Only in The First Pass); In Yellow, Soft Contact (Share in Estimation Passes 1 and 2)

	1	2	3	4
1	0		2	
2	3	0		
3	2	3	0	
4	3	3	3	0

Figure 71: Contact Matrix, Au
In Red, Hard Contacts (No Sharing); In Green, Semi-Soft Contact (Share Only in The First Pass); In Yellow, Soft Contact (Share in Estimation Passes 1 and 2)

14.8 Variography

For the required variogram models for estimating with ordinary kriging, most of the domains in the Warintza deposit were obtained using the software SAGE 2001 (Isaaks. 1999). The estimator used was the correlogram, which is robust because of the use of lag-specific mean and variance values in its calculation. In practice, it has become a very popular option when dealing with grade variables.

Except for two Cu domains and one Mo domain, all the remaining Cu, Mo, and Au domains have their own correlogram model. An example is shown graphically in Figure 72. In Table 53, the main correlogram model parameters are shown for all modelled Cu domains; Table 54 and Table 55 show the corresponding information for the Mo and Au correlogram models.

The correlogram models are described using the GSLIB rotation convention, which can be summarized as (Z/X/Y, L/R/R). The first three letters indicate the order of the rotation. The first letter indicates the first rotation axis (Z), the second letter indicates the second rotation axis (X), and the third letter, the third rotation axis (Y). The second group of three letters indicates the rotation directions. The first letter indicates a left L hand rotation around the first rotation axis. The second letter indicates a right R hand rotation around the second rotation axis. The third letter indicates a right R hand rotation around the third rotation axis.

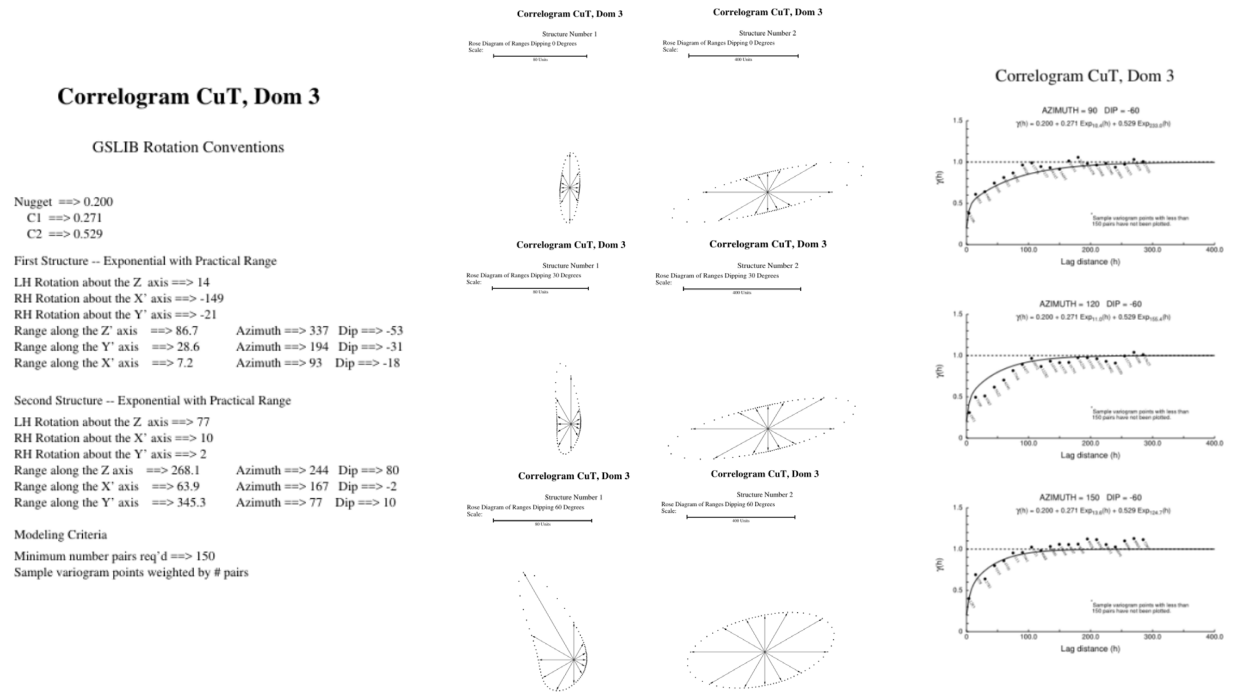

Figure 72: Correlogram Model, Cu, Domain 3
Views of the Model Parameters (Left); Main Orientations for the Two Structures Modelled (Central); and Three Directions with the Fitted Model

Table 53: Cu Correlograms Models by Domain

Cu Correlogram Models, GSLib Rotation Conventions							
Domain	**Nugget**	**Variance Structure 1**	**Rotation First Structure (Z/X/Y)**	**Ranges First Structure, m (Y/X/Z)**	**Variance Structure 2**	**Rotation Second Structure (Z/X/Y)**	**Ranges Second Structure, m (Y/X/Z)**
1	0.300	0.522	-34/-13/91	32/104/14	0.178	-125/69/-66	1152/358/7512
2	0.030	0.728	-32/50/17	64/6/30	0.242	-116/61/-60	477/86/2857
3	0.200	0.271	14/-149/-21	29/7/87	0.529	77/10/2	345/64/268
4	0.030	0.750	0/-12/84	95/32/5	0.220	-73/31/12	491/38/382
5	0.180	0.099	-107/13/-30	43/63/55	0.721	-3/-6/-15	108/619/768
6	0.270	0.132	5/3/32	71/153/74	0.598	5/3/32	76/218/1190
8	0.100	0.545	-39/46/22	14/14/19	0.355	-39/46/22	305/93/390
10	0.050	0.829	57/11/67	4/48/17	0.121	57/11/67	4887/5833/241

Table 54: Mo Correlograms Models by Domain

Mo Correlogram Models, GSLib Rotation Conventions							
Domain	**Nugget**	**Variance Structure 1**	**Rotation First Structure (Z/X/Y)**	**Ranges First Structure, m (Y/X/Z)**	**Variance Structure 2**	**Rotation Second Structure (Z/X/Y)**	**Ranges Second Structure, m (Y/X/Z)**
1	0.360	0.312	-29/-22/0	8/215/11	0.328	-29/-22/0	221/2067/2208
2	0.468	0.219	60/15/26	47/20/32	0.314	60/15/26	422/46/2447
3	0.050	0.857	16/-65/83	94/53/6	0.093	16/-65/83	1405/151/525
4	0.500	0.340	-66/5/3	12/39/47	0.160	-66/5/3	848/588/1909
5	0.420	0.269	-86/14/6	51/107/14	0.311	-86/14/6	3172/396/2433
7	0.150	0.356	-104/60/79	7/204/80	0.494	45/-38/-10	544/1217/345

Table 55: Au Correlograms Models by Domain

Au Correlogram Models, GSLib Rotation Conventions							
Domain	**Nugget**	**Variance Structure 1**	**Rotation First Structure (Z/X/Y)**	**Ranges First Structure, m (Y/X/Z)**	**Variance Structure 2**	**Rotation Second Structure (Z/X/Y)**	**Ranges Second Structure, m (Y/X/Z)**
1	0.400	0.285	-122/-53/33	19/135/40	0.315	0/-2/-75	119/969/711
2	0.500	0.185	66/90/63	203/46/3	0.315	27/66/-14	1472/10/578
3	0.300	0.361	-100/-16/-20	27/40/7	0.339	15/10/3	174/443/1138
4	0.180	0.629	14/46/16	45/71/7	0.191	-107/51/-136	1717/42/223

14.9 Block Model and Grade Estimation

The block model is defined in Datamine using a 25 x 25 x 15 m parent block size with a minimum 5 x 5 x 5 m sub-cell size and with the following limits, which refer to the southwest, lower corner of the block:

Minimum Easting: 799,210E

Maximum Easting: 801,760E

Minimum Northing: 9,647,410N

Maximum Northing: 9,649,385N

Minimum Elevation: -70 m

Maximum Elevation: 1,865 m

Blocks are flagged with a code for each lithology, alteration, mineralization zone, and estimation domain.

Ordinary kriging and Inverse Distance Squared (IDS) are used to estimate Cu, Mo, and Au grades.

Sulfuric-soluble Cu and Cyanide-soluble Cu have also been estimated into the model, although they do not feature in the Resource Inventory. They were estimated using the same correlogram models and search parameters as Total Cu (Cu). The soluble Cus were only used to fine-tune, as explained above, the mineralization zones' interpretation and model.

Grades were estimated into blocks using the 2 m capped composites within the corresponding domain, although, in some cases, as described above, composites were partially shared across domains.

Search orientations were guided by the correlogram models, and the search distances in every case were guided by variography but optimized to reflect a correct balance of estimated blocks in each estimation pass.

Since drill hole coverage is uneven, not all blocks are estimated due to the limitation imposed by the search ellipsoids. All non-estimated blocks are assigned a 0.0 grade. The grade estimation plans for all domains are shown in Table 56, Table 57, and Table 58, or Cu, Mo, and Au, respectively.

Table 59 shows the estimation plan for Density. Given the short search distances used, many blocks have no density estimates. Those blocks received assigned average densities by domain, which are shown in Table 60.

Table 56: Cu Estimation Plans by Domain

Cu Kriging Plans, GSLib Rotation Conventions					
Domain	**Pass**	**Search in Y, X, and Z**	**Search Angles Rotation, GSlib Convention**	**Min # Comp**	**Max # Comp**
1	1	55/110/44	60/0/0	4	8
	2	80/64/160	45/0/0	3	10
	3	170/153/340	45/0/0	2	12
2	1	90/72/72	30/0/0	6	12
	2	90/72/180	45/0/0	6	12
	3	170/153/340	45/0/0	2	12
3	1	45/36/90	0/0/0	4	12
	2	170/136/153	70/0/0	3	12
	3	350/280/315	70/0/0	2	12
4	1	85/68/42.5	0/0/0	4	12
	2	180/144/162	-70/0/0	3	12
	3	350/280/315	-70/0/0	2	12
5	1	75/90/75	0/0/0	4	12
	2	90/162/180	0/0/0	3	12
	3	180/324/360	0/0/0	2	12
6	1	55/82.5/55	0/0/0	4	12
	2	90/162/180	0/0/0	3	12
	3	180/324/360	0/0/0	2	12
7	1	70/35/35	0/0/0	6	12

	2	140/70/70	0/0/0	4	12
	3	280/140/140	0/0/0	2	12
8	1	60/60/72	0/0/0	4	12
	2	150/135/180	40/0/0	3	12
	3	300/270/360	40/0/0	2	12
9	1	70/35/35	0/0/0	6	12
	2	140/70/70	0/0/0	4	12
	3	280/140/140	0/0/0	2	12
10	1	35/87.5/63	45/0/0	4	12
	2	150/180/105	-45/0/0	3	12
	3	300/360/210	-45/0/0	2	12

Table 57: Mo Estimation Plans by Domain

Mo Kriging Plans, GSLib Rotation Conventions					
Domain	**Pass**	**Search in Y, X, and Z**	**Search Angles Rotation, GSlib Convention**	**Min # Comp**	**Max # Comp**
1	1	35/87.5/52.5	-30/0/0	4	10
	2	70/175/175	-30/0/0	3	10
	3	150/375/375	-30/0/0	2	12
2	1	90/81/90	60/0/0	6	12
	2	90/72/180	60/0/0	4	12
	3	180/144/360	60/0/0	2	12
3	1	90/81/45	20/0/0	6	12
	2	180/108/162	90/0/0	4	12
	3	360/216/324	90/0/0	2	12
4	1	45/90/90	-60/0/0	4	12
	2	100/100/180	-60/0/0	3	12
	3	190/190/342	-60/0/0	2	12
5	1	50/90/40	75/0/0	6	12
	2	180/144/180	90/0/0	5	12
	3	360/288/360	90/0/0	2	12
6	1	70/35/35	0/0/0	6	12
	2	140/70/70	0/0/0	4	12
	3	280/140/140	0/0/0	2	12
7	1	30/90/84	70/0/0	4	12
	2	120/180/120	45/0/0	3	12
	3	330/380/330	45/0/0	2	12

Table 58: Au Estimation Plans by Domain

Au Kriging Plans, GSLib Rotation Conventions					
Domain	**Pass**	**Search in Y, X, and Z**	**Search Angles Rotation, GSlib Convention**	**Min # Comp**	**Max # Comp**
1	1	30/90/60	60/0/0	4	10
	2	60/180/120	0/0/0	3	10
	3	125/375/250	0/0/0	2	12
2	1	90/81/54	90/0/0	6	10
	2	180/108/162	45/0/0	4	10
	3	360/216/324	45/0/0	2	12
3	1	60/90/48	0/0/0	6	10
	2	100/100/180	-80/0/0	4	10
	3	200/200/360	-80/0/0	2	12
4	1	45/90/36	0/0/0	6	12
	2	180/144/162	30/0/0	4	12
	3	360/288/324	30/0/0	2	12

Density is estimated into the block model using the Inverse Distance Squared method. The arithmetic averages of each type of mineralization are used to assign in-situ bulk density to un-estimated blocks. This average is done by alteration zones, which was found to be a better discriminant than lithology or mineralization zones.

This is reasonable considering that the upper levels of the deposit weathering and, in general, supergene processes weaken the rock. This is not unusual in these types of deposits.

Table 59: In-situ Density Estimation Plans by Domain – Longest Ranges are in the E-W Direction

In-situ Density Estimation Plans						
Domain	**Pass**	**Distance**			**Min # Comp**	**Max # Comp**
1	1	30	20	20	6	12
	2	45	30	30	4	12
	3	60	40	40	2	12
2	1	30	20	20	6	12
	2	45	30	30	4	12
	3	60	40	40	2	12
3	1	30	20	20	6	12
	2	45	30	30	4	12
	3	60	40	40	2	12
4	1	30	20	20	6	12
	2	45	30	30	4	12
	3	60	40	40	2	12
5	1	30	20	20	6	12

	2	45	30	30	4	12
	3	60	40	40	2	12

Table 60: In-situ Density Assigned Values by Domain

In-situ Density Assigned Values		
Alteration Code	**Description**	**In-situ Density Assigned Value**
311	Calco-Sodic	2.743
321	Pottasic-Biotite	2.783
331	Green Sericite	2.764
351	Propilitic	2.735
361	Qz-Sericite	2.650
381	Sericite-Clays	2.430

14.10 Validation

14.10.1 Visual Validation

Cross sections, longitudinal sections, and plan views were used to check whether the block estimated grades in relation to the nearby composites are reasonable; whether the composited assay data itself was reasonable; whether the oxide/transition/sulfide topographic surfaces, and the lithological and mineralized envelopes were correctly tagged onto the block model; and whether the estimated and assigned in-situ density values and final estimated Au grades are reasonable. No evidence of any block being wrongly assigned or estimated was found. Two examples are shown in Figure 73 and Figure 74.

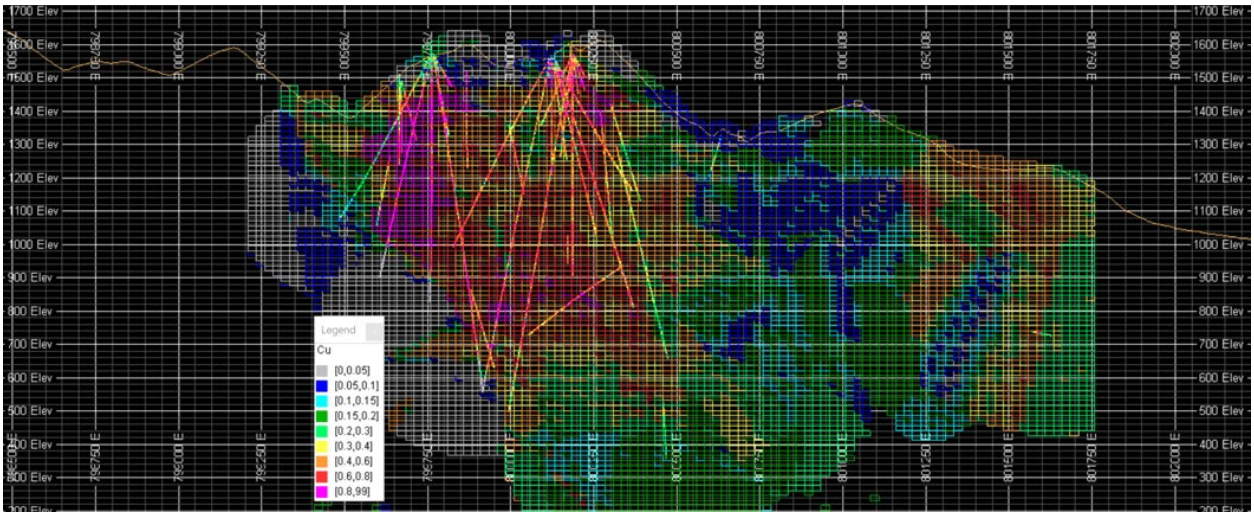

Figure 73: Warintza Central and Warintza East, Cu Grade Estimates, N9648050 Section

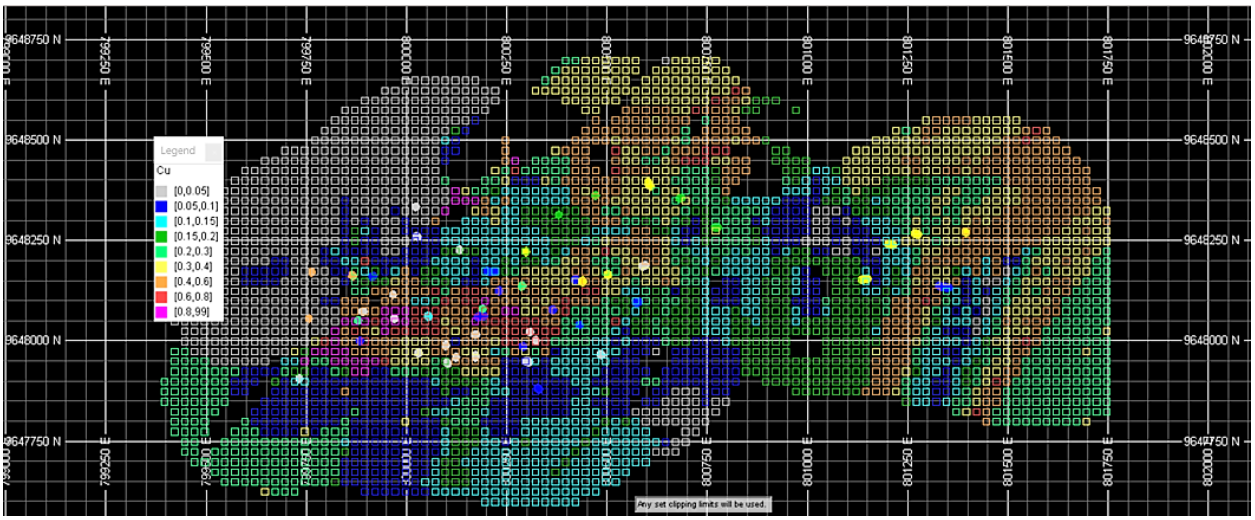

Figure 74: Warintza Central and Warintza East, Cu Grade Estimates, 820m Plan View

14.11 Statistical Validation

The comparison of the global averages and basic statistics between the block model at cut-off grade of 0 g/t Au and the declustered composites were obtained for each domain. The relative differences between the average estimated grades and the NN-declustered composites are acceptable for most domains for all three variables, Cu, Mo, and Au, as shown in Table 61, Table 62, and Table 63, respectively.

Note that those domains for which the differences are more important is either because they are low grades, such that the relative differences are more significant, or because there are few blocks and estimates considered in the averaging.

Table 61: Global Means by Domain, Nearest-Neighbor Model, and Estimated Grades, Cu

DOMAIN	ESTIMATION PASS	NUMBER OF BLOCKS	MEAN_NN_CU	MEAN_CU	Diff_%
1	1	2116	0.196	0.186	-5.02%
	2	1234	0.168	0.176	4.67%
	3	3703	0.196	0.196	-0.05%
2	1	8711	0.092	0.103	11.79%
	2	2209	0.105	0.096	-8.60%
	3	8185	0.108	0.097	-9.82%
3	1	8015	0.305	0.298	-2.14%
	2	35467	0.243	0.225	-7.71%
	3	74232	0.220	0.216	-2.15%
4	1	1037	0.660	0.670	1.60%
	2	264	0.447	0.719	60.73%
	3	488	1.001	0.468	-53.23%
5	1	16355	0.228	0.234	2.63%

	2	7815	0.210	0.197	-6.14%
	3	13047	0.190	0.186	-1.93%
6	1	5710	0.556	0.548	-1.37%
	2	1520	0.415	0.405	-2.42%
	3	2736	0.348	0.414	18.92%
7	1	30	0.107	0.098	-8.63%
	2	202	0.241	0.331	37.57%
	3	4105	0.147	0.243	66.03%
8	1	2202	0.627	0.624	-0.44%
	2	387	0.584	0.629	7.61%
	3	58	0.464	0.540	16.47%
9	1	9	0.324	0.298	-8.17%
	2	171	0.139	0.209	50.19%
	3	461	0.240	0.256	6.53%
10	1	7053	0.052	0.061	16.52%
	2	12792	0.049	0.049	0.99%
	3	21330	0.042	0.037	-10.49%

Table 62: Global Means by Domain, Nearest-Neighbour Model and Estimated Grades, Mo

DOMAIN	ESTIMATION PASS	NUMBER OF BLOCKS	MEAN_NN_MO	MEAN_CU	Diff_%
1	1	2432	0.009	0.010	5.06%
	2	7509	0.009	0.010	12.04%
	3	24462	0.010	0.011	9.09%
2	1	3247	0.003	0.003	14.20%
	2	1257	0.003	0.003	31.03%
	3	5822	0.003	0.004	31.68%
3	1	2457	0.006	0.006	-1.74%
	2	5365	0.005	0.005	-2.42%
	3	20411	0.005	0.005	7.83%
4	1	19312	0.024	0.024	0.08%
	2	7751	0.016	0.017	4.97%
	3	12991	0.014	0.014	5.98%
5	1	15983	0.015	0.015	1.56%
	2	28578	0.011	0.011	0.43%
	3	45635	0.007	0.007	-0.60%
6	1	1	0.001	0.001	37.70%
	2	21	0.001	0.002	37.87%
	3	413	0.002	0.002	-3.63%
7	1	3951	0.030	0.030	1.15%

	2	8615	0.023	0.024	5.44%
	3	9142	0.008	0.010	23.46%

Table 63: Global means by Domain, Nearest-Neighbor Model, and Estimated Grades, Au

DOMAIN	ESTIMATION PASS	NUMBER OF BLOCKS	MEAN_NN_AU	MEAN_AU	Diff_%
1	1	18262	0.040	0.040	0.29%
	2	17278	0.035	0.034	-4.72%
	3	35912	0.037	0.038	5.10%
2	1	4368	0.028	0.027	-2.08%
	2	7361	0.030	0.030	-0.37%
	3	16323	0.027	0.027	0.08%
3	1	26476	0.058	0.057	-1.30%
	2	13446	0.050	0.049	-1.14%
	3	30472	0.043	0.046	6.78%
4	1	2278	0.013	0.012	-7.45%
	2	11371	0.020	0.014	-31.64%
	3	37754	0.025	0.015	-38.30%

Drift Plots

It is important to check whether the estimated grades reproduce the same grade trends observed in the declustered composites. This can be accomplished by plotting declustered drill hole composite grades (nearest neighbor model) vs. block model averages based on the three main Cartesian coordinates and considering significantly large volumes at a time. The slices (swaths) are defined considering block sizes in each direction. In this case, the width was two blocks (50 m) in the Easting and Northing directions and two levels (30 m) in the elevation direction.

These graphs were obtained globally for Cu, Mo, and Au in each of the three directions, considering the first two estimation passes, and are shown in Figure 75, Figure 76, and Figure 77, respectively.

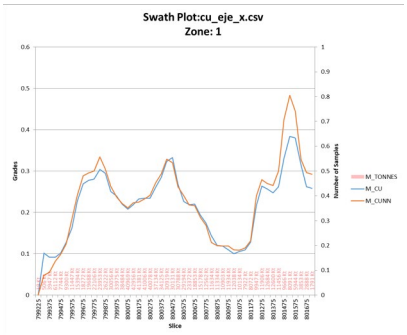

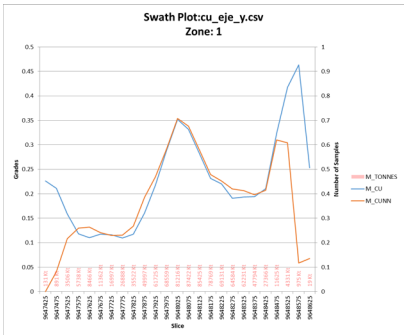

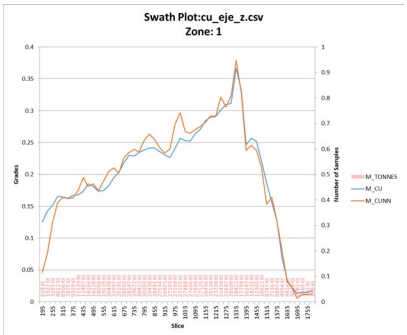

Figure 75: Drift Plots, Cu

From Left to Right: Easting; Northing; and Elevation, Average Cu Nearest Neighbor (NN) Model Grades (Orange Line) and Average Cu Estimated Grades (Blue Line).
Swaths are 50 m; 50 m; and 30 m wide, respectively

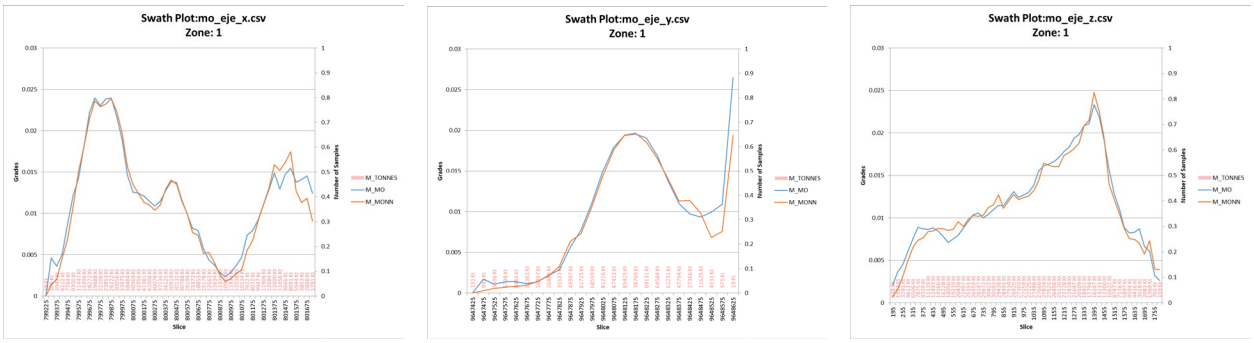

Figure 76: Drift Plots, Mo

From Left to Right: Easting; Northing; and Elevation, Average Mo Nearest Neighbor (NN) Model Grades (Orange Line) and Average Mo Estimated Grades (Blue Line).
Swaths are 50 m; 50 m; and 30 m wide, respectively

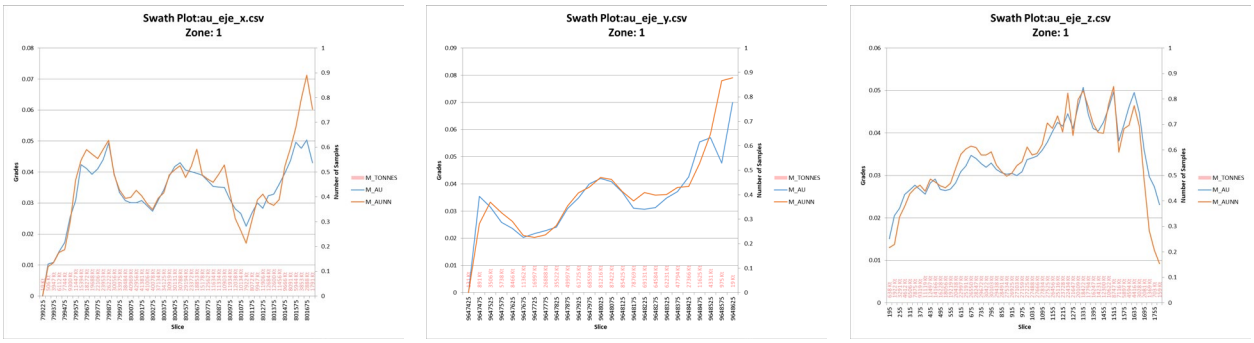

Figure 77: Drift Plots, Au

From Left to Right: Easting; Northing; and Elevation, Average Au Nearest Neighbor (NN) Model Grades (Orange Line) and Average Au Estimated Grades (Blue Line).
Swaths are 50 m; 50 m; and 30 m wide, respectively

14.12 Classification of Mineral Resources

The MRE is classified into Indicated and Inferred categories. There are no Measured resources at this point. The classification was done after considering observed continuity of mineralization, continuity of the geological units/domains, knowledge of lithological, alteration, and structural controls on mineralization, and reliability of the sampled data. Also, consideration was given to the quality of the geological model, including the lack of true width information, which in this case does not affect the confidence on the geologic model given that it is a three-dimensional interpretation of large volumes.

The implementation of the resource classification process was completed in two steps:

1. A specific estimation run using the Cu kriging plans was implemented with a maximum range between 100 to 120 m (longest axis depending on the Cu estimation domain) and using the same anisotropic searches on a domain-by-domain basis. This classification pass is slightly more relaxed than the first-grade estimation pass but significantly more restrictive than the second-grade estimation pass. The result is an indicator for each block in the model, flagging that it could have been estimated under those specific conditions, which is the basis for the indicated classification.

2. A manual interpretation and adjustment of the indicator classification was then done on plan views (by bench). The interpretation was intended to:

    a. Restrict further the indicated areas to about 90-100 m maximum in extrapolating areas.

    b. Eliminate isolated blocks marked as potentially Indicated (avoid the “spotted dog” issue), converting them to Inferred.

    c. Eliminate blocks marked as potentially Indicated in areas where there were isolated drilling platforms. In these areas, grade estimation is based on multiple drill holes but all drilled from one or two platforms. The affected areas were El Trinche and Warintza East, which are classified as Inferred.

Additional restrictions were imposed based on elevation to account for where drill holes become sparser at depth. The additional restrictions implemented were:

1. Any estimated block flagged as Indicated below 545 m elevation was classified as Inferred.

2. Any estimated block flagged as Inferred below the 200 m elevation was reset to not estimated. Similarly, any estimated block with Northing coordinates greater than 9,648,700N was re-set to not estimated.

A plan view (level 740 m) of Warintza’s resource classification and drill hole traces is shown in Figure 78, with Indicated blocks in green and Inferred blocks in blue. Also, shown in yellow, is the outline of the resource pit used to report the mineral resources. A cross section (N9648200) is shown in Figure 79, also showing the Resource Pit used to define the mineral resources, See Section 14.13 below.

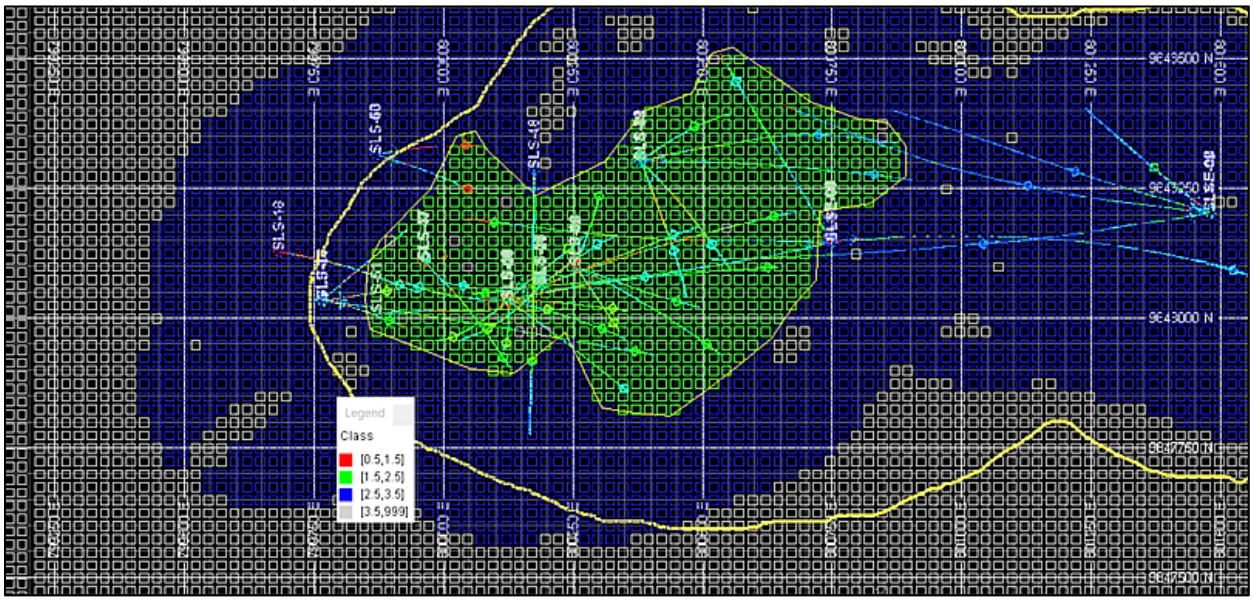

Figure 78: Warintza Resource Classification Plan View, Level 740 m
Indicated Blocks in Green; Inferred Blocks in Blue; Waste/Not Estimated in Gray; Yellow Outline is Resource Pit

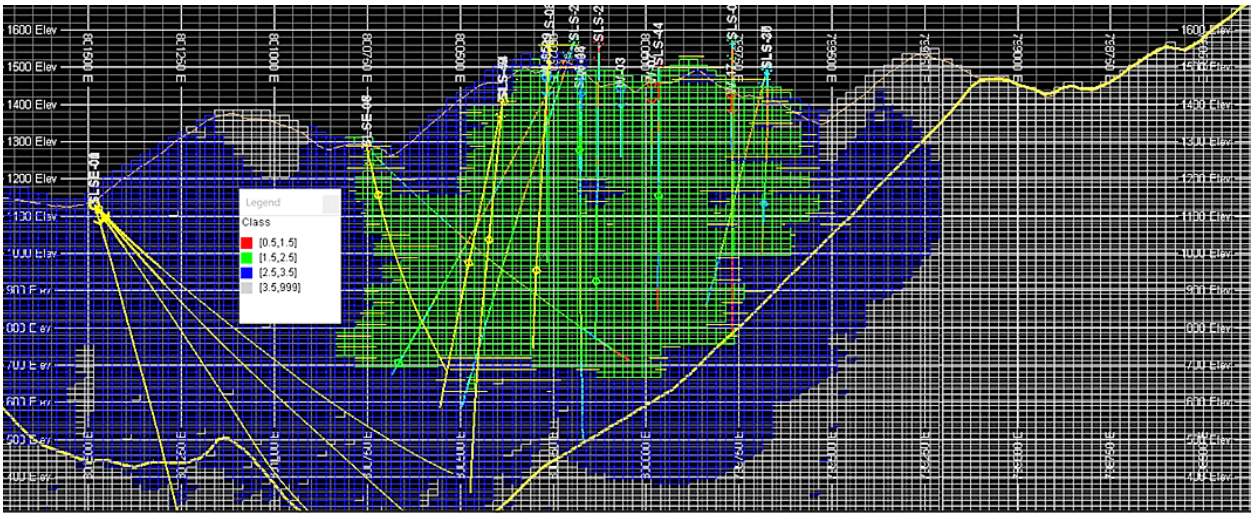

Figure 79: Warintza Resource Classification East West Section, N9648200
Indicated Blocks in Green; Inferred Blocks in Blue; Waste/Not Estimated in Gray; Yellow Outline is Resource Pit

14.13 Reasonable Prospects of Eventual Economic Extraction

The Warintza mineralization is assumed amenable to open-pit mining and milling and recovery through a concentrator (flotation plant) with a Mo recovery circuit. Au is assumed to be recoverable in a Cu concentrate and payable as a credit. All these assumptions are common for these types of Cu-Mo-Au porphyry deposits.

Warintza was evaluated for reasonable prospects for eventual economic extraction by constraining the mineral resources within a conceptual pit shell optimized in NPV Scheduler™. The assumptions used in preparing the conceptual pit include mining, processing, and general and administration costs; metallurgical recoveries; metal prices; a single global slope angle for the ultimate pit walls; and other technical parameters. The primary assumptions are shown in Table 64 and correspond approximately to a 0.09 % Cu breakeven economic cut-off.

Table 64: Warintza Conceptual Resource Pit Parameters

Parameter	Value
Cu price (USD/lb)	3.50
Mo price (USD/lb)	15.00
Au Price (USD/ounce)	1,500
Mining Cost (USD/tonne)	1.50
Incremental Mining Cost (USD/vertical every 15m)	0.02
Process Cost (USD/tonne of ore)	4.50
Cu Recovery (%)	90
Mo Recovery (%)	85
Au Recovery (%)	70
General and Administration (USD/tonne)	0.90
Overall and Global Ultimate Pit Slope Angle (degrees)	47.5º

14.14 Mineral Resource Inventory

The effective date of the MRE is April 1, 2022. The MRE is presented in Table 65.

Resources are presented based on CuEq grades, as well as the individual metals. The calculation of the CuEq grade is based on both metallurgical recoveries and metal prices, the same shown in Table 64 above. The CuEq formula used is:

$$CuEq = Cu\ (\%) + \frac{Mo\ Rec(\%)}{Cu\ Rec\ (\%)} \times \frac{Mo\ Price\left(\frac{USD}{lb}\right)}{Cu\ Price\ \left(\frac{USD}{lb}\right)} \times Mo\ (\%)$$
$$+ \frac{Au\ Rec(\%)}{Cu\ Rec\ (\%)} \times \frac{Au\ Price\left(\frac{USD}{oz}\right)}{Cu\ Price\ \left(\frac{USD}{lb}\right)} \times Au\ \left(\frac{g}{t}\right)$$

Appropriate conversion factors for Au, in particular, need to be applied. The resulting final factors are:

$$CuEq = Cu\ (\%) + 4{,}0476\ \times Mo\ (\%) + 0{,}487 \times Au\ \left(\frac{g}{t}\right)$$

In other words, under the stated assumptions, a 100ppm Mo grade in a block contributes an equivalent of 0.04% Cu (approximately), while a 0.05 g/t Au grade contributes and equivalent of 0.025 % Cu (approximately).

Although it is not certain that additional drilling will add to the current resource base, the incorporation of 87% of the current mineral inventory into the open-pit-constrained resource highlights the fact that the current resource base and constraining pit is limited by the current drilling and the early stage of the Project. The Inferred open-pit mineral resources in the Warintza Central deposit within the constraining optimized pit shell are reported at a 0.3% CuEq cut-off grade summarized in Table 655.

Table 65: Warintza Mineral Resource at 0.3 % CuEq Cut-Off Grade, Effective April 1, 2022

Cut-off	Resource Category	Tonnage Above Cutoff	Grade Above Cutoff				Contained Metal Above Cutoff			
CuEq (%)		(Mt)	CuEq (%)	Cu (%)	Mo (%)	Au (g/t)	CuEq (Mt)	Cu (Mt)	Mo (Mt)	Au (Moz)
0.3	Indicated	579	0.59	0.47	0.03	0.05	3.45	2.7	0.15	0.93
	Inferred	887	0.47	0.39	0.01	0.04	4.17	3.48	0.13	1.08

Notes to Table 1:

1. *The mineral resource estimates are reported in accordance with the CIM Definition Standards for Mineral Resources & Mineral Reserves, adopted by CIM Council May 10, 2014.*
2. *Reasonable prospects for eventual economic extraction assume open-pit mining with conventional flotation processing and were tested using NPV Scheduler™ pit optimization software with the following assumptions: metal prices of US$3.50/lb Cu, US$15.00/lb Mo, and US$1,500/oz Au; operating costs of US$1.50/t + US$0.02/t per bench for mining, US$4.50/t milling, US$0.90/t G&A; recoveries of 90% Cu, 85% Mo, and 70% Au.*
3. *Resource includes grade capping and internal dilution. Grade was interpolated by ordinary kriging populating a block model with block dimensions of 25m x 25m x 15m.*
4. *Mineral resources that are not mineral reserves do not have demonstrated economic viability.*
5. *Copper equivalent assumes recoveries of 90% Cu, 85% Mo, and 70% Au based on preliminary metallurgical test work, and metal prices of US$3.50/lb Cu, US$15.00/lb Mo, and US$1,500/oz Au. CuEq formula: CuEq (%) = Cu (%) + 4.0476 × Mo (%) + 0.487 × Au (g/t).*
6. *The Qualified Person is Mario E. Rossi, FAusIMM, RM-SME, Principal Geostatistician of Geosystems International Inc.*
7. *All figures are rounded to reflect the relative accuracy of the estimate.*
8. *The effective date of the mineral resource estimate is April 1, 2022.*

Table 66: Warintza Mineral Resource Estimate Summary and Cut-Off Grade Sensitivity

Cut-off	Category	Tonnage	Grade	Contained Metal

CuEq (%)		(Mt)	CuEq (%)	Cu (%)	Mo (%)	Au (g/t)	CuEq (Mt)	Cu (Mt)	Mo (Mt)	Au (Moz)
0.2%	Indicated	736	0.52	0.40	0.02	0.05	3.84	2.95	0.18	1.11
	Inferred	1,558	0.37	0.31	0.01	0.03	5.80	4.80	0.19	1.63
0.3% (Base Case)	**Indicated**	**579**	**0.59**	**0.47**	**0.03**	**0.05**	**3.45**	**2.70**	**0.15**	**0.93**
	Inferred	**887**	**0.47**	**0.39**	**0.01**	**0.04**	**4.17**	**3.48**	**0.13**	**1.08**
0.4%	Indicated	442	0.67	0.54	0.03	0.05	2.97	2.38	0.12	0.77
	Inferred	539	0.55	0.47	0.01	0.04	2.96	2.53	0.08	0.71

Notes to Table 64:

1. *The mineral resource estimates are reported in accordance with the CIM Definition Standards for Mineral Resources & Mineral Reserves, adopted by CIM Council May 10, 2014.*
2. *Reasonable prospects for eventual economic extraction assume open-pit mining with conventional flotation processing and were tested using NPV Scheduler™ pit optimization software with the following assumptions: metal prices of US$3.50/lb Cu, US$15.00/lb Mo, and US$1,500/oz Au; operating costs of US$1.50/t + US$0.02/t per bench for mining, US$4.50/t milling, US$0.90/t G&A; recoveries of 90% Cu, 85% Mo, and 70% Au.*
3. *Resource includes grade capping and internal dilution. Grade was interpolated by ordinary kriging populating a block model with block dimensions of 25m x 25m x 15m.*
4. *Mineral resources that are not mineral reserves do not have demonstrated economic viability.*
5. *Copper equivalent assumes recoveries of 90% Cu, 85% Mo, and 70% Au based on preliminary metallurgical test work, and metal prices of US$3.50/lb Cu, US$15.00/lb Mo, and US$1,500/oz Au. CuEq formula: CuEq (%) = Cu (%) + 4.0476 × Mo (%) + 0.487 × Au (g/t).*
6. *The Qualified Person is Mario E. Rossi, FAusIMM, RM-SME, Principal Geostatistician of Geosystems International Inc.*
7. *All figures are rounded to reflect the relative accuracy of the estimate.*
8. *The effective date of the mineral resource estimate is April 1, 2022.*

Cautionary Note

Mineral resources that are not mineral reserves do not have demonstrated economic viability. Mineral resources do not account for mine selectivity, mining loss, and dilution. The reported mineral resources include material classified as Inferred mineral resources that have a lower level of confidence than Indicated mineral resources and, as such, have not been converted to mineral reserves. It is reasonably expected that the majority of Inferred mineral resources could be upgraded to the Indicated category through further exploration.

14.15 Factors That May Affect the Mineral Resource Estimate

Other than as discussed in other sections of this Report, there are no known environmental, permitting, legal, title, taxation, socio-economic, marketing, political, or other relevant issues that may materially affect the mineral resource estimates. Other relevant factors that may materially affect the mineral resources, including mining, metallurgical recovery, and infrastructure, are reasonably well understood according to the assumptions presented in this Report.

15.0 MINERAL RESERVE ESTIMATE

Not applicable at the current stage of the Project.

16.0 MINING METHODS

Not applicable at the current stage of the Project.

17.0 PROCESSING METHODS

Not applicable at the current stage of the Project.

18.0 PROJECT INFRASTRUCTURE

Not applicable at the current stage of the Project.

19.0 MARKET STUDIES AND CONTRACTS

Not applicable at the current stage of the Project.

20.0 ENVIRONMENTAL STUDIES, PERMITTING & SOCIAL / COMMUNITY IMPACT

21.0 CAPITAL AND OPERATING COSTS

Not applicable at the current stage of the Project.

22.0 ECONOMIC ANALYSIS

Not applicable at the current stage of the Project.

23.0 ADJACENT PROPERTIES

Two large porphyry Cu-Au districts occur within the same mineralized belt as the Warintza cluster. Mirador and San Carlos-Panantza porphyry clusters share geological characteristics with Warintza (Figure

80). The following sections on Mirador and San Carlos-Panantza are summarized from publicly available reports and research literature.

Mirador District

The Mirador District, located some 40 km south of the Warintza cluster, has two main porphyry deposits – Mirador and Mirador Norte – as well as some lesser mineralized structures that comprise the Mirador District (Drobe et al., 2013). These deposits are characterized by disseminated to blebby chalcopyrite, which is most abundant within potassically altered plutonic rocks of the Zamora Batholith. Chalcocite-bearing, supergene-enriched zones overly the primary mineralization as at Warintza. Radiometric age dating (Drobe et al., 2013) indicates that the main Zamora Batholith granodiorite host rocks are ca. 164 Ma, whereas the causative subvolcanic intrusive rocks are approximately 8 million years younger.

The Mirador mine is currently owned and operated by EcuaCorriente S.A., a wholly-owned subsidiary of CRCC-Tongguan Investment Co. Ltd., which is a joint venture formed between China Railway Construction Corporation (“CRCC”) and Tongling Non Ferrous Metal Group.

Mirador commenced commercial production on July 18, 2019, and has a current projected mine life of 30 years (Harris, 2019). The mine is expected to produce 11 Mt of Cu concentrates annually, containing 137 Mlbs of Cu, 34,000 ounces of Au, and 394,000 ounces of Ag for 30 years. The Cu concentrates it produces will be exported to China. Mirador hosts probable reserves of 3.18 Mt of Cu, 3.39 million ounces of Au, and 27.11 million ounces of Ag.

San Carlos-Panantza

San Carlos-Panantza deposits are located approximately 18 km west of Warintza. San Carlos-Panantza contain mainly hypogene Cu with minor overlying oxide and secondary enrichment horizons (Drobe et al., 2007). Typical hypogene mineralization consists of disseminated chalcopyrite and molybdenite within quartz veins, whereas higher-grade zones (>0.8% Cu) are associated with more concentrated chalcopyrite with pyrite and locally magnetite (Drobe et al., 2007).

The San Carlos-Panantza porphyry Cu deposits are currently owned and operated by EcuaCorriente S.A., a wholly-owned subsidiary of CRCC-Tongguan Investment Co. Ltd., which is a joint venture formed between CRCC and Tongling Non Ferrous Metal Group. The concessions that cover the San Carlos-Panantza deposits are directly adjacent to the concessions covering the Warintza deposit.

Corriente Resources Inc.’s Panantza and San Carlos Cu Project Preliminary Assessment Report, dated October 30, 2007 (Technical Report, Mirador Copper-Gold Project 30,000 TPD Feasibility Study) contains historical estimates for the two deposits.

The reported San Carlos historical Inferred mineral resource estimate is 600 Mt of 0.59% Cu for 7,738 Mlbs of Cu at a 0.4% Cu cut-off. The reported Panantza historical Inferred mineral resource estimate is 463Mt of 0.66% Cu for 6,688 Mlbs of Cu at a 0.4% Cu cut-off. Between the two deposits, there have been 22,580 m of drilling in 79 holes.

The historical estimates in the Corriente report are thought to be relevant and reliable as of their date of issue. The following summary of assumptions, parameters and methods is an abridged version of disclosure provided in the summary of the Corriente report:

Corriente engaged Mine Development Associates ("MDA") in April 2007 to provide a block-model based mineral resource estimate for Panantza in order to provide a current resource estimate. In addition, MDA was asked to provide a block-model based mineral resource estimate for San Carlos so that the mining potential of both projects could be evaluated using block-model based mine scheduling and floating pit cones. In working with MDA, Corriente re-estimated the resources of both deposits by developing block models incorporating the 2006 drill data for Panantza, and using new geology solid models for San Carlos. The resource estimate excludes oxide copper mineralization within the leached zone of the deposits.

The historical estimates use mineral resource categories prescribed by NI 43-101 and are the most recent estimates available to Solaris. To be updated to current mineral resources, Solaris anticipates the assumptions used to derive the historical estimates would need to be updated to be more appropriate for current times. A qualified person has not done sufficient work to classify the historical estimates as current mineral resources and Solaris is not treating the historical estimates as current mineral resources.

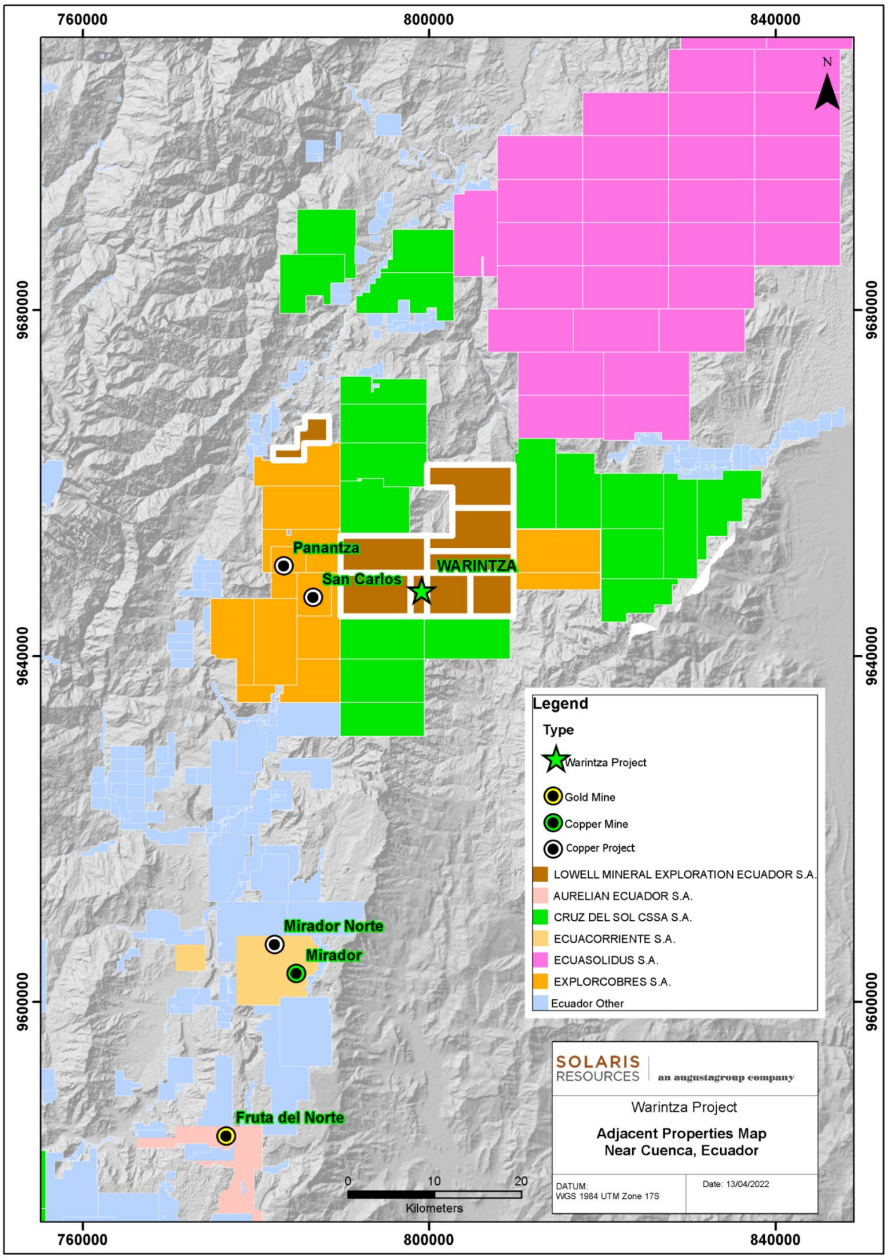

Figure 80: Map of Concessions, Known Prospects and Mines Surrounding Warintza Property
Source: Solaris Resources Inc. (2022)

The Author of the Report has been unable to verify the foregoing information, and the information is not necessarily indicative of the mineralization on the Warintza Project.

24.0 OTHER RELEVANT INFORMTION

No other relevant information.

25.0 INTERPRETATION AND CONCLUSIONS

Warintza is a highly prospective Cu-Mo-Au porphyry deposit within the Cordillera del Cóndor. Exploration efforts in the belt have identified numerous porphyry, Au skarn, and epithermal Au deposits, all related to Late Jurassic magmatism. Warintza is a typical porphyry system that has the potential to become a world-class Cu-Mo-Au resource, while the potential for other deposit types exists but have not been explored.

After less than two years and less than 65,000 m of core drilling, which have tested mainly the Warintza Central area, this MRE shows a very significant tonnage amenable to open-pit mining. It also shows that the mineralization is open in several directions and that there are several additional deposits which have significant target footprints, adjacent and nearby to Warintza Central, that require further exploration.

Infill drilling is required within both Warintza Central and Warintza East, but more importantly, drilling to date has not defined the limits of mineralization, with a reasonable expectation that additional drilling will result in an increase in the known dimensions of the mineralization.

Straightforward grass-roots exploration techniques work well in the Cordillera del Cóndor. Numerous porphyry deposits have been discovered in the area by initial panned concentrate stream sediment sampling, followed by prospecting, rock sampling, ridge soil sampling, grid soil sampling, and finally, scout drill-testing of geochemical anomalies. At Warintza, there are additional targets that have yet to be investigated by drilling.

Warintza Central and Warintza East are the subjects of this MRE. Both are open at depth and laterally. These are good prospects for additional drilling to expand the Resource in both areas.

Early exploration at Warintza prior to Solaris' involvement was hampered by community and social issues, and although this still presents a risk, efforts by the Company have allowed for the development of a supportive relationship and advancement of the Project. The return of the surface rights covering the Shuar communities, along with ongoing community consultation and community development efforts, have culminated in the Company entering into an Impact and Benefits Agreement with the host communities.

Metallurgical testing is ongoing, and a full characterization of Warintza's mineralization is still pending. It is merited that, in the near-term, a PEA be developed, which will require a more complete understanding of the mineralization's response to beneficiation methods. From the testing completed to date, plus comparisons to similar porphyry deposits, it is likely that mineralization is amenable to conventional metallurgical processes.

25.1 Risks and Uncertainties

25.1.1 Risks and Uncertainties Affecting the Resource Estimate

The factors that normally create risk in a resource estimate are not unusual and common to many exploration-stage projects. Additional infill and resource-extension drilling are required. Although, to date, drilling has confirmed prior models and assumptions regarding geological and grade continuity, this

can change in areas with relatively sparse information. This is a normal exploration risk, and, in fact, the uncertainty implies both downside risk and upside potential.

The reported resources can be impacted by social, political, and government affairs, issues that remain a risk. While at this point in time, Solaris has done considerable work to ensure that this risk is minimized, social and political factors external to the Company's control can materially impact the prospects for economic exploitation of Warintza.

Other technical issues, such as the lack of a formal quality control monitoring program for the older holes (2000 campaign), have been largely resolved by confirming the characteristics of the mineralization with new drilling. The 2001 drill campaign (holes W-17 through W-33) did include a formal quality control monitoring program. While relatively conventional for that time, they were incomplete and less rigorous than is currently recommended for such programs. This is considered a minor risk and, after the additional drilling, has no impact on the resource estimate or classification.

25.1.2 Risks and Uncertainties Affecting Potential Additional Discoveries

The Warintza Property contains targets for future exploration that could lead to the discovery of additional mineralization having the potential to add to the current resource estimates. There is no certainty; however, that future exploration will lead to significant discoveries as part of normal exploration risk.

26.0 RECOMMENDATIONS

26.1 Drilling Program

A total of 99 drill holes and 64,541 m were used to develop the Warintza 2022 MRE.

Additional diamond core drilling for the Warintza Central deposit is recommended. There are two simultaneous objectives: resource expansion and increase in resource confidence (categorization). Among these two objectives, if additional geologic information warrants it, targeting new areas of higher-grade mineralization (supergene enrichment or high-grade primary mineralization) should be prioritized.

Infill, resource expansion, exploration and geometallurgical drilling (at PQ diameter) and studies to support a PEA based on an updated mineral resource Estimate should be completed. The combined objectives are likely to require an additional 44,000 m of drilling, with the resource expansion drilling component at Warintza Central and Warintza East and follow-up drilling at the Warintza West discovery amounting to approximately 24,000 m of this total. Together, these programs would cost approximately $25 million, inclusive of camp costs, infrastructure development, and community costs. Further infill drilling, geometallurgical and geotechnical drilling, together with other technical, environmental and market studies in support of a Pre-Feasibility Study could cost an additional $40 million.

It is also recommended that a total of no less than 5% of the meters drilled in mineralization be tested for in-situ density.

A geometallurgical program is recommended for flowsheet development and optimization, in addition to assessing the mineralization's heterogeneity. Comminution variables such as SAG power and Bond Mill indices should be tested for in different domains, as well as metallurgical recovery variability from composites and variability tests.

Mineral liberation analysis and quantitative mineralogy should also be completed to determine the presence of pyrophyllite, talc, gypsum, and anhydrite that may require special processing and mining considerations. Preliminary metallurgical testing suggests that conventional floatation can achieve good recovery.

26.2 Preliminary Economic Assessment

Based on the results of the MRE for Warintza, the QP recommends further developing the Project through the completion of a PEA. The PEA study will form the basis for the mine development plan and will include detailed scopes, schedules, and work plans for inputs to a Pre-Feasibility Study to be completed at a later date. Solaris has estimated a budget of $1.4 million for the PEA and supporting input studies, including a preliminary metallurgical test work program to establish metal recoveries, metallurgical definitions, and comminution parameters, which the Company is already pursuing.

Solaris will continue to develop environmental, social, health, safety, and security programs in parallel to support the exploration program and technical studies.

27.0 REFERENCES

1. Arias, W., Core shed facilities and sample preparation laboratories visit at the Warintza project. Wood PLC. June 14, 2021. 1-5 pp.
2. Aspden J.A., Litherland M., (1992) The geology and Mesozoic collisional history of the Cordillera Real, Ecuador. Tectonophysics 205:187-204
3. Berger, B. R., Ayuso, R. A., Wynn, J. C., and Seal, R. R., 2008, Preliminary model of porphyry Cu deposits: US Geological Survey Open-File Report 2008-1321, 55 p.
4. Bloom, L., Solaris Drill Core Quality Control Procedures. Analytical Solutions Ltd. Canada. June 29, 2021. 1- 7pp.
5. Bloom, L., Recommendations for Warintza Drill Core Duplicates. Analytical Solutions Ltd. Canada. August 25, 2021. 1- 19pp.
6. Chiaradia M, Vallance J, Fontboté L, Stein H, Schaltegger U, Coder J, Richards J, Villeneuve M, Gendall I (2009) U-Pb, Re-Os, and $^{40}Ar/^{39}Ar$ geochronology of the Nambija Au-skarn and Pangui porphyry Cu deposits, Ecuador: Implications for the Jurassic metallogenic belt of the Northern Andes. Mineralium Deposita 44:371-387
7. CIM, 2003, Estimation of Mineral Resources and Mineral Reserves Best Practice Guidelines: Adopted by CIM Council on November 23, 2003, 10 p.
8. CIM, 2014, CIM Definition Standards for Mineral Resources and Mineral Reserves: Prepared by the CIM Standing Committee on Reserve Definitions, Adopted by CIM Council May 10, 2014, 10p.
9. Corriente Resource Inc. Annual Information Form, 2000.
10. Corriente Resources Inc. Annual Report 2003, 24p.
11. Corriente Resources Inc. Annual Report 2004, 24 p.
12. Deustch, C.V., 1989, “DECLUS: a FORTRAN 77 Program for Determining Optimum Spatial Declustering Weights”, Computers & Geosciences, 15(3): 325-332.
13. Donoso, A., 2019, Legal Report Lowell Mineral Exploration Ecuador S.A.
14. Drobe J, Lindsay D, Stein H, Gabites J (2013) Geology, mineralization, and geochronological constraints of the Mirador Cu-Au porphyry district, southeast Ecuador. Economic Geology 108:11-35
15. Drobe, J., Hoffert, J., Fong, R., Haile, J., and Collins, J., 2008, Technical Report, Mirador Cu-Au Project 30,000 TPD Feasibility Study.
16. Equity Exploration Consultants Ltd. Resource Estimate of the Warintza Central Ci-Mo Porphyry Deposit. Warintza Project, Cordillera del Cóndor, Ecuador. Prepared for Solaris Inc. Authors: Trevor Rabb, Darcy Baker & Eleanor Black. Effective Date: December 13, 2019. Report Date: December 18, 2019. Revised Date: February 13, 2020, 94 pp.
17. Fontboté L, Vallance J, Markowski A, Chiaradia M (2004), Oxidized Au skarns in the Nambija district, Ecuador. Society of Economic Geologists Special Publication 11:341-357
18. Gendall IR, Quevedo LA, Sillitoe RH, Spencer RM, Puente CO, Leon JP, Povedo RR (2000) Discovery of a Jurassic porphyry Cu belt, Pangui area, southern Ecuador. SEG Newsletter 43(1):8-15
19. GeoSystems International, Inc.: Warintza Project, Informe Visita a Proyecto y Laboratorio de Preparación. de Muestras, ALS, Quito, Ecuador. Preparado para Lowell Mineral Exploration Ecuador S.A., Solaris Inc. November 4, 2021, 50 pp.
20. GeoSystems International, Inc.: Warintza Project. Informe de Visita a Laboratorio de Análisis de Muestras, ALS Chemex Lima, Perú. Preparado para Lowell Mineral Exploration Ecuador S.A., Solaris Inc. February 3, 2022, 3 pp.

21. Gustafson, LB, Quiroga J (1995) Patterns of mineralization and alteration below the porphyry Cu orebody at El Salvador, Chile. Economic Geology 90:2-16
22. Harris, P., 2019, EcuaCorriente starts Mirador production.
23. Hartley, A. J., and Rice, C. M., 2005, Controls on supergene enrichment of porphyry Cu deposits in the Central Andes – a review and discussion: Mineralium Deposita, v. 40, p. 515–525.
24. Isaaks, E.H., 1999, "SAGE2001 User's Manual", Software License and Documentation.
25. Jaillard E (1997) Síntesis estratigráfica y sedimentológica del Cretáceo y Paleógeno de la Cuenca Oriental del Ecuador. Informe final del convenio ORSTOM-Petroproducción, Paris, ORSTOM, 164 p
26. Larrondo, P. and Deutsch, C.V., "Accounting for Geological Boundaries in Geostatistical Modeling of Multiple Rock Types., Geostatistics Banff 2004, Vol. 1, Leuangthong and Deutsch, editors, Springer, November 2005, pp 3-12.
27. Leary S, Sillitoe RH, Stewart PW, Roa KJ, Nicolson, BE (2016) Discovery, geology, and origin of the Fruta del Norte epithermal Au-Ag deposit, southeastern Ecuador. Economic Geology 111:1043-1072
28. Litherland M, Fortey NJ, Beddoe-Stephens B (1992) Newly discovered Jurassic skarn fields in the Ecuadorian Andes. Journal of South American Earth Sciences 6:67-75
29. Litherland M, Aspden JA, Jemielita RA (1994) The metamorphic belts of Ecuador. Overseas Memoir of the British Geological Survey, no. 11, 147 pp
30. Lowell, D. J., 2005, Warintza Project: Internal report for Lowell Mineral Exploration, 15 p.
31. Lowell Mineral Exploration: Guía de Métodos de Ensayos Geoquímicos y Físicos. Testigos de Perforación. Proyecto Warintza. Fecha: 01 Setiembre 2021. 1-11 pp.
32. Lowell Mineral Exploration: PROCEDIMIENTO DE REGISTRO Y RESPALDO FOTOGRAFICO A SONDAJES DDH. PROYECTO WARINTZA. Fecha: mayo 2020 v1, actualización octubre 2021. 1-16 pp.
33. Lowell Mineral Exploration: PROCEDIMIENTO DE MUESTREO (TESTIGOS DE PERFORACIÓN). PROYECTO WARINTZA. Fecha: mayo 2020 v1, octubre 2020 v2, actualización octubre 2021. 1-20 pp.
34. Lowell Mineral Exploration: PROCEDIMIENTO DE MUESTREO DE PULPAS. PROYECTO WARINTZA. Fecha: octubre 2020 v1, actualización agosto 2021. 1-12 pp.
35. Lowell Mineral Exploration: PROCEDIMIENTO DE PERFORACIÓN. PROYECTO WARINTZA. Fecha: mayo 2020 v1, actualización octubre 2021. 1-13 pp.
36. Lowell Mineral Exploration: Protocolo de QA/QC. Manual de cálculos y fórmulas. PROYECTO WARINTZA. Fecha: noviembre 2021 v1. 1-13 pp.
37. Lowell, J. D., and Guilbert, J. M., 1970, Lateral and vertical alteration-mineralization zoning in porphyry ore deposits: Economic Geology, v. 65, p. 373–408.
38. Puente, C., 2001, Warintza Este, Exploración Geológica Previa a la fase de Perforaciones, Provincia de Morona Santiago, SE Ecuador.
39. Richards, J. P., 2003, Tectono-magmatic precursors for porphyry Cu-(Mo-Au) deposit formation: Economic Geology, v. 98, p. 1515–1533.
40. Richards, J. P., 2005, Cumulative factors in the generation of giant calc-alkaline porphyry deposits, in Super porphyry Cu and Au deposits – a global perspective: PGC Publishing, p. 7–26.
41. Roa, K. J., 2017, NI 43-101 Technical Report on the Lost Cities – Cutucu Exploration Project, Province of Morona-Santiago, Ecuador.
42. Romeuf N, Aguirre L, Soler P, Féraud G, Jaillard E, Ruffet G (1995) Middle Jurassic volcanism in the Northern and Central Andes. Revista Geológica de Chile 22:245-259
43. Ronning, P., and Ristorcelli, S., 2006, Technical Report, Warintza Project, Ecuador: Lowell Mineral Exploration LLC, 138 p.

44. Ronning, P., and Ristorcelli, S., 2018, Technical Report, Warintza Project, Ecuador: Equinox Gold Corp. and Solaris Copper Inc., 128 p.
45. Sillitoe, R. H., 2000, Au-rich porphyry deposits: descriptive and genetic models and their role in exploration and discovery: Reviews in Economic Geology, v. 13, p. 315–345.
46. Sillitoe, R. H., 2005, Supergene oxidized and enriched porphyry Cu and related deposits: Society of Economic Geology 100th Anniversary Volume, p. 723–768.
47. Sillitoe, R. H., and Thompson, J. F. H., 2006, Changes in mineral exploration practice: consequences for discovery: Society of Economic Geologists Special Publication, v. 12, p. 193–219.
48. Sillitoe, RH (2010) Porphyry Cu systems. Economic Geology 105:3-41
49. Sillitoe RH, Perelló J (2005) Andean Cu province: Tectonomagmatic settings, deposit types, metallogeny, exploration, and discovery. Economic Geology 100th Anniversary Volume, 845-890
50. Spikings RA, Winkler W, Seward D, Handler R (2001) Along-strike variations in the thermal and tectonic response of the continental Ecuadorian Andes to the collision with heterogeneous oceanic crust. Earth Planet Science Letters 186:57-73.
51. Sivertz, G., Ristorcelli, S., Hardy, S., and Hoffert, J., 2006, Technical Report Update on the Cu, Au, and Ag Resources and Pit Optimizations, Mirador Project, Ecuador: Corriente Resources Inc., 144 p.
52. Tschopp HJ (1953) Oil explorations in the Oriente of Ecuador, 1938–1950. Bulletin of the American Association of Petroleum Geologists 37:2303-2347
53. Vaca, E., and León, J., 2001, Proyecto Warintza, Anomalías Central y Oeste; Evaluación Inicial y Recomendaciones de las Fases de Perforación.
54. Vallejo CF, Spikings R, Luzieux L, Winkler W, Chew D, Page L (2006). The early interaction between the Caribbean Plateau and the NW South American Plate. Terra Nova 18:64-269.